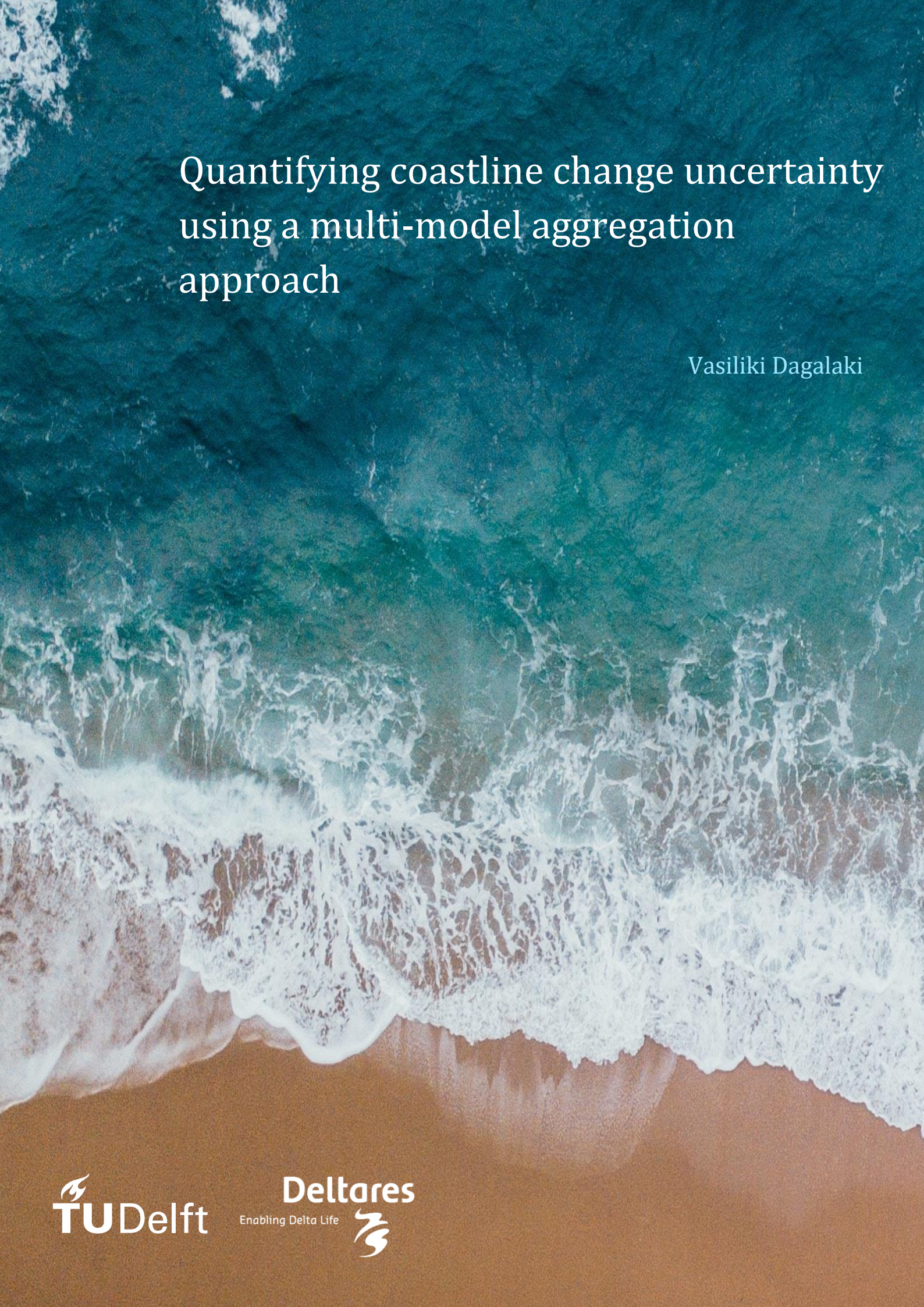

Quantifying coastline change uncertainty using a multi-model aggregation approach

Vasiliki Dagalaki

TU Delft

Deltares
Enabling Delta Life

Quantifying coastline change uncertainty using a multi-model aggregation approach

by

Vasiliki Dagalaki

in partial fulfilment of the requirements for the degree of

Master of Science
in Civil Engineering

at the Delft University of Technology,

to be defended publicly on Wednesday December 12, 2018 at 15:00.

Thesis committee:	Prof. dr. ir. S.G.J. Aarninkhof,	TU Delft
	Ir. W. P. de Boer,	Deltares/TU Delft
	Ir. F. Scheel,	Deltares
	Ir. A. Kroon,	TU Delft/ Svasek

TU Delft Delft University of Technology

Deltares Enabling Delta Life

Abstract

Evolution of coastline position under the influence of natural and anthropogenic processes is directly linked to the development of seaside societies. In the context of coastal zone management, process-based morphodynamic models are often used to predict coastline evolution and support the decision-making process for adaptation/mitigation strategies. Frequently, the processes driving the morphodynamic evolution transcend the applicability limits of a single model. In those cases, model ensembles can be used to estimate coastline change under the joint effect of the relevant processes. However, model output and in extent the aggregated result are characterised by uncertainty originating among others from forcing variability and parameter imprecision. The increasing exposure of coastal societies to coastal recession risks and emergence of risk-informed coastal zone management create the need for aggregated coastal recession estimates with quantified uncertainty.

This study investigates different statistical methods for forcing and parameter uncertainty quantification around coastline change estimates from process-based morphodynamic models. Subsequently a numerical convolution approach for the aggregation of the probabilistic coastal recession estimates from multiple models was formulated to account for the combined uncertain effect of processes acting on different timescales.

The methods of this study were applied on Anmok beach, South Korea, a coastal stretch experiencing erosion caused by long, intermediate and short timescale processes. Available UNIBEST-CL+ and Delft3D model schematizations from the CoMIDAS research program, capable of simulating the relevant processes, were utilised. Following a literature review, two methods were considered applicable for process-based morphodynamic models: Standard Monte Carlo (SMC) and Latin Hypercube Sampling (LHS). The application of both methods on the UNIBEST-CL+ model schematisation enabled the evaluation of their relative performance based on the precision of the different coastline change estimates achieved for the different sample sizes. Only LHS was applied on the Delft3D model schematisation due to computational demands limitations.

Subsequently, the scenario-based approach currently used for the aggregation of multi-model coastline change outputs was extended to explicitly account for the uncertainties quantified in the individual model outputs. A numerical convolution approach, using Monte Carlo sampling, was suggested for linear superposition of the contributing probability distribution functions. The advantages of this approach include speed, ease of implementation, comprehensibility and high resolution even at the tails of the aggregated distributions. Utilising this approach, the effect of alternative interventions (combinations of various breakwater designs with a small-scale nourishment) on the coastline change probabilities was quantified.

The results showed that both methods (i.e., SMC and LHS) with adequate sampling can produce probability distribution outputs for coastline change when applied to the process-based models. SMC remains the most suitable method for coastline change uncertainty quantification for models with small simulation durations. The method gives quantified estimates of the precision, enabling the achievement specific target precisions, with the respective computational cost. For the smaller sample sizes used, LHS gave better precision results, proving more suitable for models with longer computational time. On the downside, without extra iterations of the procedure only upper estimates of the achieved precision for a specific sample size can be obtained.

The probabilistic aggregation framework presented in this thesis has several advantages compared to the scenario-based approach currently used. It allows for quantified coastline change uncertainty estimates with the respective precision estimates and provides the distribution of the uncertainty across its range, information that could not be derived using the scenario-based approach. Different coastline change percentile estimates or confidence intervals with practical use to decision makers and the likelihood of any coastline change realisation of interest can be evaluated. The probabilistic uncertainty quantification and aggregation framework is believed to be useful for intervention assessment and comparison. It allows for the assessment of uncertainty around the morphological response under the combined effect of the processes acting on the coast with/without the intervention and thus the evaluation of the probabilistic intervention impact. Different interventions can be compared in terms of the probability of inducing desired/undesired morphodynamic realisations as well as in terms of the uncertainty range in the coastline change estimates.

Preface

This thesis marks the completion of my Master of Science in Hydraulic Engineering at Delft University of Technology. The research was carried out in Deltares from March to December 2018.

To start, I would like to thank my thesis committee members -Stefan Aarninkhof, Wiebe de Boer, Freek Scheel and Anna Kroon, for their contributions to this study. The feedback, guidance and support I received from you made the completion of this study possible. Wiebe and Freek thank you for giving me the opportunity to start my thesis on a topic I find fascinating, and for giving me inspiration when I lacked it.

I am grateful for the opportunity to work for the last 7 months in the welcoming, respectful and inspiring environment of Deltares. Special thanks to Bas Huisman for the expertise he provided on the use of UNIBEST-CL+ model. I would also like to thank Panos Athanasiou for the insight and information on sandbar related processes in Anmok beach.

To my fellow stagiaires, I enjoyed my time with you in and out of Deltares. Our plans, and slightly irrational lunch and coffee-break conversations made the last months unforgettable. I would like to thank my friends back home and my new friends in Delft for all those everyday moments that make my stay in the Netherlands much nicer. Special thanks to Fontas, Teni and Lina for the long walks and conversations.

Lastly, I would like to thank my family for enabling me to follow my dreams. Mum, Dad, Maria thank you for always being there when I needed you, for your love and generosity.

Vassia Dagalaki

Delft, December 2018

Table of Contents

1 Introduction

1.1 Background

Coastal zones worldwide are places of dense population, high economic, social and environmental value, while in some places they comprise the first line of coastal defence against flooding of the low-lying hinterland. According to recent estimates, 24% of the world's sandy beaches are affected by chronic erosion (A. Luijendijk et al., 2018), driven by natural and anthropogenic causes of varying time and spatial scales. Extreme forcing conditions, coastal structures in the littoral zone, and climate change are some of the causes of coastline retreat. Both chronic and episodic erosion can disrupt the environment and negatively affect economic growth of seaside areas. Additionally, coastal recession combined with rising water levels threatens the functionality of expensive coastal developments and poses risks for low-lying inlands and islands (Nicholls et al., 2010; Ranasinghe et al., 2012). In the case of high risk associated with coastal erosion, adaptation (e.g., set back lines) or mitigation (e.g., breakwaters, revetments, nourishments) measures are implemented in the context of coastal zone management. Future projections show that the exposure of coastal societies and infrastructure to coastal recession risks will continue to increase as the effects of climate change become more pronounced (IPCC, 2014) and the coastal zones develop further (McNamara et al., 2013; Ranasinghe, 2016). Under these conditions, there is an emerging need for risk quantification and mitigation strategies in the coastal zones and in extent, for risk informed coastal zone planning/management.

Prediction of the coastline position and the effects of the adaptation and mitigation measures form a cornerstone of risk informed coastal zone management. In current engineering practice, process-based models are used to simulate the hydrodynamic and morphodynamic processes in the coastal zone and predict the impact/effectiveness of suggested adaptation/mitigation measures. Nevertheless, despite the ongoing research and advancement in the coastal morphodynamic modelling, the outputs cannot directly facilitate risk informed coastal zone management. This can be traced back to the deterministic character of the model output that cannot directly capture the stochastic character of the simulated processes and the sources of uncertainty that relate to process based modelling, such as natural variability, model uncertainties and parameter value limitations (Fortunato et al., 2009; Scheel et al., 2014). In a morphodynamic simulation, those uncertainties are transferred through the mathematical equations and the generated outcome is in turn characterized by uncertainties and imprecision.

In present coastal engineering studies, the uncertainty in the simulated coastal morphology is usually addressed by means of expert opinions and a sensitivity analysis. Both methods can raise the awareness of the end users for the uncertainty in the model outputs and provide a first estimate of the possible range of coastline changes. However, they do not provide insight into the likelihood of predictions and do not account for the combined system sensitivity i.e. the output from simultaneously incident extreme values of parameters values (Klis, 2003; Vrijling et al., 1992).

On the other hand, information on the likelihood of different coastal evolution realizations has high value for coastal managers and decision makers. Management of the coastal zone involves multiple stakeholders, communal uses and high value assets. The decisions should satisfy economic, social and environmental criteria and should be made in an informed and transparent manner. Disregarding or misinterpreting uncertainty could lead to misplaced investments, loss of assets and unsafe situations. Proposed solutions should be judged and compared based on the full spectrum of the possible effects and, equally important, on the probability distribution of those effects. This information can neither be acquired through expert judgment, nor through sensitivity analysis. It should be noted that solutions with the same range of probable outcomes may vary significantly in the distribution of probabilities across this range, leading to different robustness levels. Those can be in turn translated to different risk levels when the quantified consequences are considered and used as indicators in the decision-making process.

Identification and quantification of coastline recession uncertainties implies that the morphodynamic model output is no longer a single coastline/profile determined by a deterministic approach. On the contrary we aim for a range or bandwidth of possible coastlines/profiles with a distribution function or confidence bandwidths that accommodate the stochastic character of the processes involved and the uncertainties of the models. Associating coastline recession with a probability distribution or confidence band, allows insight into the likelihood of the deterministic prediction and opens the way for effective assessment of the associated risk. It facilitates a better understanding for the elements of the system in question, the nexus between those elements and the properties of the system they form, such as robustness and flexibility. Additionally, it enables the quantification of the potential effects of proposed mitigation/ adaptation measures and allows for comparisons. In conclusion, it supports risk informed decision making and allows for flexibility in the decisions of coastal planners regarding the level of risk societies are willing to undertake, compared with economic and social benefits and the preservation of ecosystem services (Ranasinghe, 2016; Ranasinghe et al., 2012).

In the last years increase in computational resources enables the expansive use of process-based models in larger scales and the exploration of the morphodynamic effects of climate change. In the context of managing a complex coastal environment under changing and uncertain pressures assessing the reliability of morphodynamic predictions becomes increasingly important.

1.2 Problem definition

Despite the continuous rise of computational power, computational time remains a very important limiting factor in probabilistic morphodynamic analysis. The latter generally demands more iterations than a traditional deterministic analysis. The use of crude Monte-Carlo simulations is possible in combination with a fast coastline model like Unibest-CL+ (Scheel et al., 2014), however pairing it with more computationally expensive models may require time that exceeds the scope of the project.

Additionally, engineering problems frequently relate to a range of timescales/spatial scales/processes that cannot be simulated using a single model. When a combination of different models is required to simulate the different aspects of the problem, the models can be interconnected either by means of aggregation, coupling, or by boundary conditions extracted from a model and used in another. For coastal engineering, the impact of proposed interventions on the coast should be assessed beyond the initial impact in combination with processes of shorter timescales (e.g., storms) and longer timescales (e.g., climate change, large scale interventions). A set of morphodynamic models, such as UNIBEST-CL+, Delft3D and XBeach, with different spatial and temporal applicability ranges (Figure 1.1) can be used to simulate the processes that act on different timescales and contribute to the evolution of the coastline. In the context of risk informed coastal zone management, the uncertainties present should be accounted

explicitly and propagated not only through the morphodynamic simulations but also through the aggregation process to enable quantitative assessment of shoreline position estimates under the effect of interventions.

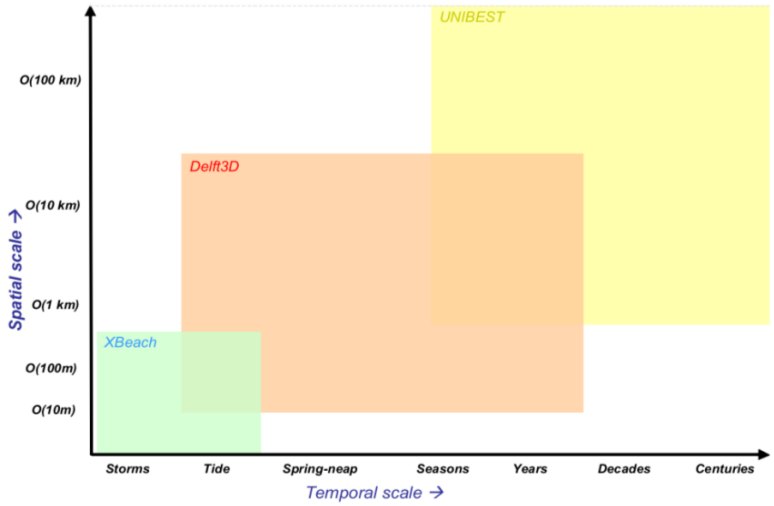

Figure 1.1: Common application ranges of coastal models, after A. Luijendijk et al. (2011).

1.3 Research objective and research questions

The aim of the present study is to gain insight in the statistical methods that can be applied together with processed-based morphodynamic models (such as Delft3D, Unibest-CL+) to quantify probabilities of coastline recession precisely and efficiently. Subsequently, we aim to suggest an approach for the aggregation of the resulting probabilistic model outputs from different timescales to systematically assess the effect of interventions on coastline recession risk/probabilities.

Obviously, it is not possible to study all nearshore processes that may affect coastal morphology, consider all the statistical methods and the total of the available coastal morphodynamic process -based models. The research domain of this project is therefore restricted by the specifications of case study, time and resources available. It is expected however, that the conclusions drawn from this study can prove useful for uncertainty quantification and aggregation for similar or more complex cases.

The methods will be applied specifically for a case study in South Korea, at a coastal stretch that is affected by erosion processes of varying timescales (episodic erosion, response to human interventions, climate change). Data, model configurations and knowledge from a recent research program (CoMIDAS) carried out by Deltares and the Korean Institute of Ocean Science and Technology (KIOST) for the area of interest are used in the present study. They foster a better understanding of the system and support the implementation of the proposed methods in the case study.

The selection of the above mentioned morphodynamic models, was based on the findings of the CoMIDAS research project (Deltares, 2016, 2017). The models were found capable of simulating the processes acting at Anmok beach on individual timescales as well as the required spatial scales. Nevertheless, these models could also be used with different schematisations to model different sets of processes and be applied to simulate different interventions than the existing, or processes on other coastal stretches, thus serving the general aim of this project.

Based on the problem definition and objectives, the following main research questions and sub-questions are formulated.

1. Which statistical methods can be used with process-based morphodynamic models (such as Delft3D, Unibest-CL+) to provide precise probabilistic estimates of coastline change on varying timescales in a computationally efficient way?

2. How can the probabilistic model results of the individual timescales be integrated to assess the impact of the selected mitigation/adaptation measures?

a. What are the steps in a generic approach for the aggregation of probabilistic model outputs to arrive to one probability distribution function of coastal recession?

b. What is the impact of the considered measures on the uncertainty of the coastline position for the case study of Anmok beach?

1.4 Research approach

The methodology followed to answer the research questions presented above will be presented in the following paragraphs. The approach consists of (1) literature review and data acquisition, (2) selection of the uncertain variables (3) application of the statistical methods for uncertainty quantification, (4) aggregation of the coastline change uncertainties from different processes/models and (5) analysis of the results of coastline change uncertainty evolution after the application of different adaptation/ mitigation measures. The general approach is presented in the flowchart of Figure 1.2.

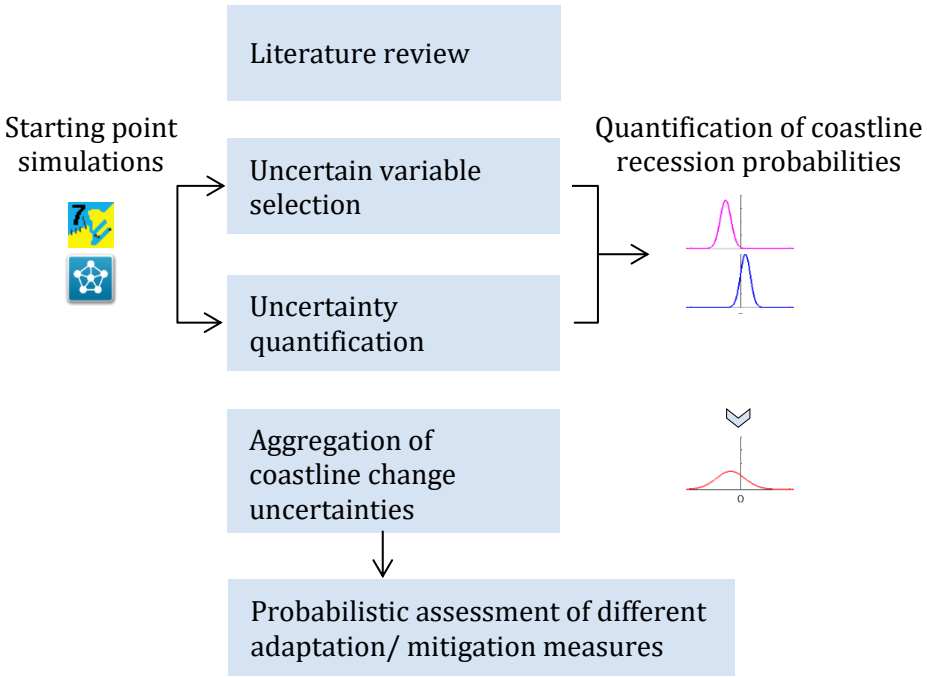

Figure 1.2: Flowchart of the approach followed to address the research questions

Phase 1- Literature review & data acquisition

As a first step a study of the available literature was carried out to obtain knowledge on the different aspects of the research problem (Chapter 2). The aim is to familiarise with the sources of uncertainty in simulations and the methods available for uncertainty quantification, the benefits and drawbacks of each one as they have been identified by other researchers. Among the reviewed methods, those considered more suitable to be used with coastal morphodynamic

models were selected. A study on the applications of uncertainty quantification in coastal morphodynamic modelling with process-based models and present aggregation frameworks was used to identify potential gaps.

An important aspect of this phase is acquiring more information regarding the case study. Model schematisations and scenarios selected to support the application of the statistical methods were selected and presented in this phase.

Phase 2- Selection of uncertain variables
Phase 2 includes the identification of the parameters that were included as stochastic in the uncertainty analysis (Section 3.2). Focusing on forcing and parameter uncertainty, sensitivity analysis and expert judgement were used to select those variables for which imprecision/value variability have significant influence on the model output. The range and distribution of each parameter were obtained from expert judgement.

Phase 3- Uncertainty quantification
Having selected the variables that introduce the uncertainty in process based morphodynamic model simulations, this phase centres on the quantification of the uncertainty as manifested in the model outputs (Sections 3.3, 4.1 and 4.2). Standard Monte Carlo and Latin Hypercube sampling, selected as the 'best candidates', were applied on UNIBEST-DL+ and Delft3D model schematisations of the case study area. In this phase, the applicability of the statistical methods with each model was investigated in terms of the precision of the results and the computational resources required to reach this precision.

Phase 4- Aggregation of coastline change uncertainties from different processes
Phase 4 focuses in the combination of the probability distribution functions of coastline change of individual processes/different timescales (as described in phase 3) on a single probability distribution function of coastal recession in the time horizon of interest (Sections 3.4 and 4.3). The application of a numerical convolution approach for the propagation of uncertainty through the aggregation process was investigated. The method was applied on the case study area to quantify the coastline change uncertainty from the combined effects of long-term processes, sandbar dynamics and a submerged breakwater-nourishment implementation.

Phase 5- Probabilistic assessment of adaptation/mitigation measures
In the final stage alternative interventions were simulated. The probabilities of coastline change with and without the interventions were quantified and combined with the coastline change probabilities of the autonomous evolution and the long-term wave climate variation. This enabled the assessment of the effect of each intervention on the coastline change uncertainty in a 20-year management horizon. Apart from the submerged breakwater-nourishment, two other designs were considered: a set of submerged-breakwaters-nourishment and an emerged breakwater-nourishment. Comparisons were made in terms of the location, dispersion of the aggregated probability distributions, the probability of several coastal change scenarios as well as in terms of the spatial scale of the intervention impact.

2

Literature Review

In the following paragraphs a short literature review will be presented to illustrate the present state of knowledge concerning the topics directly relevant with the research objective. An overview of the process-based models to be used is presented, the sources of uncertainty in morphodynamic models are introduced as well as statistical methods available for uncertainty analysis. Subsequently, an initial selection of methods to be investigated further regarding their applicability with process based morphodynamic models is carried out. Current knowledge and existing research in the quantification and aggregation of uncertainty in coastal engineering are presented.

2.1 Process based morphodynamic models

Coastal morphodynamic models, either empirical or process based, are widely used to predict or hindcast coastal development on different spatio-temporal scales by assessing values of different system behaviour indicators. Process-based models (Delft3D, Unibest etc.) couple different numerical modules to simulate wave and current propagation, hydrodynamics, sediment transport and bathymetry changes. They can give detailed information on the effect of processes on the morphodynamics of a coast and in extent on the impact of potential interventions in the littoral zone. Currently, process-based models are often designed to simulate natural processes on specific spatial and temporal timescales.

UNIBEST-CL+ (Deltares, 2011) is a 1D coastline model able to simulate morphodynamic change due to wave driven longshore sediment gradients at locations along the coast. The model does not account for cross-shore transport or complex bathymetry and is widely used to assess coastal impacts of structures. The small computational costs allow for simulations over large scales (~100km, 100 yrs), multiple scenarios and detailed schematization of the wave climate. Delft3D (G. Lesser et al., 2004) can simulate non-steady flow and transport from tidal and meteorological forcing and the resulting morphodynamics in 2 or 3 dimensions. It is capable of handling complex geometries and is applied to cases of small to intermediate scales (up to kms, yrs).

2.2 Sources of uncertainty in morphodynamic models

The output of coastal morphodynamic models depends on the forcing input time series, the model structure and several parameters which describe the simulated system. Inaccuracy and uncertainty of the output are inherent characteristics of morphodynamic modelling as the model itself is a simplification of the physical system. These simplifications lead to inaccurate representation of the present state; however, uncertainty is certainly more pronounced in predictive simulations.

There are different classifications of uncertainty in literature. In the present study a classification of uncertainty based on the source will be used, as presented by Scheel et al. (2014):

- *Forcing uncertainty*, stemming from natural variability, spatial and temporal, which characterise the forcing input series. Forcing uncertainty cannot be reduced by selecting

more refined models, additional data, or better calibration techniques. Forcing uncertainty becomes quite pronounced especially for long-term predictive simulations, where it is not guaranteed that historical data will describe adequately future forcing e.g., under the effect of climate change.

- *Parameter uncertainty* refers to initial condition imprecision, approximation of uncertain factors as probability distribution functions (statistical uncertainty) and use of parameters with unclear physical context either due to data or knowledge gaps, inaccurate measurement or recording etc.
- *Model uncertainty,* uncertainty is introduced by the approximation of the natural system in a model with inevitable simplifications, the schematization, accuracy limitations, unsuccessful calibration etc.
- *Unknown uncertainty sources,* including all the uncertainty sources natural and operational that have not yet been identified.

Some kinds of uncertainty can be decreased by additional data collection or further knowledge acquisition. Model uncertainty for example, could be reduced by developing more representative models that are able to approach better natural processes. However, extra data collection would result in additional cost, sometimes disproportionate to the achieved uncertainty reduction. Additionally, the more representative models are generally more expensive in computational resources, require larger input sets and involve a greater number of parameters, thus contributing to the output inaccuracy through higher parameter uncertainty (Loucks et al., 2017). Uncertainty sources that relate to natural variability cannot be eliminated. Lastly, unknown uncertainty sources cannot be confronted without prior identification.

It is evident that eliminating uncertainty from predictive model simulations is for the time impossible while reducing uncertainty is not always a practical choice. Therefore, it is wise for engineers to communicate the existing uncertainties in a quantified manner to enable coastal recession risk assessments and risk informed decisions concerning potential adaptation or mitigation strategies.

2.3 Statistical methods for model uncertainty analysis

According to Uusitalo et al. (2015), there are 3 ways to derive information about the uncertainty of a variable of interest, in this case coastline recession, to support decision making:

- Using field observation data, in this case coastline recession measurements.
- Probabilistic modelling, incorporating uncertainties into every stage of the modelling procedure,
- Performing uncertainty analysis on deterministic model outputs.

Coastline recession observations are however scarce and for the time being cannot facilitate a statistical analysis that would enable prediction of the future trends. Additionally, the widely used morphodynamic models have not yet been developed to accommodate probabilistic modelling. They provide a clearly deterministic output, characterised by uncertainty that must be evaluated separately by means of uncertainty analysis.

The techniques presented in the following paragraphs vary in terms of their conceptual approach, the computational cost and the power of the results. They have been applied in engineering problems of varying nature and compared in literature. It is generally accepted that there is no objectively 'best' method but the choice of the method to be applied should be based on the specifications of each problem and the resources available for the uncertainty analysis. The general principles of each method, their advantages and limitations derived from literature are presented below.

2.3.1 Probability tree

In the context of uncertainty analysis through scenarios, and for a limited number of possible values for each uncertain input variable/parameter, the uncertainty of the model output can be presented as a discrete probability distribution. Morgan et al. (1992) present the use of a probability tree as the method to define the discrete distribution of the output. A probability tree consists of branches -possible values of the uncertain variables, and terminal nodes that define the possible paths -the possible scenarios. The probability of each scenario can be calculated as the product of the conditional probabilities of the crossed branches.

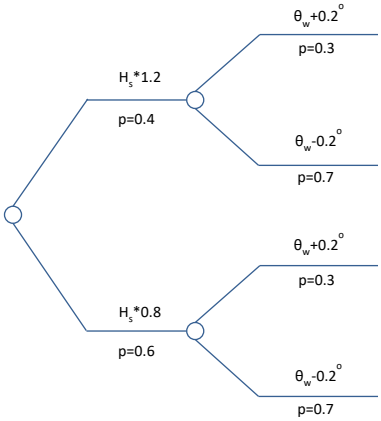

Figure 2.1: Example of a probability tree. Two branches (possible values) have been defined for each uncertain variable (θ, H_s). The terminal nodes define the possible paths -the possible scenarios. The probability of each scenario can be calculated as the product of the conditional probabilities of the crossed branches.

Probability tree is not a preferred method for uncertainty analysis in coastal morphology engineering models where the uncertain variables are mostly continuous rather than discrete. Nevertheless, when climate change effects are considered and variables such as the water levels are expressed as discrete scenarios, probability trees could be used in conjunction with other methods.

2.3.2 Analytical derivation

Uncertainty analysis on deterministic model outputs yields the distribution of the model output given a joint distribution for the input variables/parameters. When the model structure is simple, and equations are relatively linear this can be achieved analytically. Numerical models like Delft3D are constructed to approximate numerically the solution to complex equations simulating natural processes. Therefore, deriving the probability distribution of the outcome analytically is not possible in this case, and simulations using sampling techniques have to be used (Kurowicka et al., 2006).

2.3.3 Standard Monte Carlo sampling

Standard, or Crude, Monte Carlo sampling technique, has a wide range of applications due to the advantages it offers. The technique involves generating a set of random scenarios for the uncertain input of a model using the prescribed probability distributions and correlation functions. Scenarios are subsequently fed to the model which generates a set of output realisations. These realisations are used as random and independent samples of the model output and the model output distribution can be estimated using standard statistical techniques (Morgan et al., 1992).

According to Klis (2003) the advantages of SMC method include ease of implementation, accommodation of the non-linearity of models and the different uncertainty distributions, and

lastly use of standard statistical methods to estimate the total of the statistical properties of the output as well as the precision of the output distribution without the need for any assumptions on its distribution. These properties constitute SMC technique a robust method for uncertainty analysis with complex non-linear models.

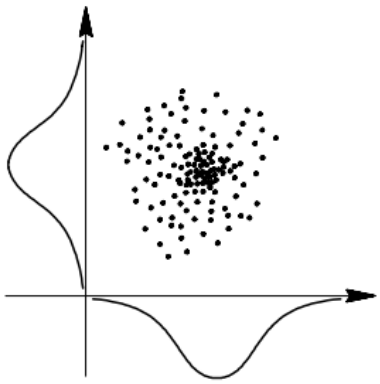

Figure 2.2: Cloud of points generated by Standard Monte Carlo, (Hurtado et al., 1998). The uncertain input space is framed from the probability distributions assigned to the uncertain variables.

However, the coupling of SMC simulations with complex morphodynamic models such as Delft3D for the time being presents obstacles related to time requirements. The generally large number of numerical simulations needed to arrive to a desired convergence level, can lead to a computational time that exceeds the budget of the project.

Keeping into account the advantages and the drawbacks of the Standard MC approach, aiming to the reduction of the required simulations for a model seems reasonable. According to Morgan et al. (1992) the number of simulations in a Standard MC approach decreases with a decreasing desired accuracy level. Additionally, sample size in an MC simulation depends on the demand on convergence in the extreme percentiles of the probability distribution.

Variance reduction techniques have been developed for the cases when the rate of convergence of the output distribution is slower than desired. Variance reduction refers to the statistical error in Standard MC results and exploits information about the structure of the model in an effort to reduce this error in the output distribution. The different techniques developed include Importance Sampling, Stratified Sampling, Latin Hypercube Sampling etc. Each technique is characterised by different limitations and thus needs to be adapted to each specific problem. Some of the variance reduction techniques will be briefly presented in the following paragraphs.

2.3.4 Latin Hypercube sampling

Latin Hypercube Sampling (M. D. McKay et al., 1979) is a variance reduction technique that aims towards equal, more spread-out coverage of the input space. The range of each uncertain input variable is divided in *n* equiprobable intervals and the variable gets a value randomly in each interval. The randomly selected values for the variables are grouped at random so that no replacement happens and the Latin Hypercube requirements are met, i.e. only one sample at each axis-aligned hyperplane (Kurowicka et al., 2006). The resulting sets of input are used as input in the numerical model to obtain the corresponding output realisations. Subsequently, distribution and statistical characteristics of the output can be estimated using standard statistical methods. **Midpoint LH** sampling is a variation of the standard method in which each variable takes the value of the median of each equiprobable interval.

LH sampling technique is concluded to perform better than Standard MC sampling for linear and monotonic systems or for systems with uncertainty dominated by one or two variables (Morgan

et al., 1992). For non-linear and/or non-monotonic system the efficiency of the sampling technique can reduce to the levels of Standard MC or lower. In general midpoint LHS performs better than standard LHS but attention should be paid when the model outputs are periodical. The drawbacks of LHS technique relate to determination of the sample size and precision assessment. More specifically, there is no method available to estimate the required sample size based on the desired accuracy before the application. Model precision can be estimated by repeating the model several times and assessing the variation in the cumulative distribution functions. This process can lead to an increase of the simulations needed in the end and defeat the purpose of variance reduction technique application.

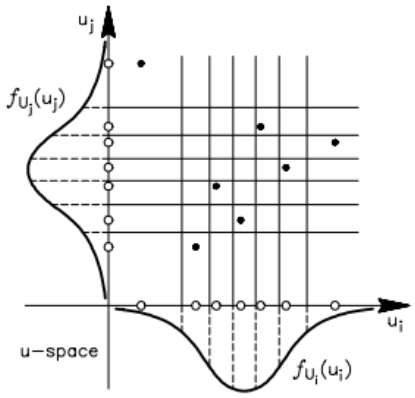

Figure 2.3: Cloud of points generated by Latin Hypercube sampling, (Hurtado et al., 1998). The uncertain input space is framed from the probability distributions assigned to the uncertain variables, divided into equiprobable parts -the strata.

2.3.5 Stratified Sampling

Stratified sampling resembles Latin Hypercube sampling. Similarly, the range of each uncertain input variable is divided in *n* equally probable intervals and the variable gets a value randomly in each interval. In stratified sampling each subset of the variable values forms a sample and is used as input scenario in the model.(Hurtado et al., 1998)

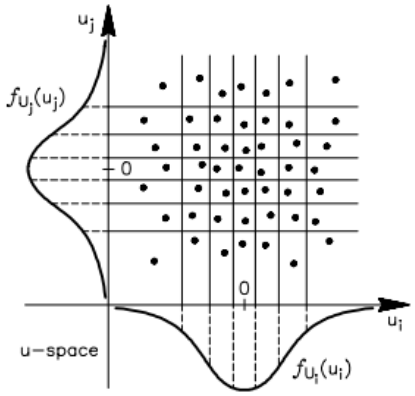

Figure 2.4: Points generated by Stratified Sampling (Hurtado et al., 1998)

2.3.6 Importance Sampling

When the end user is not interested at the output distribution, but only a part of it, Importance Sampling technique can be applied. This variance reduction technique aims at generating more points in the area of interest that will lead to the output of interest. This target is achieved by adjusting the probability distributions of the input variables so that the 'important' values are

encouraged. To avoid the bias in the output mean, the sampled values are corrected. Importance sampling finds frequent application in structural uncertainty analysis used in conjunction with a limit state function and a design point estimated using approximate analytic techniques. Morgan et al. (1992) highlight the potential of using this method to predict low likelihood, high consequence events, when the emphasis lies on the tail of the distribution.

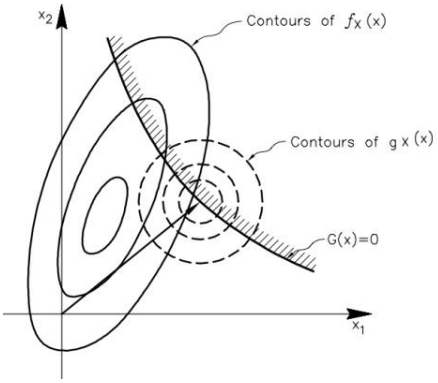

Figure 2.5: Importance sampling on a two variable space (Hurtado et al., 1998)

2.3.7 Directional Sampling

Directional Sampling technique was developed for multivariate distribution functions and is a method that, like Importance sampling, depends on the limit state function. In literature it is described as particularly efficient compared to SMC, for systems with almost spherical failure surface, as in this case only one simulation is needed to calculate the probability of failure (Bjerager, 1988).

2.3.8 Approximate Analytic Techniques

First Order Reliability Method (FORM), known also as First Order Variance Estimation is one of the approximate analytic techniques that use first or higher order moments of probability distributions to estimate the output uncertainty. FORM method is applicable with the assumption of independent and Gaussian distributed inputs and output. FORM makes use of the Taylor expansion and more specifically the first order terms to express the deviation of the output from its nominal value in terms of the deviations of the inputs from their expected value (Beckers et al., 2017; Morgan et al., 1992; Villaret et al., 2016). In engineering problems FORM method is generally used to define the probability of a certain state of the system named 'limit state' and described by the 'limit state function' that distinguishes the 'Failure space' from the 'Safe space' (Figure 2.6).

According to the review of Klis (2003) and Morgan et al. (1992), FORM performs well when the function is smooth and close to linear in the region of interest and the range of uncertain variables is small. For a strongly non-linear model an even shorter range needs to be considered.

Second Order Reliability Method (SORM) utilises up to the second order terms in the Taylor expansion. Effectively, instead of linearizing the limit state function around the design point, a parabola is obtained. Using second order (or even higher) Taylor terms can improve the accuracy of the analytical approximation for nonlinear functions. However, using higher order terms of Taylor expansion can quickly increase the complexity of the algebra (Morgan et al., 1992).

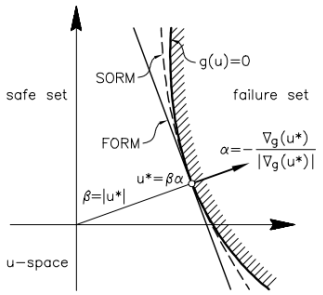

Figure 2.6: FORM/SORM methods (Hurtado et al., 1998)

2.3.9 Other methods for uncertainty propagation

Except from the above mentioned there are several other methods that could be used for uncertainty propagation through a numerical model. **Bayesian networks** make use of the Bayes theorem and are used to represent graphically a set of variables and their probabilistic relations. After the model is trained, observed evidence are used to update the joint distribution by conditioning on the observation (Nielsen et al., 2009). Applications of Bayesian networks can be found in literature (Kroon et al., 2017; Plant et al., 2011) and the method remains out of the scope of this study. **Response surface methods** or **meta-models** are approximate versions of more complex sophisticated models that can reduce significantly the computational cost when a large number of simulated e.g., for a SMC simulation for an uncertainty analysis (Morgan et al., 1992; Villaret et al., 2016).

2.4 Applicability of statistical methods

The selection of a suitable statistical method for the description of uncertainty propagation through numerical models requires the consideration of several factors that relate to the model, the method itself, the analysis requirements and the available resources. Morgan et al. (1992) provide a detailed inventory of decision factors for the selection of a statistical method. Assuming that for the models to be used, Delft3D, UNIBEST-CL+, model uncertainty does not dominate over input uncertainty, the criteria to be used for the selection of a method are presented below:

- Statistical method limitations that relate to the structure and the nature of the model: Can the method be applied to complex models, nonlinear, non-smooth relations? Does it accommodate the different uncertainty types or the uncertainty ranges that we want to propagate?
- Uncertainty analysis requirements: What is the aim and impact of this analysis? Does the analysis aim to calculate failure probabilities or the full output distribution? Is the emphasis placed on achieving a certain precision for a certain fractile, for the mean, for the tails? What is the desired level of precision to achieve?
- Available resources: how much computational time is required per computational run? What is the computational time and resources budget of the project?

Based on the above criteria, the initial analysis of the statistical methods, the models to be used and the uncertainties the following remarks can be made:

- The present study aims to gain insight in the uncertainty propagation through coastal morphology models. The desired output is the probabilistic estimate of shoreline position change for different processes. That translates to the distribution function(s) for one or more coastal positions. For different projects, the probability of 'failure' i.e. probability of exceedance of a particular threshold could be of interest but this is not the case for the specific thesis.

- Monte Carlo simulation is a robust method that can accommodate the nonlinearity and complex nature of coastal morphodynamic models as it does not make any assumptions in the output distributions or the model function. This method estimates the whole probability density function of the output and can accommodate space and time variability if expressed in the input variables. However, it becomes very laborious for long simulation durations. It is therefore recommended for coastline models with short simulation durations so that the required number of simulations is in the budget of the project. Such models are Unibest-CL. Delft3D computations even in 2DH are not expected to be efficient coupled with SMC.
- Applying Latin Hypercube Sampling on Delft3D could prove effective in reducing the required iterations/resources for the uncertainty analysis especially if only a few variables are considered uncertain. However, caution is recommended in the initial selection of the sample size and the subsequent precision estimation.
- For Stratified sampling with equiprobable strata the number of samples is related to the number of uncertain input variables and strata. For example, for n=3 variables and m=4 strata defined the number of samples is n^m=81. The steep increase in sample size for each extra variable/stratum renders the method unsuitable for the computationally expensive morphodynamic models with more than 2 uncertain inputs. Although Stratified Sampling could be applicable with models such as UNIBEST-CL+, the limited applicability on Delft3D excluded it from further investigation.
- Although the selection of variables to be considered has not yet been applied, it is expected that the uncertainty ranges will be large. Due to the large uncertainties, the complexity and non-linearity of the equations in Delft3D the application of moments methods is not expected to produce accurate results. Additionally, moments methods as well as directional sampling technique depend on the definition of the limit state function that is not always clearly defined in a coastal recession study. As mentioned before, these methods could be utilised if we wanted to estimate the probabilities of recession past a certain threshold (e.g., assessment of the failure likelihood of a setback line), however, generally in the uncertainty analysis for coastal recession modelling the desired outcome is the range of probable outcomes and not only the likelihood of a single realisation.
- Lastly, the method of probability tree paired with numerical integration could be used to arrive to an approximation of the probability distribution function of the model output. The accuracy of this method to estimate for a limited number of scenarios is expected to be low.

The conclusions presented above are summarised in the following table (Table 1).

	UNIBEST-CL+	**Delft3D (2DH)**
Monte Carlo	✓	× computational resources
Latin Hypercube	✓	✓
Stratified Sampling	× computational resources	
Importance Sampling	× require limit state function, suitable for smooth functions, (close to) linear in the region of interest, short range of uncertainty, not recommended for complex models	
FORM, SORM etc		
Directional Sampling	× developed for systems with (approaching) spherical failure surface	
Probability tree	× low accuracy for a limited number of scenarios	

Table 1: Initial selection of the statistical methods that will be investigated further per morphodynamic model

2.5 Combination of probability distribution functions

There are several methods listed in literature for combining probability distributions: convolution, moments method, Taylor's series, Monte Carlo, to mention a few (Fullwood, 1999). The most common way to combine individual continuous or discrete probability distribution functions as a union is by using the convolution operation. The convolution operation for two independent variables A,B continuously distributed with marginal cumulative distributions F_A,F_B respectively can be described as follows $(F_A * F_B)(z) = \int_{-\infty}^{\infty} F_A(z-y)dF_B(y)$ (Regan et al., 2004).

As mentioned in Regan et al. (2004) numerical evaluation of the convolution integral is preferred due to ease of implementation over analytical calculation. Numerical evaluation can be performed among others by discretising the variable range and subsequently calculating the convolution integral on a number of points, or through a Monte Carlo approach -by sampling from the individual distributions and performing linear addition of the realisations to obtain the aggregated probability distribution. Monte Carlo approach can also be used when there is a specific dependence between the uncertain variables aggregated with the assumption that the uncertainty of the random variables is fully described in the prescribed probability distribution functions.

2.6 Current progress in coastline change uncertainty quantification

Uncertainty quantification has found frequent application in fields like flood risk management and river morphodynamics. As far as coastal recession is concerned, probabilistic studies emerged just in the last decades with the effects of climate change becoming more pronounced on the coastal stretches worldwide and consequently stressing the need for uncertainty quantification in coastal morphodynamic modelling. Studies about the quantification of coastal morphodynamic uncertainty have had varying objectives and applications. Most studies however focused on input variable and parameter uncertainties due to limitation of methods available to quantify other kinds of uncertainties. One would also note that MC sampling techniques dominate in the literature while there is an effort to investigate the use of more computationally efficient models so that multiple simulations are possible.

Vrijling et al. (1992) compared long term coastal recession estimates derived using deterministic approach, sensitivity analysis approach and probabilistic approach on a single line model. An implementation of a probabilistic approach was presented, using Monte Carlo sampling methods to generate sets random input parameter values. Applying these sets of values to the structural function (transfer function) of the model allows for multiple realisations of coastline position and for the estimation of the distribution function of coastal change in time. Vrijling et al. (1992) highlighted the relation between the coastline change distribution function (standard deviation and skewness) not only with the characteristics of the input distribution functions but also with the transfer function as a function of time. For a coastal system immediately after an abrupt disturbance from the equilibrium, a strongly nonlinear transfer function will result in skewed coastline position distribution function with increased standard deviation. As the system approaches equilibrium again the coastline position distribution function will become more symmetrical and narrow. For the total probabilistic description of the coastline evolution in time, superposition of coastline models and shorter scale models is suggested.

The use of importance sampling technique is presented by den Heijer et al. (2012) in a probabilistic assessment of dune failure to counterbalance the necessity of multiple integrations of Standard MC in order to converge on small probabilities of failure. Fortunato et al. (2009) investigated the space and time variability of uncertainty in a 2D morphodynamic modelling system for an estuarine environment with an ensemble of simulations; varying each time several

input parameters as well as the transport formulae. The authors concluded that uncertainty increases with time scales and with larger morphological changes, while uncertainty is smaller in systems that evolve slowly.

Ranasinghe et al. (2012) developed the Probabilistic Coastline Recession model (PRC model) aiming for probabilistic assessment of SLR induced coastal recession, as a replacement of the Bruun rule that has been for decades the standard deterministic approach. In PCR model, coastline recession is defined as the landward movement of the foot of the dune, while the processes of SLR, storm erosion and dune recovery are assumed to affect the long-term movement of the dune foot. Water level and wave measurement (or hindcast) timeseries as well as one or more SLR scenarios are required as input. The input data are used to fit distributions to storm conditions (maximum wave height, duration, storm surge etc.), to water levels and subsequently Monte Carlo sampling method is used to generate a 100years storm timeseries. The coastal recession of every storm is calculated using an analytical wave impact model developed by Larson et al. (2004) that is preferred over detailed process based numerical models for dune erosion mainly for computational efficiency reasons. Allowing for dune recovery between the storms, the final dune foot position is estimated, and the long term coastal erosion is defined for this timeseries. Multiple timeseries are generated until the probabilities of exceedance over the user defined threshold converge.

The model does not account for effects of climate change other than SLR such as increased storm peaks and changing wave climate, while gradients in the longshore transport can be simulated as sediment sources/sinks. It was evaluated in Narrabeen beach, Sydney, Australia, and the long-term coastal recession probabilistic estimates were compared with the respective estimates using Bruun rule, showing the latter to be highly conservative. Jongejan et al. (2016) in a proposal of a framework to estimate the economically optimal setback line, used PCR model to derive the time dependent exceedance probability distribution of the setback lines in the same beach, assuming a moving setback line that is defined by the maximum annual coastal recession.

Monte Carlo Sampling approach coupled with coastline model Unibest-CL+ was presented by Ruggiero et al. (2007) and Scheel et al. (2014) in an initial assessment of long term coastline change in Long Beach Peninsula, WA and Holland coast respectively. The latter sampled values for the uncertain variables using assigned probability density functions while the former utilised the probability tree approach. The authors investigated the graphic opportunities for communication of uncertainty and proposed the exploration of different statistical methods for coastline recession risk quantification.

Villaret et al. (2016) applied First Order Second Moment method using Algorithmic Differentiation to produce a Tangent Linear Model of a river morphodynamic 2D model. The method was compared with LH sampling method and was found to complete the research in a fraction of the time needed for the sampling method. However, the FOSM calculated variances were found to deviate from LH calculated variances as the simulation time increased due to nonlinearity.

The process of aggregation of model results in a deterministic framework does not have a much-defined framework in literature and is dependent very much on the case study specifications, the target framework and the knowledge and understanding of the engineer. Aggregation of coastal of coastal recession probabilities relating to different timescales can be encountered in literature under two different approaches. The first one, encountered in the research of Jongejan et al. (2016) involves using a model that simulates coastline recession from different timescale processes (PCR model) paired with SMC to derive probabilistic results. Alternatively, different components of coastal recession corresponding to processes on different timescales are evaluated probabilistically and the aggregated probability distribution is estimated analytical using the

convolution operation (Wainwright et al.). The work of Vousdoukas et al. (2018), using a Monte Carlo approach to aggregate extreme water level projections from different processes, provided the inspiration for the use of the Monte Carlo approach in the coastline change aggregation framework presented in the present study.

As can be seen in this section, quantification of uncertainties is more common in fields of river engineering and flood risk. Uncertainty quantification in coastal recession estimates is an emerging approach. Although SMC approaches have been applied with simple morphodynamic models there has not been an analysis concerning the feasibility of application of other statistical methods on more laborious process-based models like Delft3D.

3 Approach

The chapter gives a short description of the case study and describes the model schematisations and parameterisations used in the present thesis. The methods used to quantify the uncertainty in the coastline position estimates from process-based models are presented. Lastly, the framework followed for the aggregation of these probabilistic results for the quantification of the uncertainty reduction due to interventions in the coastal environment is described.

3.1 The case study in South Korea

Information about the case study in Anmok Beach on the East coast of South Korea has been obtained from the outputs of the 5-year research program CoMIDAS (Coastal Modelling, Intelligent Defence and Adaptation based on Scientific understanding) carried out by Deltares and KIOST (Korean Institute of Ocean Science and Technology) and financed by the South Korean government. A summary of the most relevant findings is presented here, however for more detail the reader is referred to Deltares (2016), Deltares (2017) and de Boer et al. (2017).

The South Korean East coast consists of many sandy beaches connected by rocky stretches. Both natural processes and human interventions cause a dynamic evolution of the shoreline. Severe erosion has been observed on the sandy stretches threatening infrastructure and seaside developments.

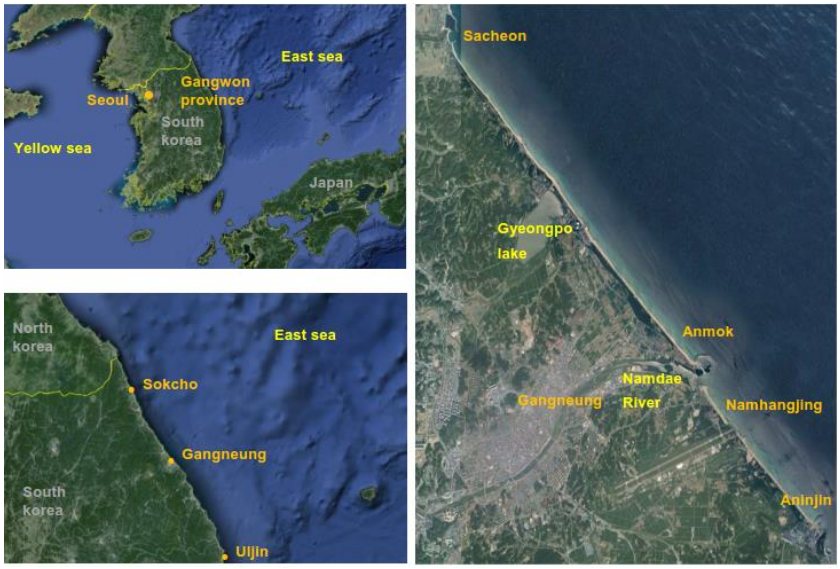

Figure 3.1: Gangwon province in South Korea (upper left), Gangneung city in Gangwon province (down left), Anmok beach near Gangneung city (right) (Deltares, 2017).

Anmok beach is located near the city Gangneung in the Gangwon province in South Korea, at the southern part of the 9.5-km long beach stretching among the port of Sacheon and Gangneung. The coastal stretch is straight, faces NNE and is characterised reflective, wave dominated, with winter swell and occasional typhoon events, while tide and currents have small amplitudes. Several

interventions implemented in the past decades have affected the morphodynamic evolution of the coast. More specifically, these interventions include the northern breakwater of Gangneung Port (constructed by 2002), the submerged breakwater at the southern end of Anmok beach (constructed by 2014) and the beach nourishment behind the breakwater (implemented by 2014).

Figure 3.2: Coastal interventions in Anmok beach, adapted from Deltares (2016)

The research carried out in the context of CoMIDAS project showcased the different physical processes that drive the coastal evolution in Anmok. Process based numerical models were selected to simulate the effect of the coastal processes thought to contribute to erosion on different timescales. The identified processes, the relevant timescales and the selected models can be seen in Table 2.

Physical process	**Time scale**	**Model**
Large scale coastline realignment due to wave climate variations	years to decades	UNIBEST-CL+
Large scale coastline realignment due to port construction	years to decades	UNIBEST-CL+
Coastline undulations due to bar dynamics	seasons to years	(Data analysis)
Effects of submerged breakwater construction and nourishment	seasons to years	Delft3D
Storm effects	hours to days	XBeach

Table 2: Numerical modelling framework for the identified coastal erosion drivers in Anmok beach (Deltares, 2017)

As a starting point, model schematisations and scenarios from CoMIDAS research program are used in the present study. Focusing on the effect of the long-term wave climate variations and the effect of the breakwater construction and nourishment, a UNIBEST-CL+ and a Delft3D model schematised and calibrated to capture the relevant properties were selected. These model schematisations were coupled with statistical methods aiming to quantify the uncertainties.

The following paragraphs present a short overview of the original model schematisations and parameterisations (Deltares, 2016, 2017) as well as a description of the modifications made for this project.

3.1.1 UNIBEST-CL+ model schematisation

The original UNIBEST-CL+ schematisation simulates the evolution of the coastline of ca. 9.5km between Sancheon and Aninjin, an area much bigger than the area of interest of the present study (Figure 3.3).

Figure 3.3: Overview of the coastal stretch modelled in UNIBEST-CL+, spanning form Sacheon to Aninjin port (Deltares, 2016). The area of interest for this present study is marked by the white line.

The wave conditions that force the model were derived by averaging long term wave data propagated from offshore to nearshore (to the 4m contour line) using a Delft3D-WAVE model. The wave climates used can be seen in Figure 3.4. The initial coastline and the 45 cross shore profiles defined were based on bathymetric survey data from 2015. The scenario simulates the effects of Gangneung port (at the south end of Anmok beach) and several other interventions at the edges and outside the area of interest for a period of 20 years. The submerged breakwater in Anmok beach (Figure 3.2) is not included in this simulation. The Van Rijn (2004) sediment transport formula was used with d_{50}=400μm, d_{10}=250μm and d_{90}=600μm. The run time is approximately 70mins for both the LT and CL modules of UNIBEST.

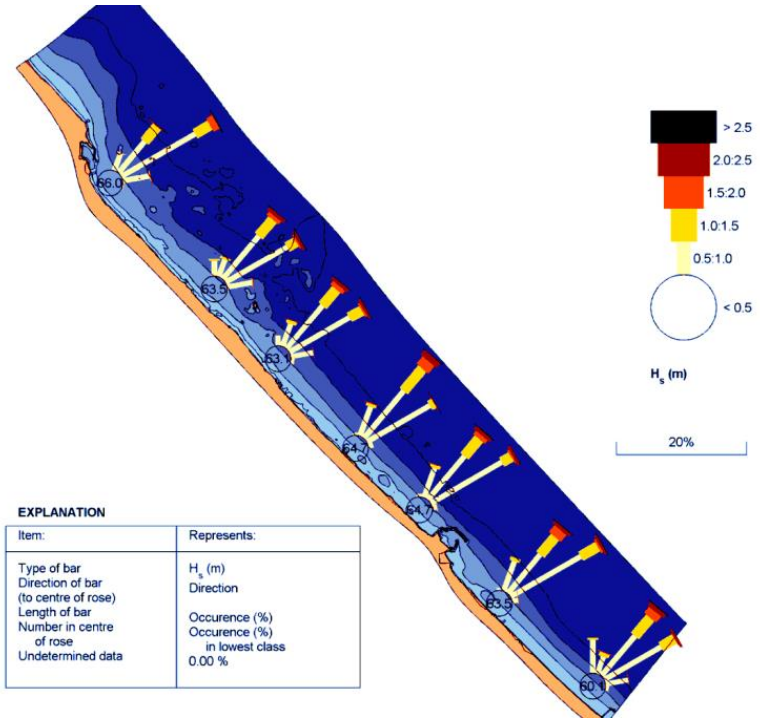

Figure 3.4: Nearshore wave climates used as boundary conditions in the UNIBEST-CL+ model (Deltares, 2016)

For the UNIBEST-CL+ simulation, run time reduction was considered in order to facilitate the Standard Monte Carlo simulations. Modifications regarding the number of cross-shore profiles considered, as well as the cross-shore grid cell size, were applied to the original model schematisation, and assessed based on the computational time reduction achieved as well as similarity of coastline change at the end of the simulations to that of the original schematisation.

In the changes applied, the full number of profiles and a dense grid resolution were preserved in the region of interest, while outside the region bigger changes were allowed. Table 3 and Figure 3.5 present an overview of the modifications applied and the results. It is clear that the changes applied in the grid cell size result in faster simulations than changes in the profile number. The model schematisation named 'mod 1' gave the best approximation of the final coastline combined with a significant decrease of the run time and was chosen to be used in the following phases of this project.

		Original schematisation	Mod 1	Mod 2	Mod3
Total number of profiles		45	45	24	24
Grid cell size	inside Anmok beach	1-2 m	4-8 m	1-2 m	4-8 m
	outside Anmok beach		6-12 m		8-16 m
Total run time		70mins	20mins	45 mins	10 mins

Table 3: Overview of modifications applied in the original model schematisation and the resulting run durations

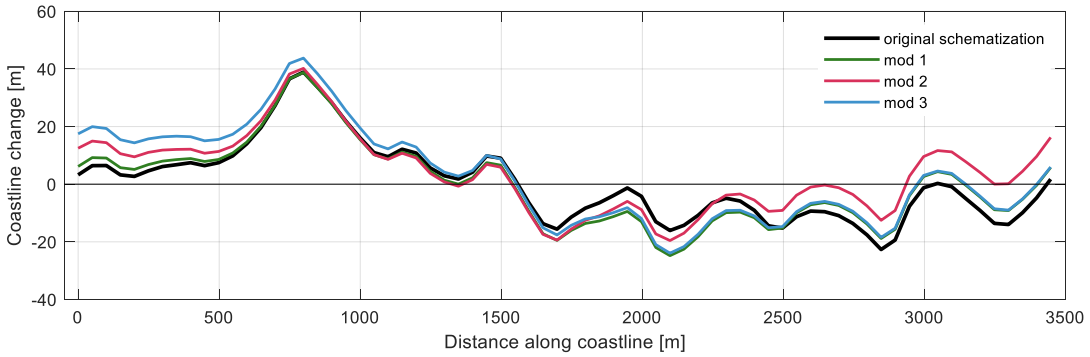

Figure 3.5: Coastline change at the end of the original and modified UNIBEST-CL+ simulations for the area of interest (Anmok beach). Positive coastline change indicates accretion.

Following the modifications described above, the value of d_{50} defined in Unibest–CL+ model (400µm) was changed to a value (450µm) for consistency across the models used.

3.1.2 Delft3D model schematisation

The scenario selected for Delft3d features Anmok beach, the Gangneung Port and the submerged breakwater and nourishment at the northern side of the port. Both interventions are indicated in the bathymetry and roughness files while thin dams are used for the port breakwater. The submerged breakwater is modelled with dimensions 250m x15m, crest level at -0.5m MSL and is located at 100m from the shore. The beach nourishment has a volume of 11000m^3 and is implemented during the timesteps 2 to 4. The modules WAVE and FLOW are used in parallel (online coupling), in 2DH mode, with communication intervals of 20min. The grid resolution varies from 5x3.5m close to the beach to 15x25m towards the lateral and offshore boundaries.

Timeseries of wave boundary conditions are applied uniformly to the open boundaries of the domain, derived from offshore measurements propagated to the domain boundaries using a SWAN model. Conditions that do not contribute significantly to sediment transport (H_s<0.5m and offshore directed waves) were not included in the timeseries. Timeseries of water levels are applied uniformly across the offshore boundaries to incorporate tidal forcing. The tidal forcing at the domain boundaries was derived using a larger FLOW model forced with astronomical boundary conditions and calibrated using local tidal station data. Neumann gradient boundary conditions are used on the lateral boundaries. Equilibrium concentration conditions are imposed at the inflow boundaries.

The van Rijn (1993) formula is used for the computation of the sediment transport with d_{50}=500μm. A morphological time scaling factor (MorFac=3) was applied to speed up the changes in morphology. The simulated hydrodynamic period is ~3.5 months, equivalent to 3 years of morphological changes using the 2015 initial bathymetry. The run time is approximately 160hrs with 6s timestep.

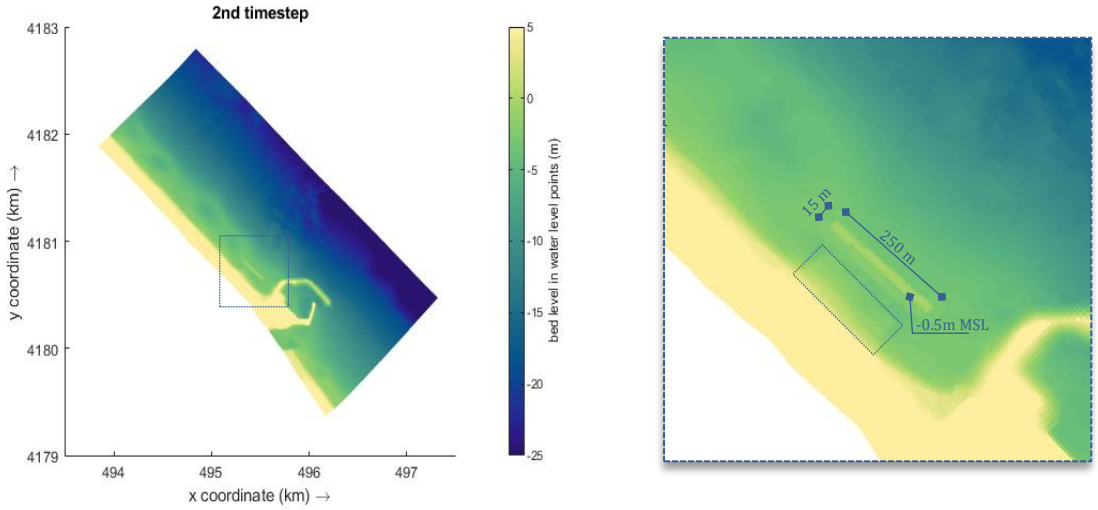

Figure 3.6: Spatial plot of bed level during the 2nd timestep of Delft3D simulation (right). Zoom in for the area of the interventions(left). The dimensions of the submerged breakwater and the location of the nourishment are shown on the figure.

To guarantee stability of the model during the probabilistic simulations the timestep was reduced to t=1.5s. Subsequently, input reduction was performed on the wave forcing conditions reducing the run duration to ~96 hrs. For more details about the performed input reduction the reader is referred to Appendix A. Lastly, the value of d_{50} defined in Delft3D model (500μm) was changed to the value 450μm, consistent across the models used.

3.2 Selection of uncertain variables

The type and amount of uncertainties that will be assessed in this project is limited both due to time constraints and limitations imposed from the statistical methods to be used. A selection of the uncertainty sources that will be considered is therefore necessary to be carried out aiming to discern those parameters whose variations affect the model output the most.

An overview of the methodology followed to identify the final set of parameters/variables that will be included as uncertain in the next phases of the current project is presented in the flowchart below (Figure 3.7). The selection of the parameters to be included as uncertain was based on literature, focusing on the study area, the uncertainty types we wish to explore (forcing and parameter uncertainty), and past uncertainty analyses on coastal morphodynamic models. Since model schematisations and configurations are already available for the case of Anmok beach, it is useful to consult the model input files as well. Expert consultation was used to further refine the initial set of parameters. Experience in coastal modelling for diverse cases and especially for the case of South Korea can support the exclusion of some of the variables whose potentially uncertain value has less significant impact on the model output. At this stage, estimates of the range and distribution of the variables were also obtained.

Subsequently a simple sensitivity analysis was performed to explore the relative impact of the value uncertainty of variables/parameters in the model output. The method used (One-at-a-time -OAT- method) includes varying one uncertain parameter value at a time, taking a high or low value, while keeping the other parameter values at the median value and evaluating the response

of the model output to these variations (Hamby, 1994; Loucks et al., 2017; Saltelli, 1999). Variables that were not described with uncertainty were considered deterministic and their value was considered to be true and accurate (without error).

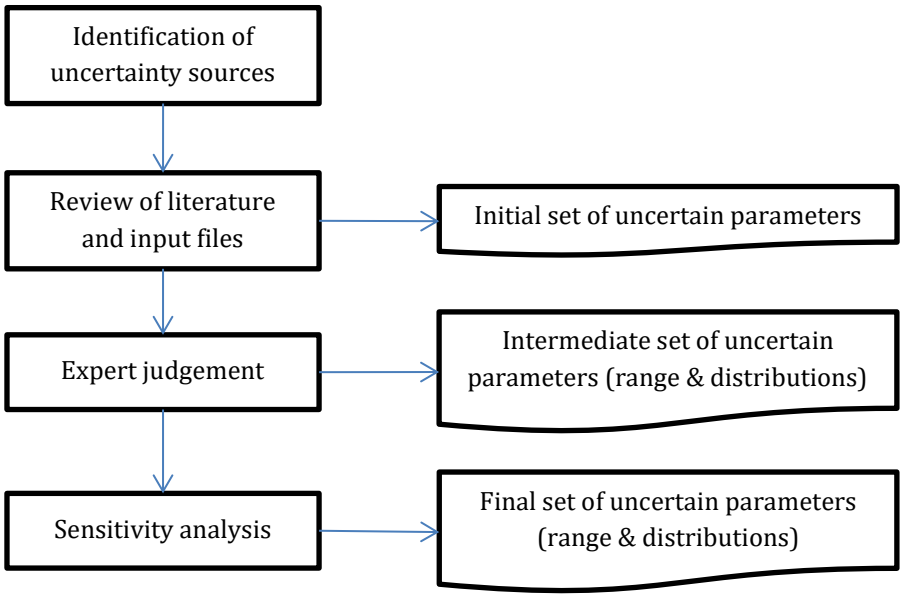

Figure 3.7: General approach for uncertain variable selection

OAT method was selected as a simple and easily implemented method for sensitivity analysis. It provides a rough estimate of the sensitivity of the model output relative to the median value of the varied parameter, not accounting for the entire parameter distribution (Hamby, 1994). Additionally, the method does not account for combined system sensitivity or correlation between the input variables and is generally recommended for linear models and narrow range variables (Saltelli, 1999; Vrijling et al., 1992). Although the assumption of non-correlation between the variables can be held valid for the set of variables considered, the morphodynamic models themselves are highly non-linear. As a result, OAT is used to assess the relative and not the absolute sensitivity of the model output to the varying input, that is to distinguish those variables whose uncertainty impacts model output the most, resulting to the final set of parameters/variables to be included as uncertain in probabilistic modelling.

The procedure described was carried out separately for each of the numerical models included in this research, Delft3D, UNIBEST-CL+, as the differences in the model input, structure and schematisation are expected to lead to different final sets of uncertain variables.

3.2.1 Selection of uncertain variables – UNIBEST-CL+

A sensitivity analysis had already been completed for the UNIBEST-CL+ model schematisation for Anmok beach developed during CoMIDAS program (Deltares, 2016). The sensitivity analysis investigated the effect of the variation of 3 parameters (H_s, d_{50}, θ) on the model output as well as the effect of using different transport formulas. The main assumptions from that sensitivity analysis were utilized in the present study. The three parameters (H_s, d_{50}, θ) were included in the new sensitivity simulations, with the same or updated ranges.

UNIBEST-CL+ was recommended for the simulation of the large scale processes acting on the coast, namely the reorientation of the coast due to the Gangneung port construction and the effect of climate change, regarding the changing wave climate, disregarding the effect of SLR or changing storm patterns (Deltares, 2017). In the present study the interest lies more on the effect of the changing wave climate due to climate change and that is reflected in the selection and the

ranges of the variables in the sensitivity analysis. The incident wave height is varied using an amplification factor on the original timeseries while the incident wave direction is varied applying a uniform addition to the timeseries. The ranges for these parameters (Table 4) have been derived from an explorative climate change impact assessment (Deltares, 2017) conducted for the same area using Global Climate Models for the intermediate and very high baseline emission scenarios (RCP 4.5 and RCP 8.5) in a hundred year period. The results suggest minor changes in the incident wave energy and a small reorientation of the yearly averaged wave climate (-1°) in a century. Accordingly, for a 20-year UNIBEST-CL+ simulation a variation in the average wave direction of ±0.2° was adopted.

The range for the median grain diameter (d_{50}) was selected in accordance with the range applied in the sensitivity analysis conducted during CoMIDAS program, derived from analysis of sediment samples from the area. Additionally, an extra parameter was introduced in the sensitivity analysis. The k_b, coefficient for bottom roughness is one of the hydraulic coefficients of UNIBEST-CL+. It appears in the definition of the Chezy friction coefficient, $C=18 \log (12d/k_b)$ (Deltares, 2011). Due to the wide range of values it can take, it can affect the transports significantly (see also de Bruijn (2005)). The range of k_b for a sandy coast was defined after expert consultation (B. Huisman, personal communication, July 25, 2018).

Parameter	Description	$P_{0.15}$	P_{50}	$P_{99.85}$
α_{Hs}	significant wave height amplification	0.8	1	1.2
d_{50} [µm]	median grain diameter	300	450	600
β_ϑ [°N]	incident wave direction addition	-0.2	0	+0.2
k_b [m]	coefficient of bottom roughness	0.02	0.1	-

Table 4: Parameter values for the sensitivity runs in UNIBEST-CL+

The values of these variables, as presented in Table 4 were varied according to the OAT method in the LT module of UNIBEST for the run configuration presented in Section 3.1.1 . The resulting transport rates were used as input for the CL module, providing in turn the varied position of the coastline at the end of the simulation. The results are presented only for the area of interest, Anmok beach, between the Anmok port northern breakwater (x=4.956*10^5 m) and the outflow of Namdae stream (x=4.93*10^5 m), (Figure 3.8).

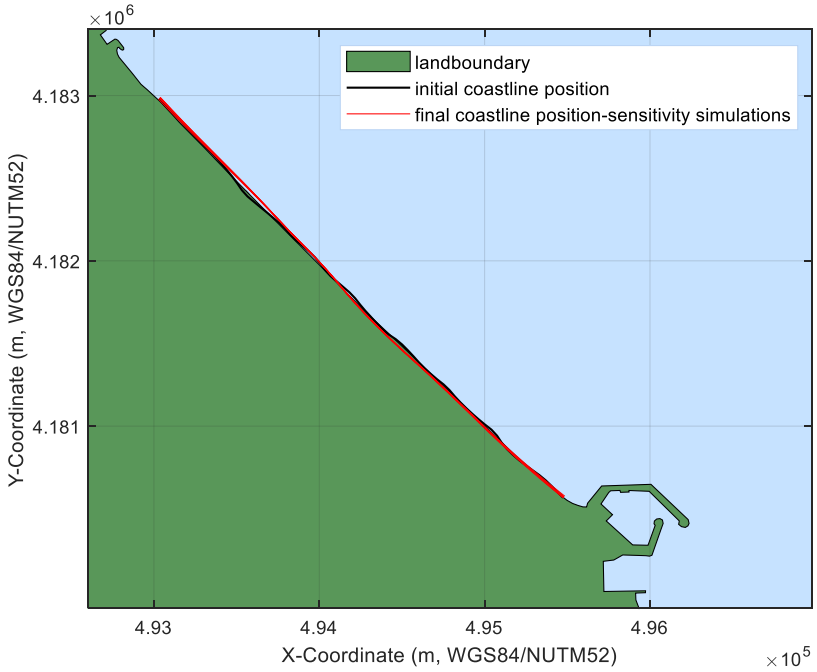

Figure 3.8: Spatial plot of the initial coastline position (black) and the final (red) coastline positions of the reference/sensitivity runs.

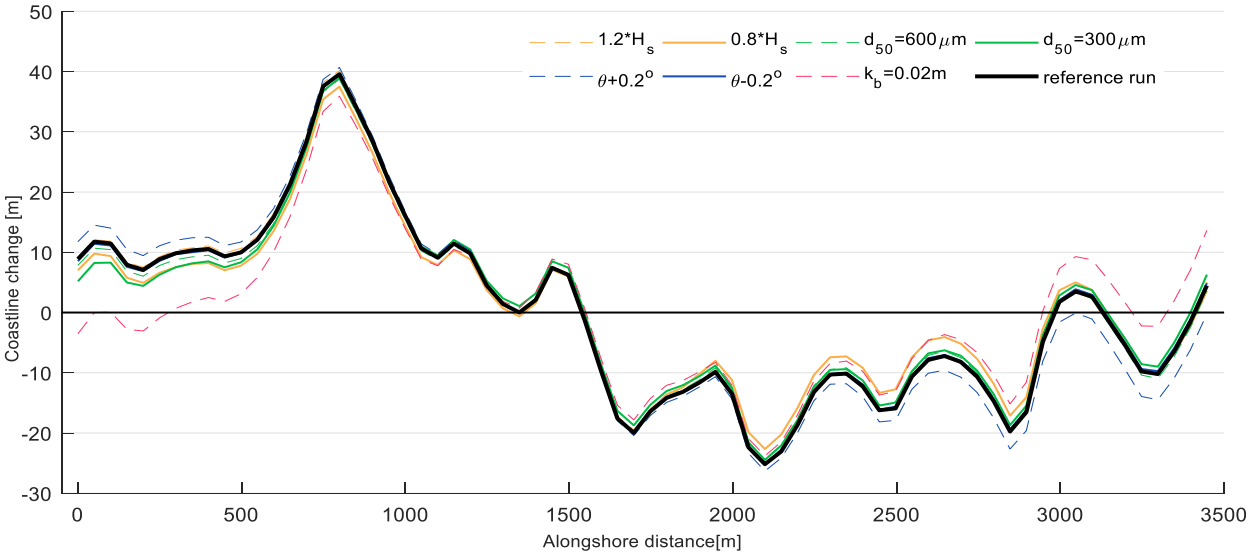

Figure 3.9: Coastline change at the end of the reference and sensitivity simulations for the points along Anmok beach. Positive coastline change indicates accretion.

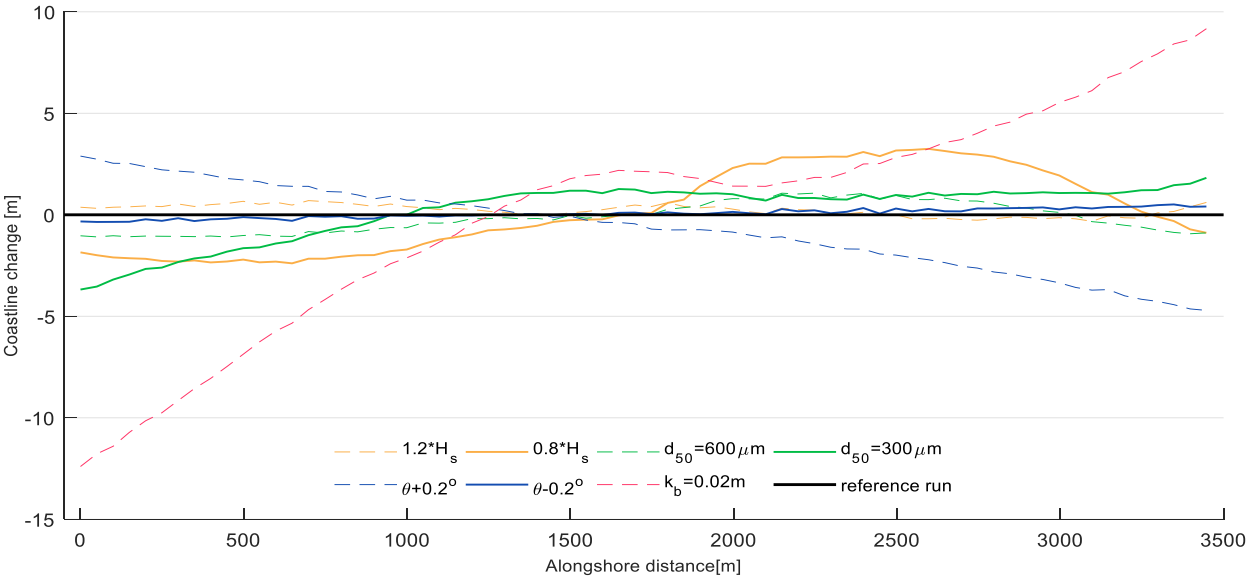

Figure 3.10: Coastline change at the end of the simulation for the different sensitivity runs relative to the coastline change of the reference simulation. Positive coastline change indicates additional accretion w.r.t. the reference simulation.

Both the reference and the sensitivity simulations result to the same trend of coastline movement: reorientation of the coastline with accretion at the northwest side of the simulated coastal region and erosion at the southeast side, suggesting that the coast is close but has not yet acquired the equilibrium position for the incident wave climate and the interventions present (Gangneung Port). The area of interest is modelled as a coastal cell, with longshore transport impeded by the port breakwater at the south end and by a shorter groyne situated at the north end. Negative and positive gradients in the longshore sediment transport at the two ends of the modelled cell create erosive and accretive disturbances locally. These disturbances grow over time forming the reorientation pattern observed and leading the coast towards an orientation in equilibrium with the incoming wave energy.

Varying the wave incidence angle for the sensitivity runs modifies the target equilibrium position of the coast leading to less or more reorientation. Additionally, variations in the significant wave height lead to changes in the equilibrium coastline position through the non-linear relation between significant wave height and resulting sediment transport. But more significantly, higher or lower values in H_s and the remaining sensitivity parameters change the speed at which the coast adapts to the wave climate. Reduced wave height/roughness coefficient or increased grain diameter are expected to yield smaller reorientations of the coast in the same simulation duration.

The results of the sensitivity analysis give rise to the following remarks:

- Variations of the variable values mostly reduce the coastline rotation compared to the reference situation except for the reduced wave incidence angle and the increased wave height.
- The model output shows increased sensitivity to variations in the k_b, wave incidence angle and incident wave height. Variations in each of these variables values trigger significant changes in different areas of the coast.
- The model output (coastline position change at the end of the simulation) displays spatially varying sensitivity to changes in the variable values. The sensitivity becomes more pronounced when moving from the centre towards the edges of the modelled coast.
- As can be seen in Figure 3.10, there are areas for which evaluating a variable at the mean value leads to more extreme (or more conservative) results than using the $P_{0.15}$ or $P_{99.85}$ values for the same variable. This can be attributed to the nonlinear processes that UNIBEST-CL+ simulates and the wide uncertainty range considered for the variables (Loucks et al., 2017).

Taking the above into consideration it is decided that all 4 variables (**H_s, d_{50}, ϑ** and **k_b**) are to be included as uncertain in the probabilistic analysis in the following chapters.

3.2.2 Selection of uncertain variables -Delft3D

Following the review of literature and the input files of the available Delft3D model schematisation for Anmok beach, and expert consultation (F. Scheel, personal communication, April 26, 2018), the list of variables to be included in the sensitivity analysis was defined.

The variables whose variability/imprecision is expected to influence the model output are the following:

- bottom roughness coefficient, C ($m^{0.5}/s$),
- median sediment diameter, d_{50} (m),
- significant wave height, H_s,
- peak period, T_p,
- Incident wave direction, ϑ(°N)
- Submerged breakwater height, defined in bathymetry

This set of variables was restricted even further so that sensitivity analysis becomes feasible for a model with long simulation time. The final set of variables and the values considered in the sensitivity analysis is presented in Table 5. Sensitivity runs were performed using a 3-year Delft3D simulation including both the port and the submerged breakwater, as described in paragraph 3.1.2 .

Parameter	Description	$P_{0.15}$	P_{50}	$P_{99.85}$
C [$m^{0.5}/s$]	bottom roughness coefficient	55	65	75
α_{Hs}	significant wave height amplification	0.8	1	1.2
β_θ [°N]	incident wave direction addition	-0.2	0	0.2
d_{50} [µm]	median grain diameter	300	450	600

Table 5: Parameter values for the sensitivity runs in Delft3D

Delft3D is an area model and does not provide coastline position output directly as coastline models such as UNIBEST do. Considering that coastline position is an indicator of interest in the current study, the Momentary Coastline (MCL) position was used to obtain the output variable of the model for the sensitivity analysis. The MCL represents the momentary horizontal position of the coastline from a reference line evaluated in a cross-shore profile using the volume of sand (A in Figure 3.11) between a landward and seaward boundary. In this study, the MSL+1m and MSL-1m contour lines were used as the landward and seaward boundaries respectively. This range was considered to enclose both the tidal range and the small storm surges incident in the area.

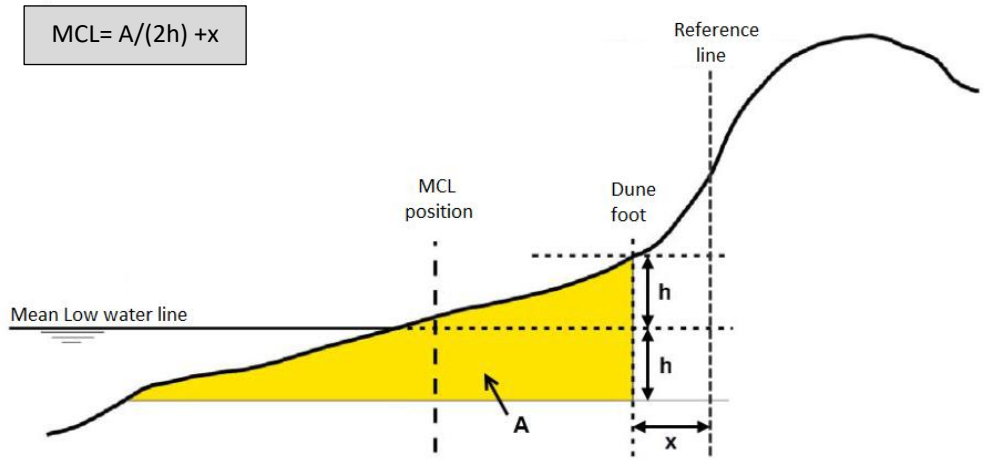

Figure 3.11: Definition sketch of the MCL, (Rijkswaterstraat, 2018).

The MCL approach was preferred over the simple contours as it allows for a single representation of the coastline, making it more suitable for comparisons. At the same time, it is less affected by local instabilities that can appear in the swash zone of Delft3D results. However, MCL might display steep shifts that do not correspond to simulated morphological features. This is especially the case when the beach evolves to a non-uniform shape, with multiple crossings of the upper and lower boundaries. In this case, the standard procedure of the MCL calculation would assume the most landward upper and lower crossings. In the present model domain, the simulated morphology yields complex contourline patterns for the area behind the submerged breakwater. Nevertheless, using a narrow range of contourlines to define the landward and seaward boundaries was found to minimize the sudden shifts in the MCL.

Lastly, the difference of the cumulative sedimentation volume in the model domain during a sensitivity simulation from the cumulative sedimentation volume in the model domain during the reference simulation was computed (Table 6). Although this indicator does not provide any spatial resolution as the previous one (MCL position), it shows the relative impact of variable values variation not only on the coastline position but also in the evolution of the active shore face.

Cumulative sedimentation for the model domain relative to that of the reference run								
Sensitivity simulation	high H_s	low H_s	high d_{50}	low d_{50}	ϑ +0.2°	ϑ -0.2°	high C	low C
Volume ($*10^5$ m^3)	1.23	-0.96	-0.19	1.85	-0.003	0.0003	1.3	-0.46

Table 6: Cumulative sedimentation at the end of the sensitivity simulations, summed over the domain, relative to the cumulative sedimentation volume of the reference run

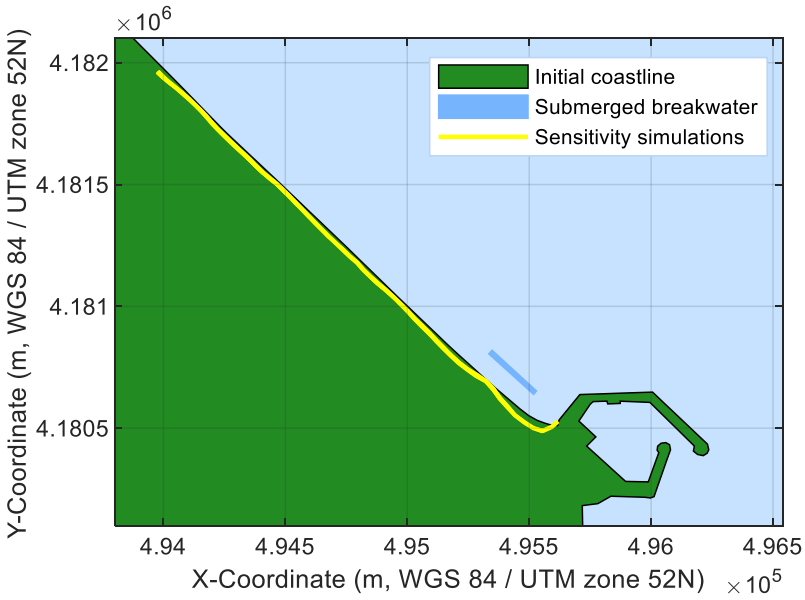

Figure 3.12: Spatial plot depicting the shoreline position at the end of the sensitivity simulations, the position of the initial shoreline and the position of the submerged breakwater.

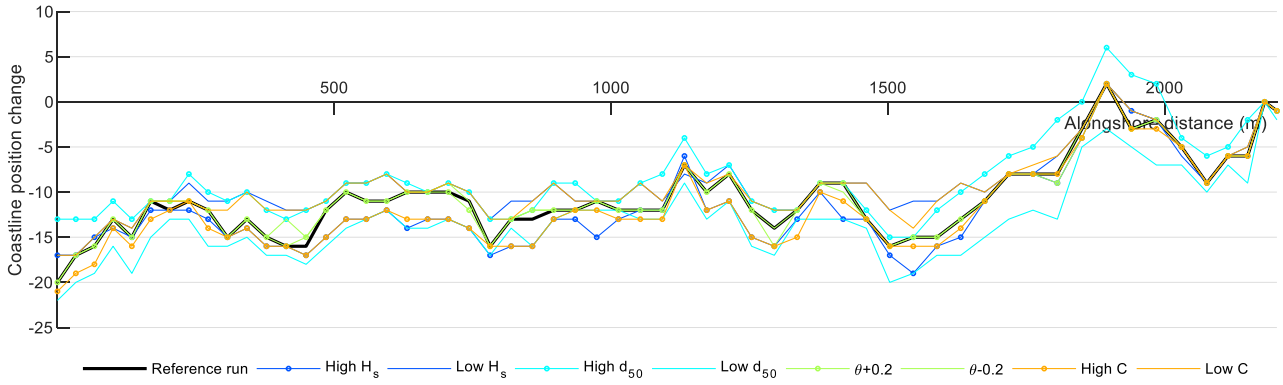

Figure 3.13: Coastline change with respect to initial coastline for the different sensitivity runs. The MCL approach is used between MSL-1m and MSL+1m. Positive coastline change indicates accretion.

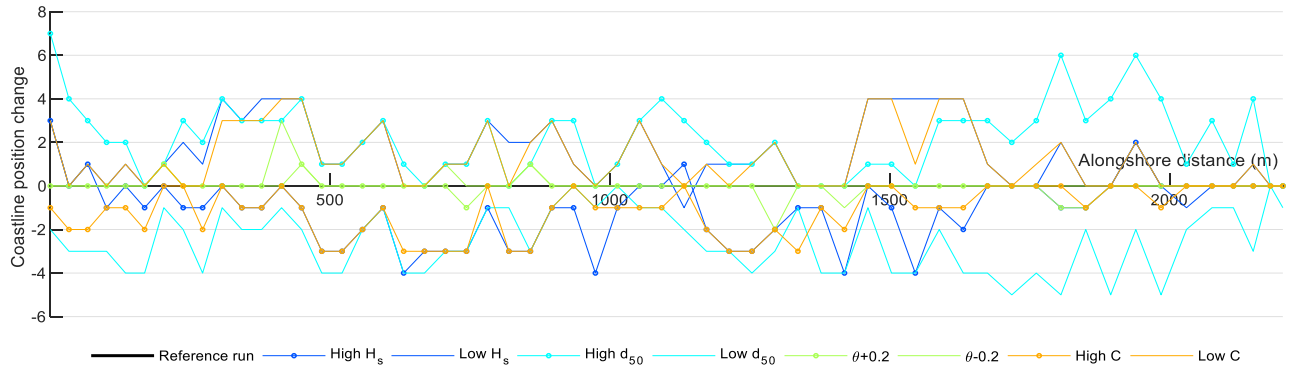

Figure 3.14: Coastline change for the different sensitivity runs w.r.t. coastline change of the reference simulation. The MCL approach is used between MSL-1m and MSL+1m. Positive coastline change indicates accretion.

The following remarks can be made based on the results of the sensitivity analysis on the described simulation of Anmok beach:

- Coastline position appears to be more sensitive to changes in the median sediment diameter, with higher grain diameters leading to more accretion/less erosion and smaller diameters leading to more erosion.
- Variations in the median grain diameter and the incident wave height cause the strongest changes in the morphodynamics of the domain as can be seen in Table 6.
- The variable, whose variation has the least effect on both the coastline position and the cumulative sedimentation in the domain, seems to be the incident wave direction. This is in contrast with the results of the sensitivity analysis on the UNIBEST-CL+ model schematisation, where coastline change proved very sensitive to the variations in the incident wave direction. This difference in the relative significance of parameters between the different model schematisations can be attributed to various reasons. The Delft3D model schematisation simulates a three-year period using wave timeseries derived from offshore wave measurements. On the contrary, the UNIBEST-CL+ schematisation simulates a 20-year period using schematised wave climate as forcing conditions. The smaller simulation period and the non-schematised forcing input could justify reduced sensitivity of the Delft3D output to the incident wave direction variations. The difference in the parameter significance could also be traced back to the different ways the relevant processes are included in the two models. In UNIBEST-CL+ the net sediment transport as a function of the coastline angle (derived from the LT) module is used in the coastline morphology simulation (CL module). On the other hand, in Delft3D alongshore sediment transports are evaluated for every wave condition and every timestep using the defined transport formula and are subsequently used to update the morphology. Differences like this, in the model structure and the modelling assumptions may lead to deviations in the relative significance of parameters between different models even when the same processes are simulated.
- The effects of uncertainty on the coastline position seem to be quite monotonic in this case. The reference scenario coastline is consistently framed between the coastline positions of the sensitivity runs. Additionally, opposite variations in the sensitivity parameters consistently give opposite results. However, the asymmetry of the sensitivity analysis' results around the reference simulation illustrates non-linearity in the response of the model to the variations in the uncertain variables.

The effect of the definition of the target variable (output variable) on the sensitivity results was investigated. Graphs of coastline change for the sensitivity runs were produced for different definitions of the coastline: MCL approach between the levels MSL [-2 2], the contourlines 0m MSL and MSL-1m. The relevant graphs are to be found in Appendix B. Although the results change as the target variable definition changes, the relative sensitivity of the output to the varied variable values is the same irrespective of the definition of the coastline.

From the variables selected, it is decided that $\mathbf{H_s}$, $\mathbf{d_{50}}$ and **C** are to be included as uncertain in the probabilistic analysis on the Delft3D simulations in the following chapters.

3.3 Uncertainty quantification

Already from literature review (Section 2.4) the statistical methods found to satisfy the applicability criteria were selected to be investigated further. Table 1 summarises the conclusions of this selection process. The application of statistical methods on the process-based morphodynamic models was carried out as described in Table 1 on each of the model schematisations described in Sections 3.1.1 and 3.1.2 for the uncertain input of 3.2.1 and 3.2.2 while assuming zero correlation.

The assumption of no correlation between the uncertain variables was adopted to simplify the next steps. This assumption is not strictly true for the significant wave height H_s and the incident wave direction θ, variables selected to be included with uncertainty in UNIBEST-CL+ simulations. Generally, these two variables are correlated, e.g., in every coastal stretch a dominant wave direction for the more energetic wave conditions can be found. However, in this specific case, where the incident wave direction is varied in a very restricted range, the assumption of uncorrelated variables can be considered valid.

Model output realisations constitute the empirical distribution i.e., samples from the yet unknown model output distribution (Kurowicka et al., 2006). It is expected that when the sample size *n* approaches infinity, the sample distribution converges uniformly to the true distribution (Glivenko-Cantelli theorem).

The performance of each statistical method on the different process-based models will be judged based on two aspects: the computational resources required, and the precision achieved. In this study, as with most engineering projects, the computational and time limitations set a ceiling to the number of samples that can be used. Precision of the model output distribution usually refers to a specific fractile of interest and is dictated by the demands for the future use of the resulting distributions, under the assumption of sufficient knowledge about the input uncertainty. In cases where the uncertainty distribution of the input variables is not adequately known (high statistical uncertainty), there is no point in demanding high precision or convergence in the extreme high or low probabilities as the statistical uncertainty will dominate the approximation uncertainty contributed by the iterative simulations. SMC sampling offers the tools for the quantification of the achieved precision. For LHS, the achieved precision can only be evaluated through comparison with results from different sample sets/LHS iterations or from the SMC application.

3.3.1 Standard Monte Carlo

As depicted in the flowchart Figure 3.15, Standard Monte Carlo involves sampling from the probability distributions of the uncertain input to obtain the samples of the model input vector. Those samples are pushed through the model to obtain an empirical distribution of the model output and to estimate the precision of the output distribution (Kurowicka et al., 2006).

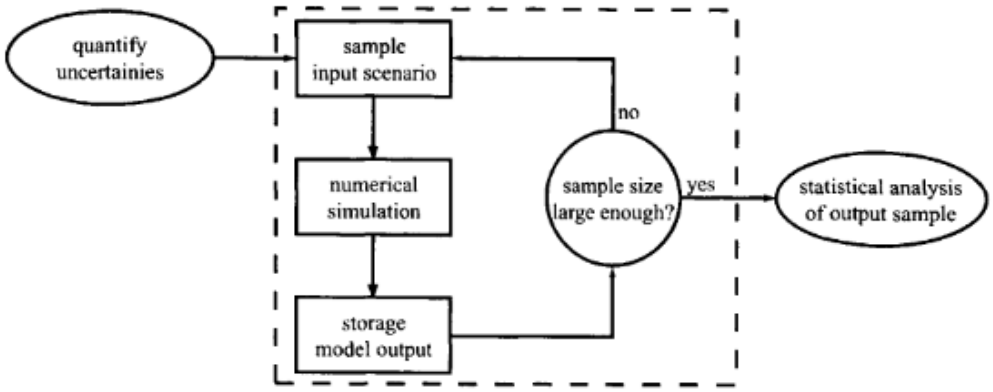

Figure 3.15: Overview of a Standard Monte Carlo Analysis (Klis, 2003)

The number of samples required in a Standard Monte Carlo simulation depends on the relative precision required of the output distribution. A first estimate of the sample size for this project will be acquired using a method presented in Morgan et al. (1992) in which the desired precision is expressed as a maximum allowed deviation from an estimated percentile in meters of coastline change.

The first step of this method as applied in the research of Klis (2003) includes the definition of the target precision: the p percentile of coastal erosion to be computed should lie within a confidence interval ci with associated confidence level α. Subsequently, SMC is applied (50 samples), an initial set of samples of the output distribution is obtained and assuming normal distribution, the initial estimates of the model output mean (μ) and standard deviation (σ) are calculated. For the probability interval $2\Delta p$ that corresponds to the allowed confidence interval ci around the percentile p the required sample size m can be calculated as:

$$m = p(1-p)(\frac{c_\alpha}{\Delta p})^2,$$

where c_α is the interval in the unit normal distribution that encloses probability α and Δp defined as in Figure 3.16. The number of samples required is independent of the number of uncertain variables considered for a given standard deviation of the output distribution.

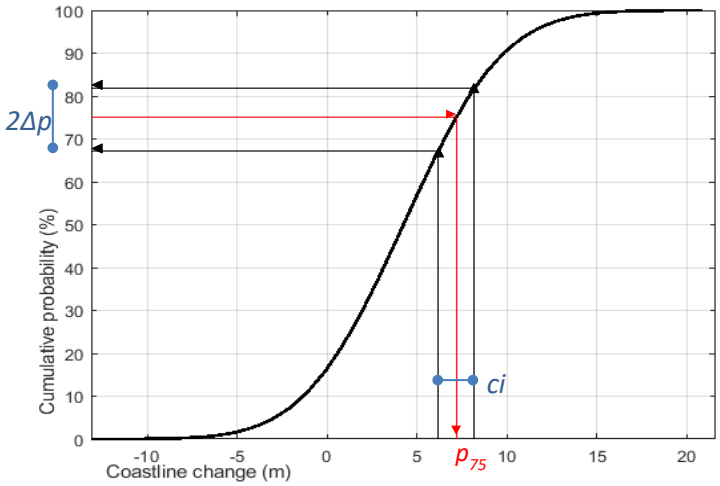

Figure 3.16: Estimating the required SMC sample size for an allowable confidence interval around p_{75} for a coastline point.

The required SMC sample sizes for every point along the coastline, for different percentiles of interest (p_5, p_{25}, p_{50}, p_{75} and p_{95}) and different error margins (±0.5m, ±1m, ±2.5m) with 95% confidence level were calculated following the steps described above for an initial set of 50 MC samples (Figure 3.17). The required sample size increases with higher precision requirements and wider ranges of possible coastline change –towards the edges of the coastal cell. It should be noted that a set of 80 SMC samples is expected to yield ci ranges up to 4m around the percentile estimates alongshore. A sample size of 1000 leading to ci ranges lower than 1m for the majority of the coastline points was selected.

Following the completion of the SMC sampling method, a check will be performed to ensure that the estimated number of samples m leads to the target precision. For m sorted values of the model output ($y_1 \leq y_2 \ldots \leq y_m$), the values y_i, y_k determine the confidence interval for the percentile p where according to Morgan et al. (1992):

$$i = mp - c_\alpha\sqrt{mp(1-p)}$$

$$k = mp + c_\alpha\sqrt{mp(1-p)}$$

In the case that the target precision is not met, the sample size can be extended easily, and the checks will be repeated.

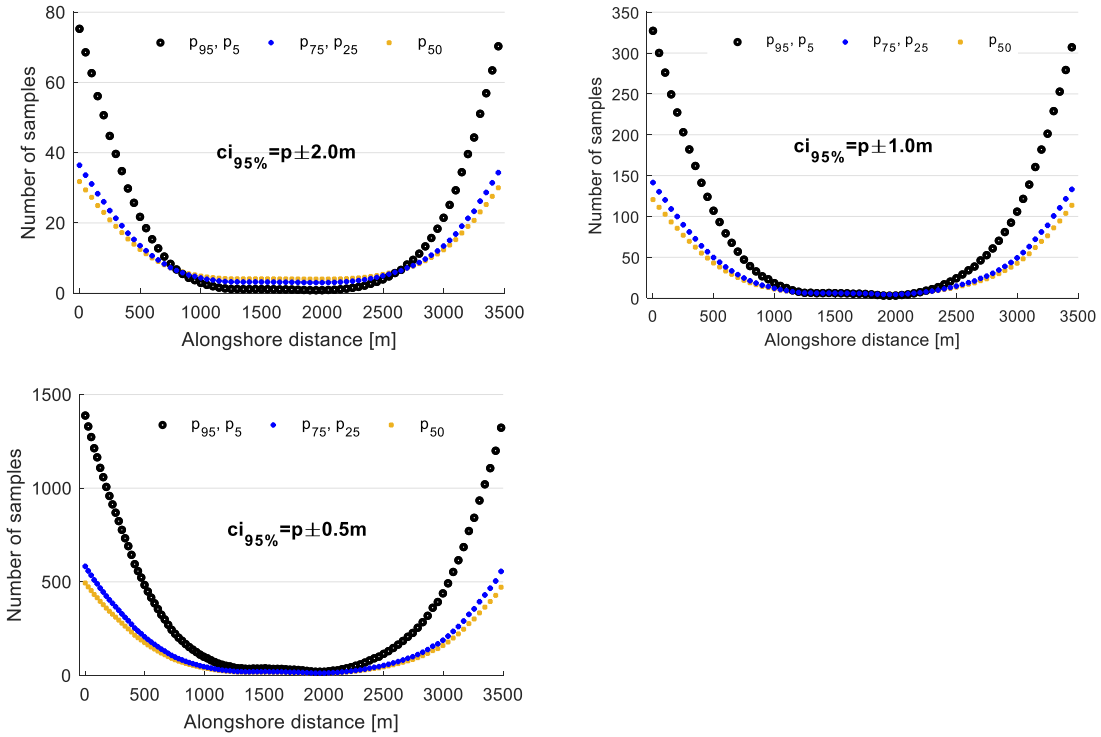

Figure 3.17: Required number of SMC samples for the points along the coastline calculated according to the method presented from Morgan et al. (1992) and employed from Klis (2003). Sample sizes computed for the different percentiles of coastline change and different confidence interval allowable ranges (4m, 2m, 1m). The confidence level is 95% in all cases.

3.3.2 Latin Hypercube Sampling

Latin Hypercube Sampling was applied by dividing the range of each uncertain variable into n non-overlapping equiprobable intervals (strata). The input vector for each simulation was created by sampling from a random stratum for each of the uncertain variables under the condition that every stratum was sampled once in the sampling process (Eamon et al., 2005). Input vectors were pushed through the model to obtain the empirical distribution of the model output.

LHS process produces random but serially dependent samples of the output distribution and thus the methods described above, used to estimate the cumulative distribution precision and sample size for SMC, are inaccurate for LHS, typically underestimating the precision achieved (Helton et al., 2003; Morgan et al., 1992). No generally applicable formulations exist in literature relating LH sample size with the achieved precision for the cumulative distribution. For n random variables, J. McKay (1988) suggests a sample size of $2n$, Iman et al. (1988) $4/3n$, while Manache et al. (2007) conclude that an even larger sample size may be required for adequate output uncertainty estimation. In the current study it was decided to perform the LHS on several different sample sizes. More specifically, sample sizes of 10, 20, 40 and 80 were selected. The samples were selected such that the bigger sample sets include the smaller ones. As a result, the computational resources required were reduced significantly as only 80 simulations instead of 150 were required for each morphodynamic model in total.

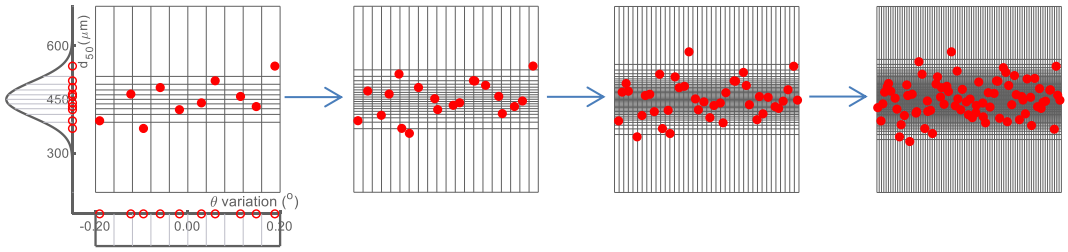

Figure 3.18: Example of sample selection for LHS. The right sample set (n=10) is included in the next sample set (n=20). That is included in the next sample set (n=40), which is in turn included in the left sample set (n=80).

In the absence of any relative formulas, the precision of the resulting empirical cumulative distributions was not quantified. Qualitative conclusions about the precision were drawn through comparison of the empirical distribution functions and percentiles resulting from the different sample sizes. Comparisons also were made between the empirical distribution functions and percentiles resulting from SMC sampling.

3.4 Multi-model coastline change uncertainty aggregation

Although information on the relevant processes needs to be obtained on individual time and spatial scales using the relevant models, the results on individual timescales can be aggregated to simulate the response of the system in a specific time horizon. The aggregation procedure followed in this chapter was based on the relevant framework developed during the CoMIDAS research program ('scenario-based' approach). The basic idea of the aggregation is that coastline change in a specific management horizon can be evaluated as the superposition of the independent coastline change resulting from the individual processes acting on different time-spatial scales. Figure 3.19 presents the main steps of the aggregation process: (1) appropriate model schematisations selection, (2) modelling of the defined scenarios and uncertainty identification, (3) result conversion to coastal impact, and (4) result visualisation (Deltares, 2017). The aggregation framework does not accommodate any interdependencies between the processes at the different timescales.

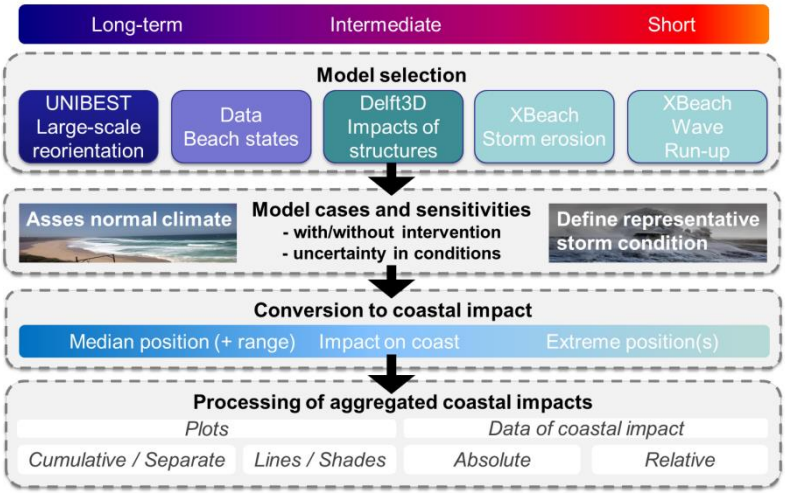

Figure 3.19: Aggregation approach steps (Deltares, 2017)

In the scenario-based approach the mean coastline change is estimated from the deterministic model outputs with all the variables estimated at their expected values. Uncertainty bandwidths around the mean coastline change are estimated using sensitivity analysis/ data analysis. The aggregation operation entails the superposition of the deterministic mean coastline change estimates as well as the superposition of the uncertainty bandwidths.

In the present thesis, this framework has been extended to account explicitly for the uncertainties propagated from the inputs, through the process-based models and the aggregation operation to the cumulative coastline change results. When the coastline evolution from individual processes is expressed in the form of probability density functions then superposition entails the linear combination of the individual pdfs, i.e. convolution of probability distributions.

A Monte Carlo approach was proposed to be applied for the convolution of the probability distributions. It requires sampling from the cumulative density functions (cdfs) of coastline change estimated using the uncertainty quantification methods (SMC, LHS) for each of the coastline evolution components and performing addition/subtraction of the samples to obtain samples of the unknown distribution of the aggregation. These samples form the empirical distribution, an estimator of the true distribution of the aggregated coastline change.

The Monte Carlo approach was selected as a simple and easily implemented method of probability distribution convolution. The method is very fast allowing for the use of large sample sizes and consequently high precision even at the tails of the aggregated distribution. Although Monte Carlo procedure can accommodate correlation between the sampled components, in this case it is applied under the assumption of independence of the aggregated processes.

The assumption of independence between the aggregated processes is not always true. For this specific application, it is assumed that the coastline evolution under the effect of the intervention is not affected by the long-term processes. Indeed, the evaluation of the net intervention impact as the difference in coastline change between a set of simulations with and without the intervention can be safely assumed to remove the effect of the initial bathymetry/coastline that is shaped by the longer-term processes. However, there are cases when interdependencies between the process become relevant and have to be accounted for in the aggregation process. One such case is explored in the results with the inclusion of the sandbar dynamics effect in the aggregation. Other cases include the effect of long-term processes on storm impact, and the effect of interventions on storm impact.

The steps that were followed in the aggregation procedure are presented below:

1) Identification of the time horizon, the variable and the spatial scale of interest. The selection of these basic elements will guide the aggregation process. There is a difference in the approach to estimate coastal recession in terms of coastline change in a coastal cell over a decade or in terms of cumulative eroded volume of the coast of Netherlands over a century. For small management horizons the effect of processes acting on significantly longer timescales may be omitted from the aggregation process.
   In this first step, a definition of any precision targets would also be useful as it can influence the decisions in the different steps of the framework: the selection of processes that will be included, the level of complexity of the models used, the statistical methods for uncertainty quantification and the variables that will be included as uncertain.
2) Identification and listing of the processes that drive the changes of the variable of interest across the time and spatial scales. With respect to coastline change, some of these processes are: relative sea level rise, climate change driven wave climate variation, initial morphodynamic impact to interventions, long term morphodynamic response to interventions, effect of sandbar dynamics, seasonal/long period coastline oscillations, storm impact, river (sediment) discharge fluctuations etc.
3) Delineation of the appropriate model schematisations to simulate the processes. The models selected must be able to simulate all the processes listed above on the corresponding timescales. At the same time, inclusion of a process effect more than once should be avoided. For this reason, one baseline simulation is selected, usually with the longest simulated period including one (or more) of the larger timescale processes. For

the remaining processes, their net effect is evaluated either by a single simulation or through comparison of the model output with and without the specific process.

4) Definition of the uncertainties that will be quantified. Literature review, expert judgement and sensitivity analysis can be used to determine the variables that introduce significant uncertainty in the model output and their distributions.
5) Quantification of the uncertainties on the individual timescales/processes. Statistical methods like the ones described in the current thesis (SMC, LHS) can be applied to obtain the probability density distributions of coastline change for the different schematisations selected.
6) Definition of the aggregation formula and aggregation of the coastline change probability distributions using the MC approach as described above.

4

Results

In this chapter the results from the implemented methodology are presented. Firstly, the results of the implementation of SMC and LHS on the Unibest-CL+ and Delft3D schematisations for Anmok beach are introduced. Subsequently, the implementation of the aggregation framework to estimate the probability distribution functions of coastline change in a management timeframe of 20 years is presented.

4.1 Uncertainty quantification for Unibest-CL

Four variables were selected to be included as uncertain in the uncertainty quantification process for the model 20-year simulation of UNIBEST-CL+ as described in paragraph 3.2.1 . The variables with their associated statistical characteristics are presented in Table 7. The statistical characteristics were derived from the sensitivity analysis ranges, assigning $p_{0.15}$ and $p_{99.85}$ (for the normally distributed variables) to the low and high values respectively.

Parameter	Description	Distribution
α_{Hs} [m]	significant wave height amplification	N (1, 0.067)
d_{50} [μm]	median grain diameter	N (450, 50)
β_{ϑ} [°N]	incident wave direction addition	U (-0.2, 0.2)
k_b [m]	coefficient of bottom roughness	U (0.02, 0.1)

Table 7: Uncertain input variables for UNIBEST-CL+.

Following the application of the statistical methods on each of the process-based models as described in Sections 3.2.1 and 3.2.2 , rescaled histograms were used for coastline change density estimation at the different points along the coast. From a total of 57 resulting probability density and cumulative distribution plots of coastline change only 12 will be presented. These correspond to the different cross-sections selected from a cross-sectional grid (Figure 4.1). The grid allows for higher resolution -denser cross-sections- in the areas close to coastal interventions. The distance between the considered cross-sections varies from 130m for those located near the port, to 530m for those at the northern end of the coast.

Additionally, different percentiles (p_5, p_{25}, p_{50}, p_{75}, p_{95}) were chosen to be computed as measures of central tendency and dispersion of the model output sample without any underlying distributional assumptions.

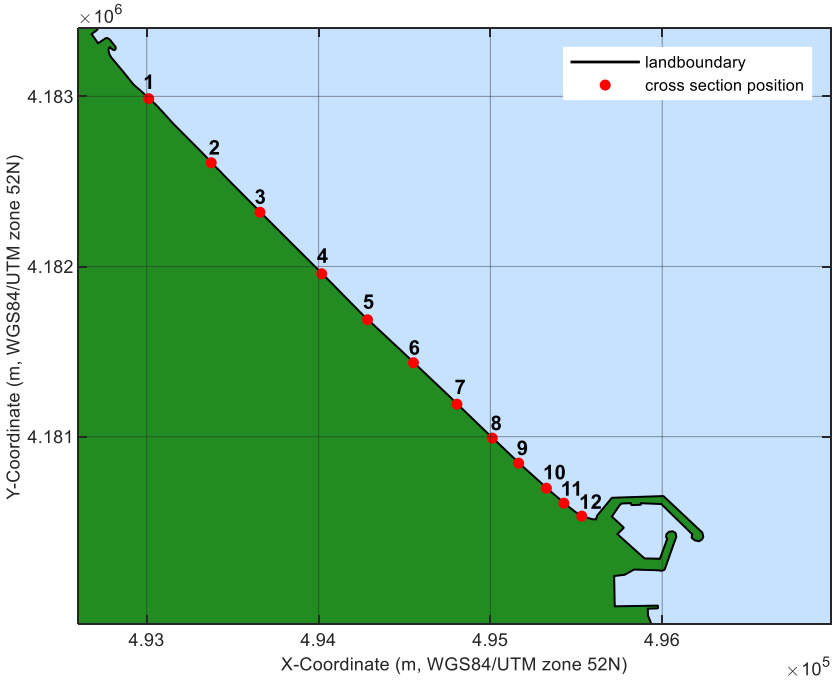

Figure 4.1: Spatial plot of Anmok beach. The markings show the location of the cross-sections for which results of the statistical methods' application on UNIBEST-CL+ application will be presented.

4.1.1 Latin Hypercube Sampling

Sample sets of four different sizes were selected for LHS; n=10, n=20, n=40 and n=80, with the smaller sample sets being subsets of the larger ones. Each sample vector includes one value for each of the four uncertain variables, sampled according to the Latin Hypercube requirements, and was used as input to the model simulations. All other input variables/parameters were treated as deterministic and used with a fixed, 'true' value in the model. The dependence between d_{50}, d_{10}, d_{90} and d_{ss} was accounted for; fixed coefficients were used to vary the diameter percentiles according to the sampled median diameter values. In Figure 4.2 2D projections of the cloud of points sampled by Latin Hypercube can be seen for n=10. The projections for the different sample sizes can be found in Appendix C.

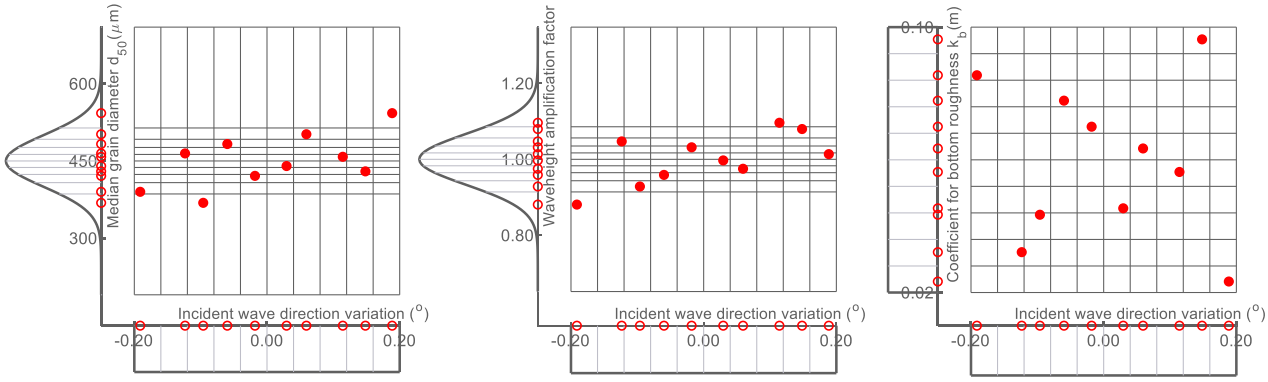

Figure 4.2: 2D projections of the cloud of sample vectors (red filled dots) generated by LHS for Unibest, (n=10). The sampled probability distributions of the variables (median grain diameter, wave-height amplification factor, coefficient for bottom roughness) have been plotted on the sides along with the sampled values from each variable (red circles).

The sample vectors created with LHS were used as input for the UNIBEST-LT module and the coastline change realizations were computed for every point along Anmok beach using the

UNIBEST-CL module. Probability distribution plots and cumulative distribution plots of coastline change for different positions along Anmok beach (as indicated in Figure 4.1) were computed based on the empirical distributions of the output for the different sample sizes used. The rescaled histogram approach was used for coastline change density estimation. Most of the resulting figures can be found in Appendix C, with the exception of Figure 4.3 below, which compares the performance of the different sample sizes.

Since there are no formulas that explicitly link the used sample size and/or the uncertain parameter statistical characteristics with the precision achieved through LHS, initially, the performance assessment of the different sample sizes will be conducted qualitatively. According to the Glivenko-Cantelli theorem, the probability distributions that resulted from the largest LH samples set (n=80) are a better estimator of the true probability distributions of coastline change in the different cross-sections. From Figure 4.3, comparing the results of the different sample sizes to those of the largest sample, it is clear that even the smallest sample size (n=10) can represent quite well the coastline change distribution for the points with the most restricted modelled coastline change range (Points 4 to 6). For the points closer to the edges of the coastal cell, where more diverse coastline change realisations are likely, there is a clear difference in the performance of the different sample sizes. Although all sample sizes produce a similar range of coastline change, the resulting shape of the distribution varies. Using too few samples, 10 or 20, leads to the distributions containing a number of peaks, overestimating the probability of specific coastline change realisations, while at the same time underestimating the probability of others. In contrast, both the shape of the distribution and the coastline change range originating from 40 samples are very similar to those of the biggest sample set.

Taking a closer look at the deviations of the smaller sample set percentile estimates (n=10, n=20, n=40) w.r.t. the largest sample set percentile estimates (n=80) along the coastline (Figure 4.5), we can see that indeed even 10 samples yield an estimate of the coastline change median within less than 0.5 m deviation from the 80 sample estimate. For the remaining percentiles, 40 samples estimates deviate no more than 1m from the 80 samples estimates, while 20 or 10 samples estimates deviate a maximum of 2m from the 80 samples corresponding percentile estimates. This indicates that being willing to sacrifice 1 or 2 meters of relative precision (keeping in mind that 80 is a practical upper limit in the number of samples used in this case) we would be able to reduce the computational time significantly, even to $1/8^{th}$ of the time required for the biggest sample size.

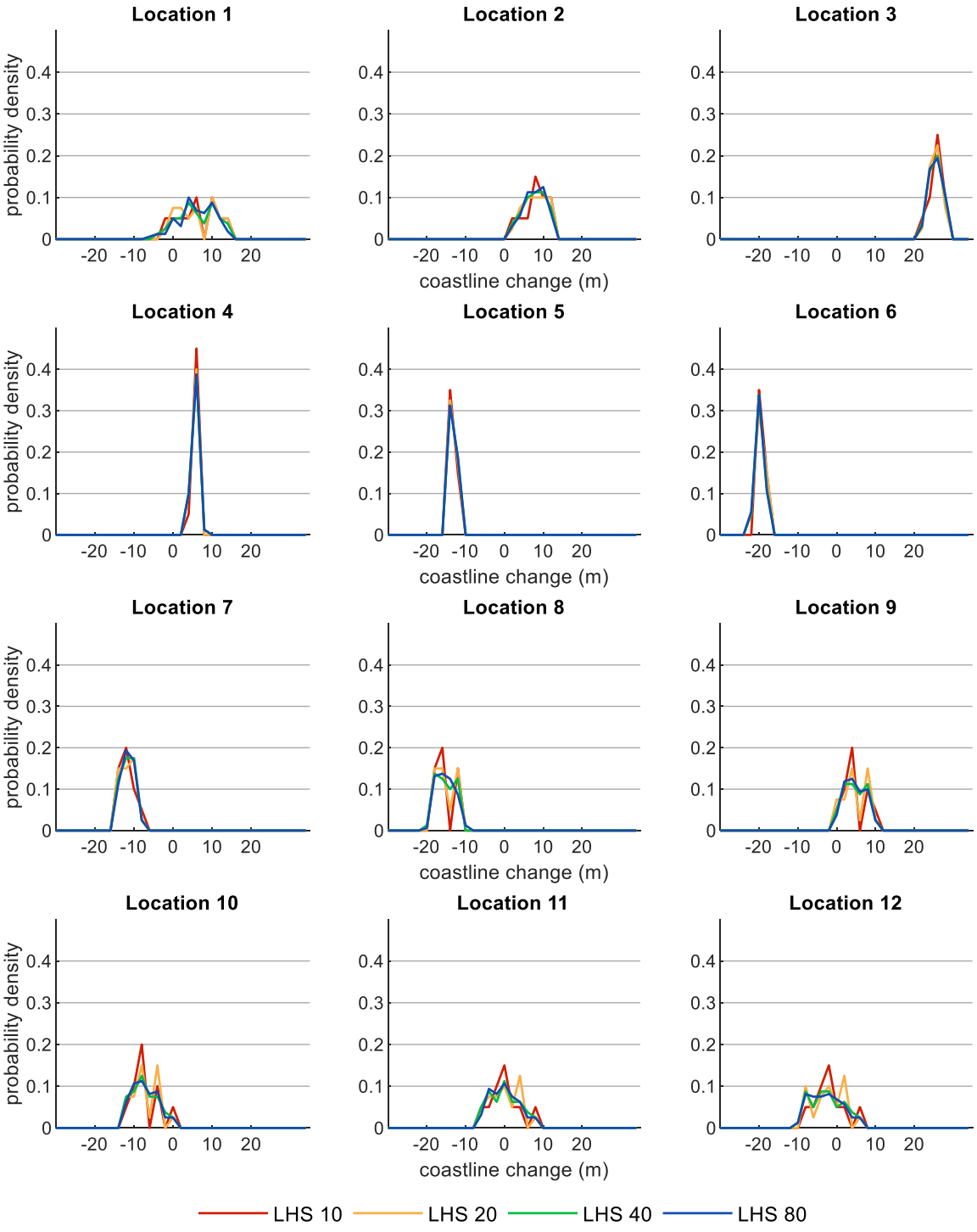

Figure 4.3: Probability density plots of coastline change at different cross-sections (as marked in Figure 4.1) along the coast for the different LH sample sizes (red: 10 samples, yellow: 20 samples, green: 40 samples and blue: 80 samples). Positive coastline change indicates accretion.

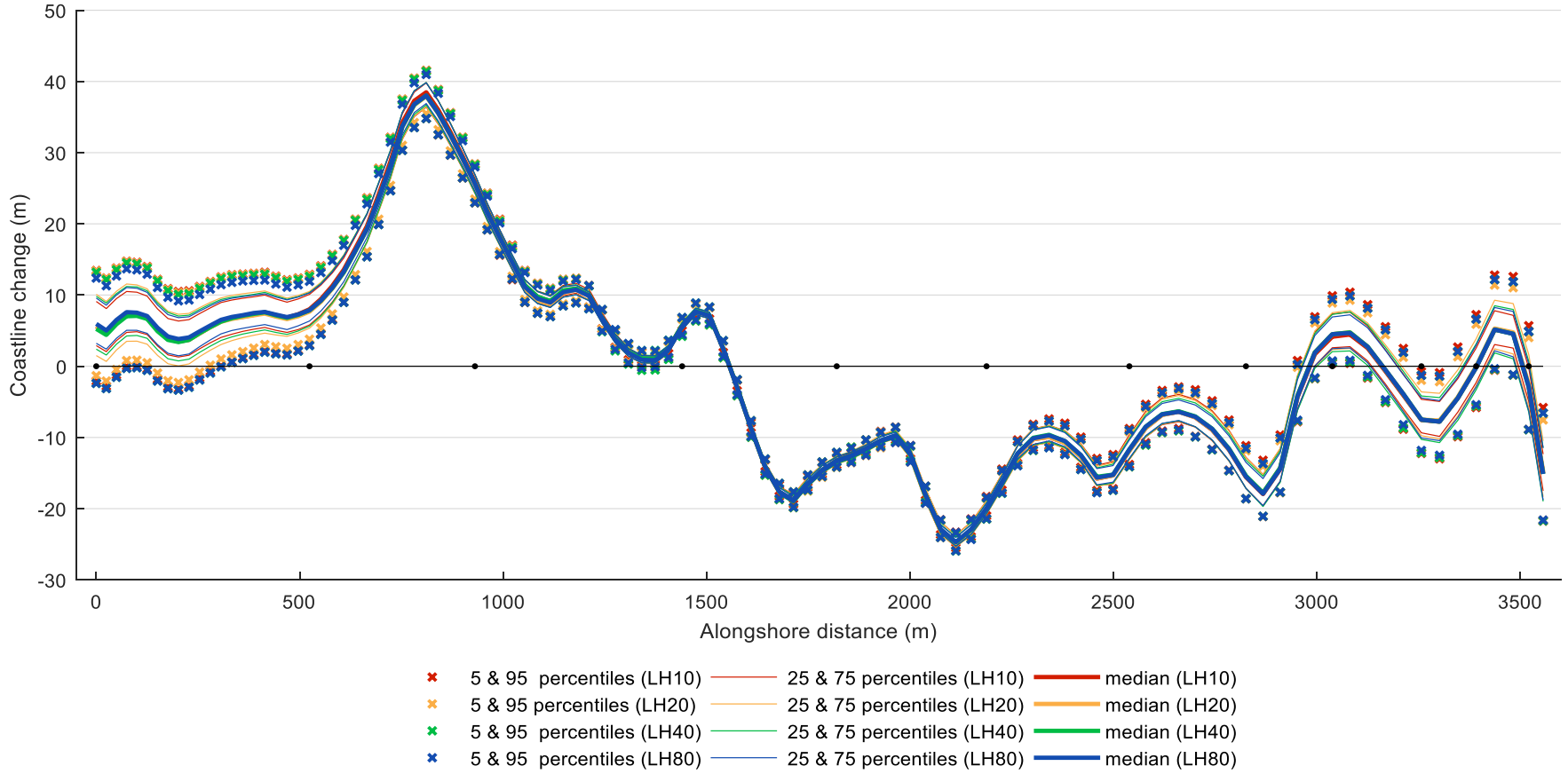

Figure 4.4: Alongshore distribution of coastline change percentile estimates for the different LH sample set sizes (red: 10 samples, yellow: 20 samples, green: 40 samples, blue: 80 samples). Positive values of coastline change indicate accretion. The black markings on the horizontal axis indicate the location of different cross-sections (points 1 to 12) presented in Figure 4.3.

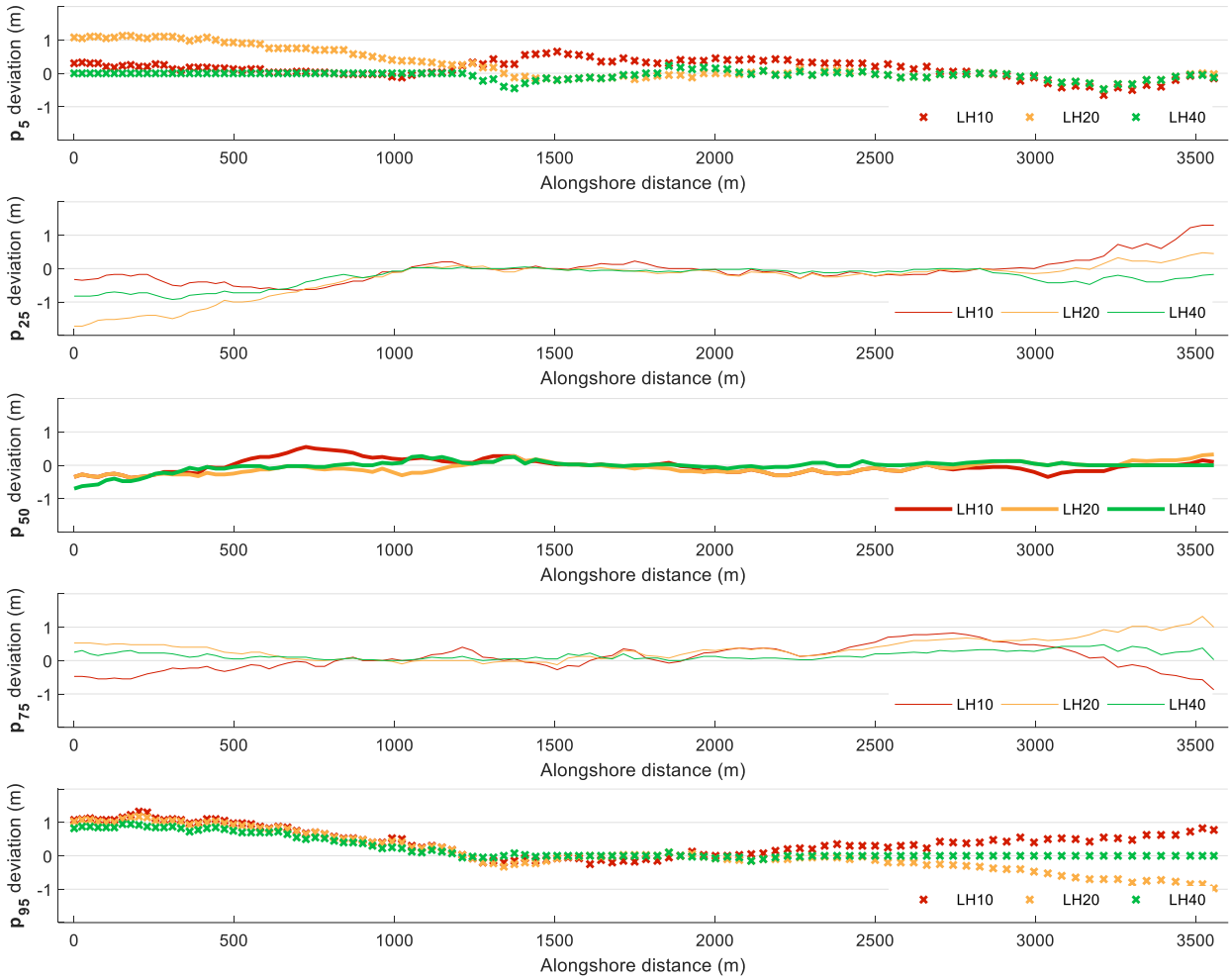

Figure 4.5: Deviations of coastline change percentile estimates using different sample sizes (red: 10 samples, yellow: 20 samples, green: 40 samples) from the percentile estimates of the biggest sample size (n=80)

To investigate whether the above observations can be attributed to a fast convergence of the model output or whether they are incidental to the specific sample set, the LH Sampling procedure was repeated 9 times. Figure 4.6 presents the resulting alongshore distributions of coastline change percentiles as estimated using the 10 LHS realisations with 10 and 80 samples. The results of the 10 LHS realisations for 20 and 40 samples can be found in the Appendix C. The dispersion of the percentile estimates is evident in both graphs. As expected, this dispersion is more pronounced for the more extreme percentiles than the median and grows towards the edges of the coast. Additionally, the percentile spread narrows for larger sample sizes, implying a better convergence of the empirical distribution function from larger sample sizes towards the true output distribution.

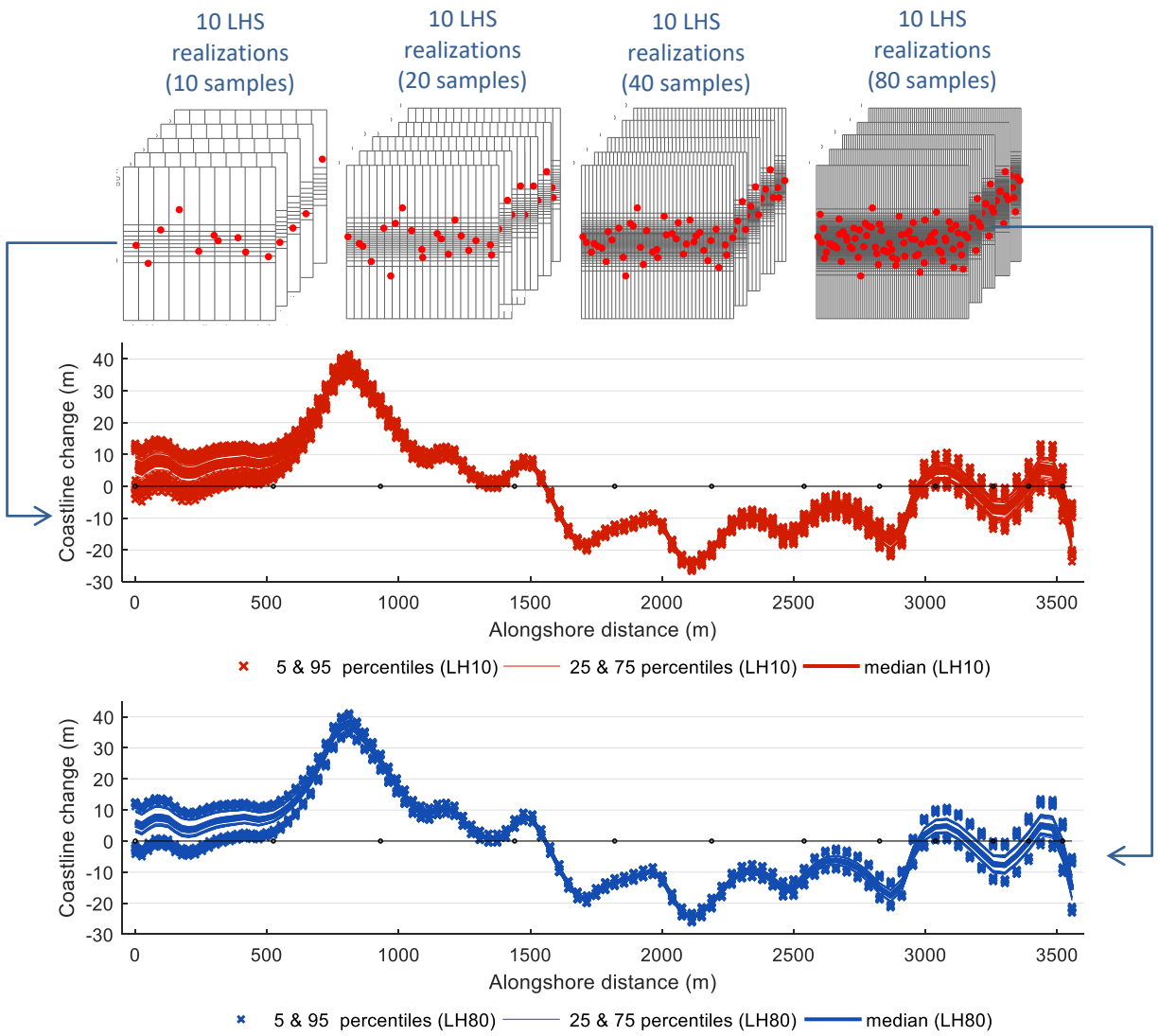

Figure 4.6: Schematic representation of the steps followed. 10 different LH sample sets were drawn for the different sample sizes (top). Alongshore distribution of coastline change percentile estimates as estimates from 10 LH sets of 10 samples (middle). The relevant graphs for the sample sets of 20 and 40 can be found in Appendix C. Alongshore distribution of coastline change percentile estimates as estimates from 10 LH sets of 80 samples (bottom). Positive values of coastline change indicate accretion. The black markings on the horizontal axis indicate the location of different cross-sections (points 1 to 12) for which the results were examined more closely.

The spread of the different percentiles derived from the 10 LHS realisations for the various sample sizes is illustrated in Figure 4.7. At the central part of the domain, where the potential coastline change range is more limited the percentile estimate spreads for all the different sample sizes converge to the minimum values, suggesting a monotonic relation between the uncertainty range and the convergence rate. At the edges of the modelled area the spread of the computed percentiles ranges from 1 up to 6 meters. This implies that the small deviations observed in Figure 4.5 are incidental of this specific sample set and cannot be attributed to the sample size related convergence.

Sufficient iterations of the LHS process could provide a statistical measure of the percentile spread, thus a measure of the achieved precision of the LHS for the specific model, the defined uncertainties and the considered sample size. However, this would raise the required model simulations (from 80 to 800 in this case), practically defeating the efficiency of the LHS technique.

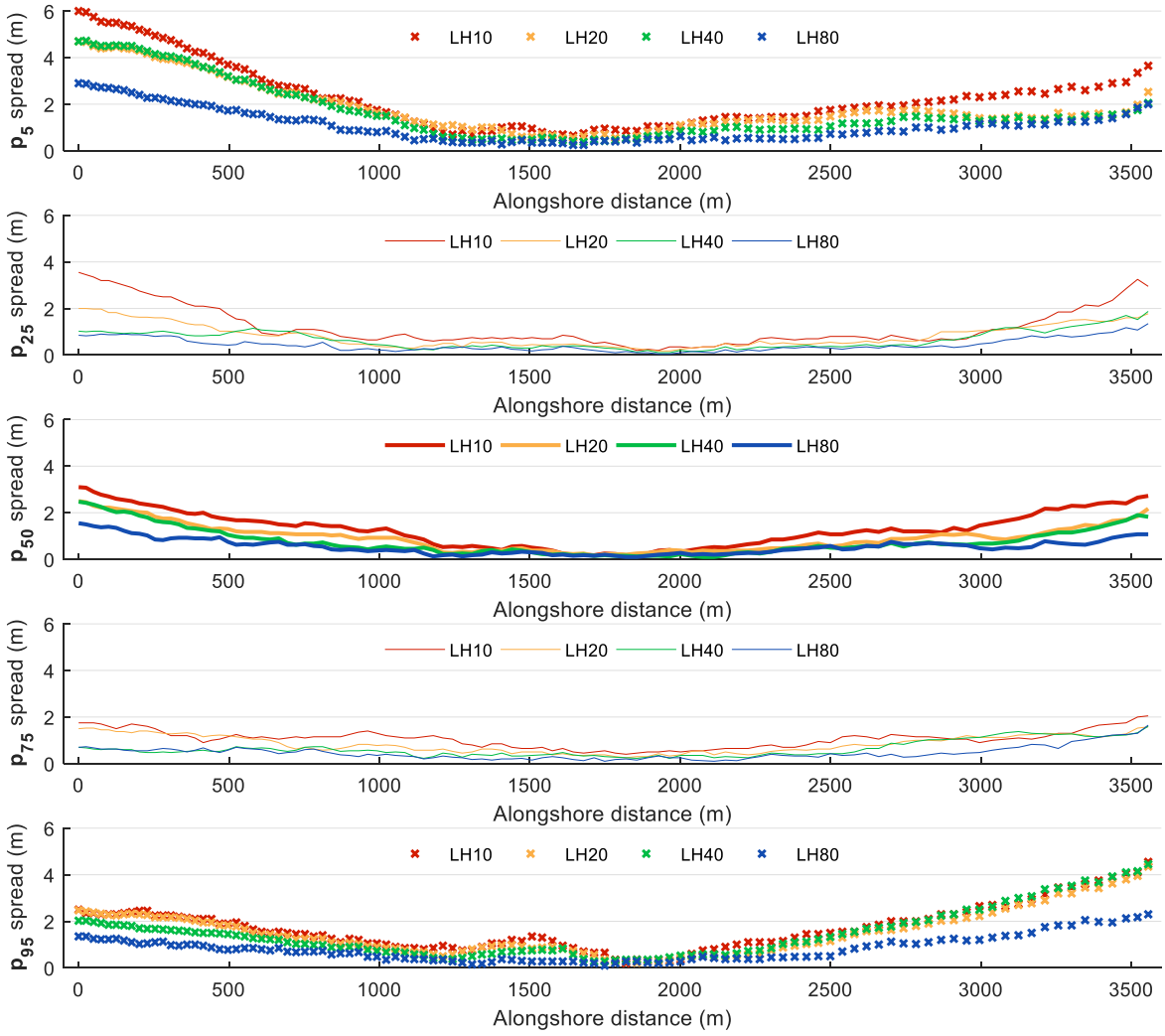

Figure 4.7: Percentile spread for the 10 LHS realisations for different sample sizes (red: 10 samples, yellow: 20 samples, green: 40 samples, blue: 80 samples) along the coast.

Apart from the uncertainty range, the choice of the sufficient sample size is heavily influenced by the uncertainty analysis requirements. In view of the results presented above, for the median estimates a sample size of 10 could be considered sufficient (with an expected spread 0.5-3m). If the emphasis is placed on estimates of the 1st and 3rd quartiles, then a sample size of 20 could be considered sufficient. When the focus lies in the acquisition of the probability distribution functions of coastline change along the coast, 40 samples can yield a good approximation of the distributions in most coastline points. However, if the emphasis is placed on the extreme percentiles or the tails of the distribution and high precision is required then a sample size of 80 or even larger sizes should be examined.

4.1.2 Standard Monte Carlo

The sample set size of 1000 was selected for SMC. Each sample includes one value for each of the four uncertain variables randomly sampled according to the assigned probability distributions. 2D projections of the samples selected by SMC on the sample space can be found in Figure 4.8. The samples were used as input to the model simulations, while all other parameters were evaluated at fixed values.

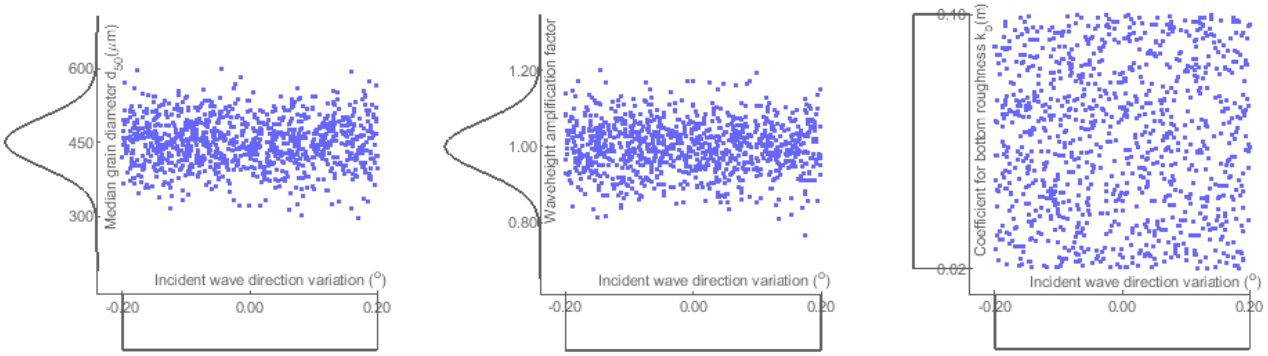

Figure 4.8 2D projection of the cloud of points generated by SMC for Unibest, (n=1000). The sampled probability distributions of the variables (median grain diameter, waveheight amplification factor, coefficient for bottom roughness) have been plotted on the sides.

Following the completion of the UNIBEST-CL+ simulations, 1000 realisations of coastline change along the coast were obtained. These constitute the empirical distribution, an estimator of the true probability distribution of the model output. Figure 4.9 shows different percentiles of coastline change along the coast, estimated using the SMC (n=1000) empirical distributions of each coastline point.

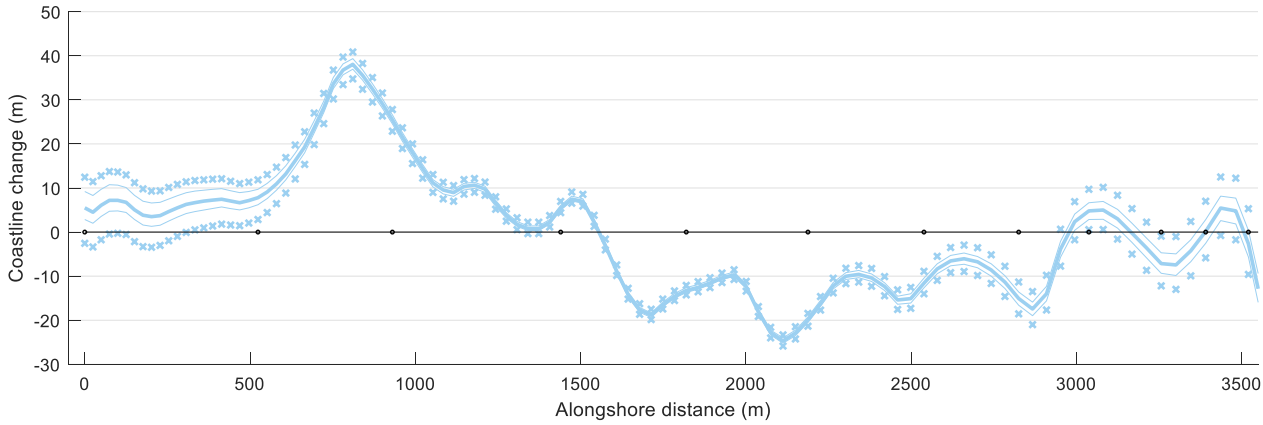

Figure 4.9: Percentiles of coastline change along the coast as estimated using 1000 SMC samples. Positive values of coastline change indicate accretion. The black markings on the horizontal axis indicate the location of different cross-sections (points 1 to 12) for which the results will be examined more closely in Figure 4.11.

As described in paragraph 3.3.1 , a check is performed to ensure that the selected number of samples (1000) indeed results in confidence interval ranges lower than 1m for the majority of the coastline points with a required level of confidence 95%. Figure 4.10 displays the range of the 95% confidence interval each of the percentiles considered (p_5, p_{25}, p_{50}, p_{75}, p_{95}), for each of the coastline points, estimated using the empirical distribution of 1000 SMC samples. For most of the coastline points we are 95% confident that the margin of error in the percentile estimates is equal or smaller than ±0.5m (equivalent to ci_{95} of 1m) while it is smaller than ±0.75m (ci_{95}=1.5m) for all of them.

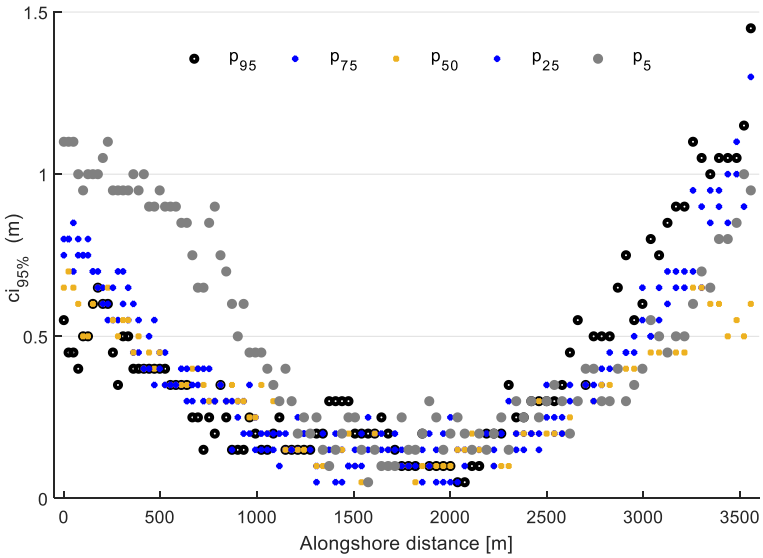

Figure 4.10: Alongshore distribution of the 95% confidence intervals (ci_{95}) around the percentiles of coastline change, derived using 1000 SMC samples. Range of $ci_{95\%}$ 1m around a percentile is equivalent to ±0.5m margin of error.

The difference between the achieved precision of the 5th and 95th percentiles that can be observed in Figure 4.10 indicates skewness or even the additional (smaller) peaks for the probability density functions of coastline change at those points. More specifically, more pronounced negative skewness is expected for the probability density functions at the right side of the modelled coast (0-1000m), while less pronounced positive skewness is expected for the probability density functions at the left side of the modelled coast (3000-3500m).

4.1.3 Methods' comparison

Applying both LHS and SMC sampling on the same model, with the same statistical characteristics for the variables allows for comparative estimates of the statistical methods' efficiency. In the following figures the SMC results have been projected over the LH results to enable this comparison.

Figure 4.11 presents the coastline change probability distribution plots for the twelve defined cross-sections along the coast estimated using LHS with four different sample set sizes (n=10, n=20, n=40, n=80) and SMC sampling (n=1000). LHS probability distributions with 80 or even with 40 samples resemble the SMC distributions very closely both in terms of coastline change range and in terms of shape, even for the cross-sections at the edges of the coastal cell. Similar conclusions can be drawn from Figure 4.12: LHS percentile estimates align closely with the respective SMC percentile estimates all along the coast. From the different LHS sample sizes used, the largest two (n=80 and n=40) have the best performance (see also graphs in Appendix C).

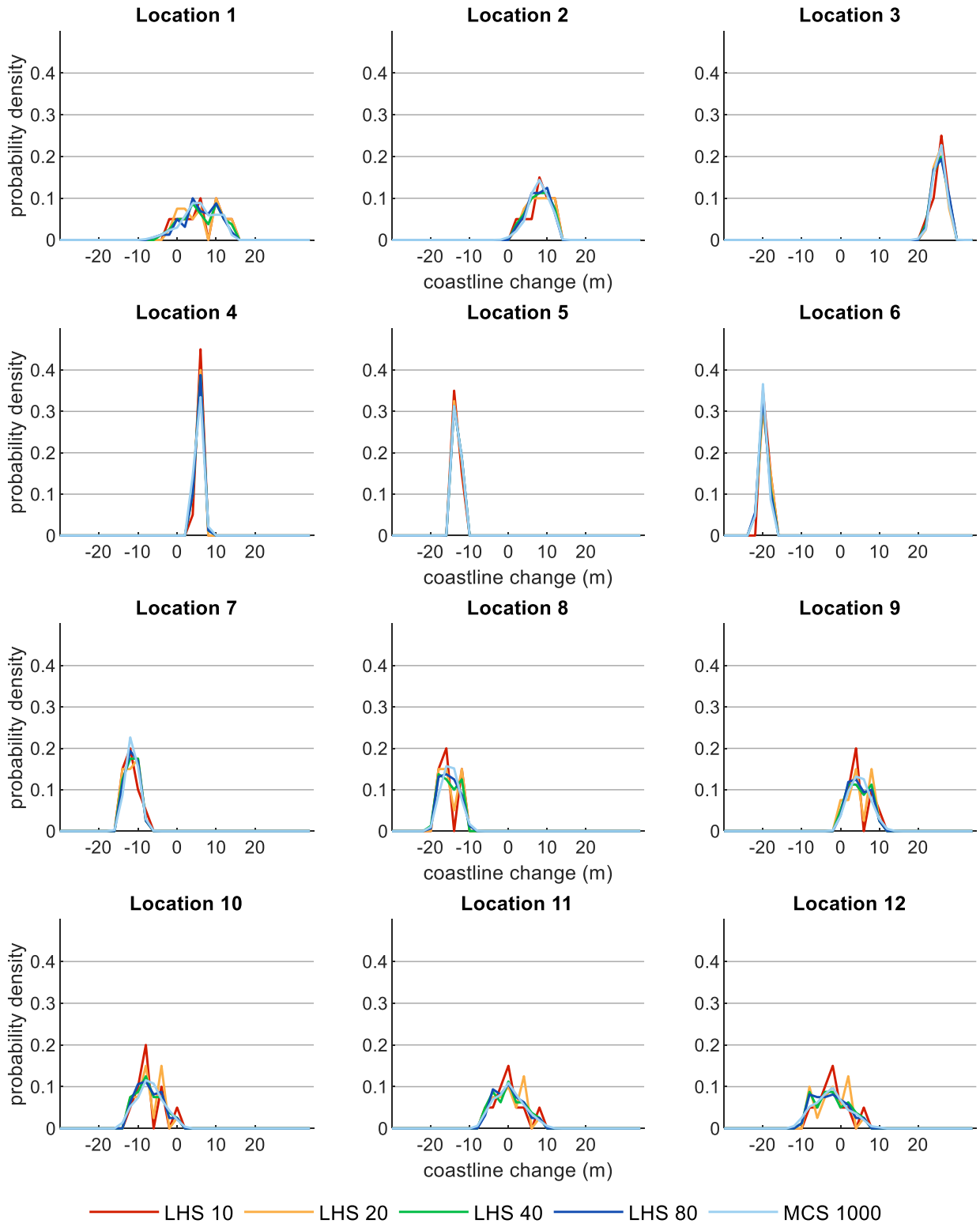

Figure 4.11: Probability density plots of coastline change at different cross-sections (defined in Figure 4.1) using different LH sample sizes (red: 10 samples, yellow: 20 samples, green: 40 samples and blue 80 samples) and SMC of 1000 samples (light blue). Positive coastline change indicates accretion.

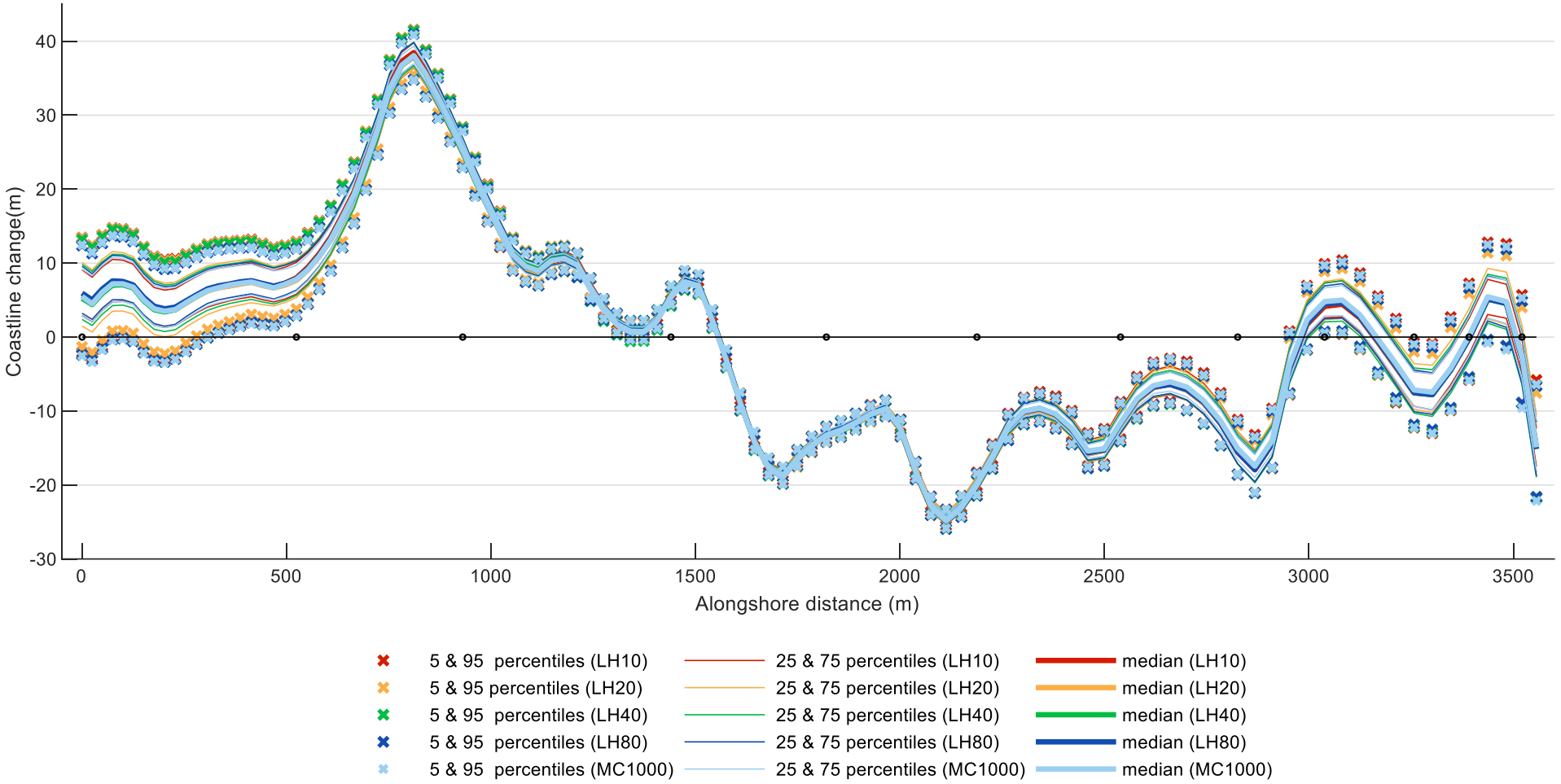

Figure 4.12: Alongshore distribution coastline change percentile estimates using different LH sample sizes (red: 10 samples, yellow: 20 samples, green: 40 samples, blue: 80 samples) and SMC (light blue: 1000 samples). Positive values of coastline change indicate coastline accretion. The black markings on the horizontal axis indicate the location of different cross-sections (points 1 to 12) presented in Figure 4.3.

However, in Section 4.1.1 we observed considerable deviations in the percentile estimates of LH when the process was independently repeated. In fact, the maximum deviation between the percentile estimates of the different LHS (n=80) realisations and SMC (n=1000) was found 2m (Figure D.4). In view of that, we can conclude that for the UB simulation and the input uncertainties considered, LH Sampling with 80 samples approaches but does not quite reach the same results' precision as with SMC (n=1000).

Nevertheless, for many computationally expensive models the computational and time limitations set a ceiling to the number of samples that can be used. To justify the statistical method selection for such cases, a comparison of LHS and SMC under the same conditions was carried out. To match the 10 LHS realisations carried out previously (Figure 4.6) for the different sample sizes, 10 SMC realisations for the same sample sizes were performed as indicated in Figure 4.13, using the already drawn set of 1000 SMC samples. Different percentiles of coastline change along the coast were estimated for each of the SMC and LHS realisations. The resulting distributions of coastline change percentile estimates for each method and location along the coast were assessed in terms of central tendency and dispersion both between the two methods and with respect to the 'benchmark' results, the results of SMC (n=1000).

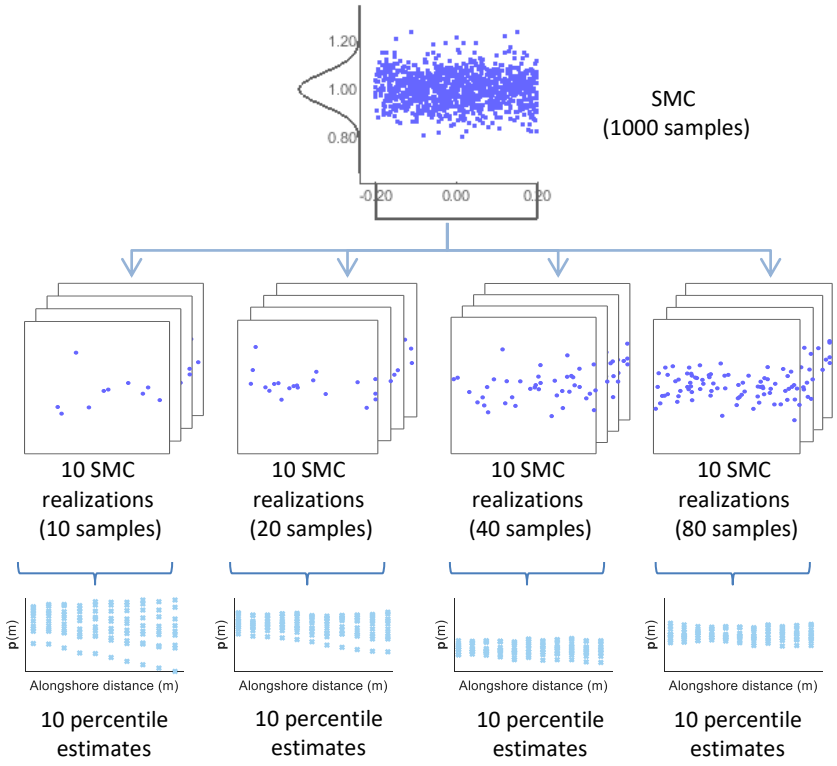

Figure 4.13: Schematic representation of the steps followed. 4 sets of 10 SMC realisations (for the 4 different sample sizes) were drawn from the initial SMC sample set (n=10). Subsequently the distributions of the different coastline change percentile estimates from the 10 SMC realisations were derived for every point along the coast.

Five different percentiles of coastline change were considered (p_5, p_{25}, p_{50}, p_{75}, p_{95}). The percentile estimate distributions along the shore resulting from the 10 LHS and 10 SMC realisations relative to the benchmark percentile estimates (SMC n=1000) can be found in Appendix D. Alongshore averaged mean absolute and bias error indicators (Figure 4.14 and Appendix D respectively) were calculated to assess the success of each method-sample size combination in approaching the benchmark results. For the same sample size LHS percentile estimates are mostly closer to the benchmark values than the SMC percentile estimates. For each LHS sample size, the performance reduces from the median towards the extreme percentiles. For SMC this tendency is not so strong.

Interestingly, the Mean Absolute Error (MAE) values across the percentiles are not symmetric. Both LHS and SMC give lower MAE values for the higher percentiles 95 and 75 compared to the corresponding lower percentiles (5 and 25 respectively). As expected, the performance of both statistical methods improves for increasing sample sizes. For the smallest sample size MAE is significantly lower when LHS is used while as the sample size grows the difference in performance reduces. Notably for n=80 the two methods have almost equal performance in terms of central tendency. Both statistical methods tend to underestimate the extreme percentiles and overestimate the quartiles (Appendix D). This tendency decreases rapidly as the sample size increases and is more pronounced for the LHS method.

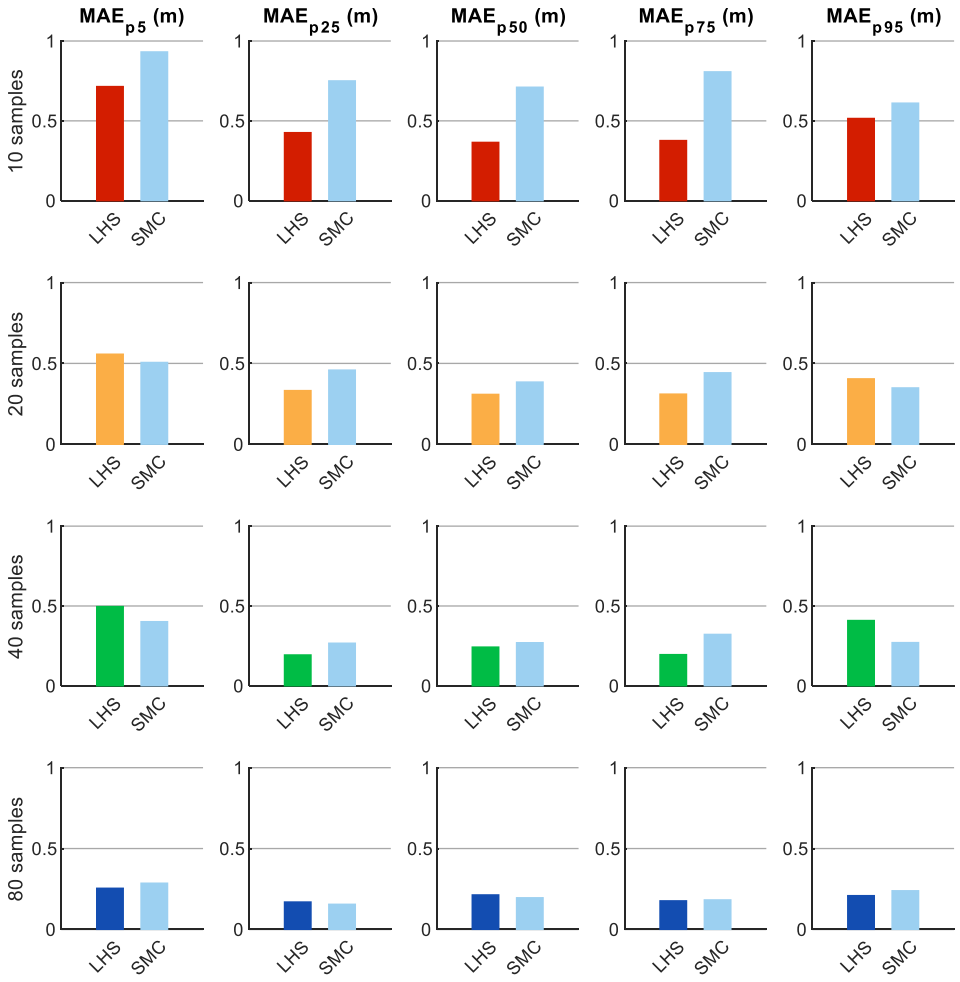

Figure 4.14: Alongshore averaged Mean Absolute Error for the different coastline change percentile estimates, for SMC and LHS with different sample sets. The results are derived using 10 LHS and SMC realisations for each of the different sample set sizes. The percentile estimates derived using SMC (n=1000) were used as the 'true' values for the MAE calculation.

The alongshore averaged standard deviation (standard error) of the different percentile estimates serves as an indicator of the convergence of the statistical method-sample size combination and allows the comparison of the achieved precision. As can be seen in Figure 4.15, LHS estimates generally converge more than the SMC estimates for the same sample size, with the exception of the extreme percentiles from 40 samples, and p_{95} from 20 samples. A clear convergence pattern can be observed for both methods as the sample set size used increases. Once again, for the smaller sample sizes LHS estimates are superior to the SMC estimates. However, as the sample set sizes increase this disparity decreases. For the largest sample size of this analysis, n=80, the difference in the performance is fractional.

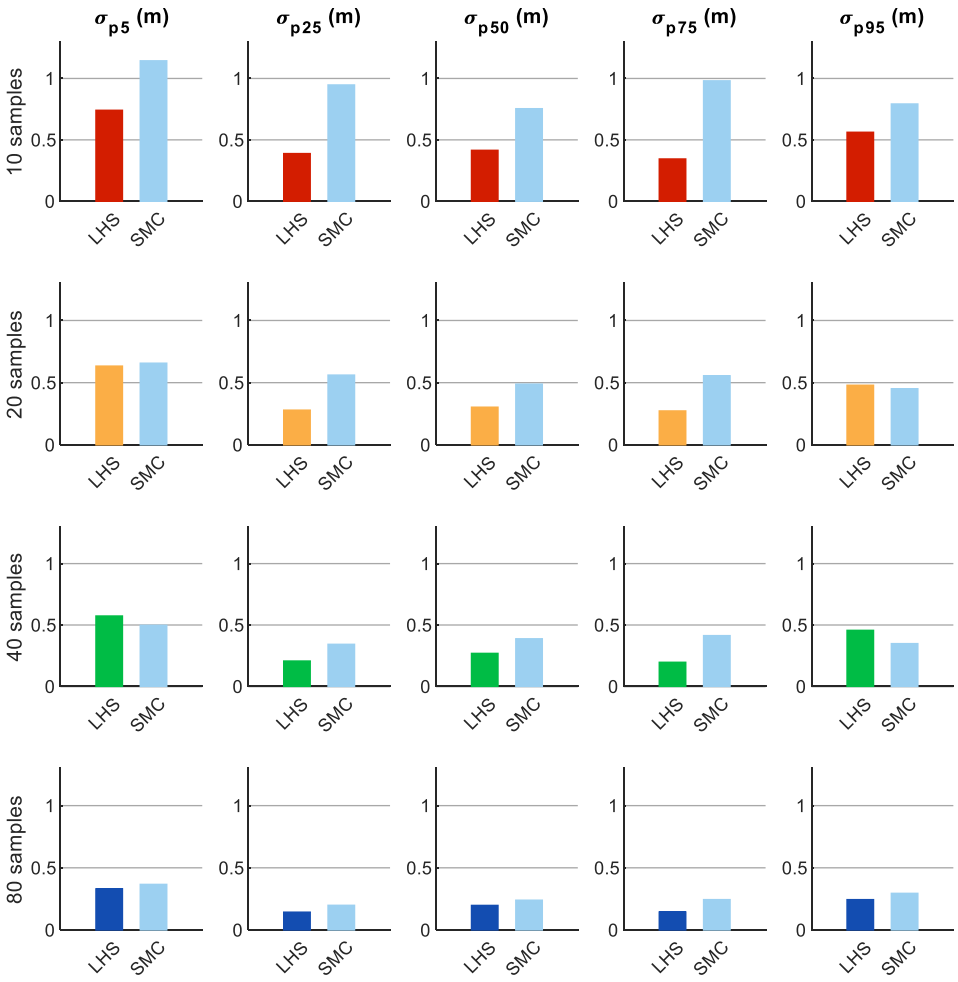

Figure 4.15: Alongshore averaged standard deviation (σ) for the different coastline change percentile estimates, for SMC and LHS with different sample sets. The results are derived using 10 LHS and SMC realisations for each of the different sample set sizes.

On balance, it appears that for small sample sets LHS performs better than SMC and should be preferred for the quantification of the uncertainties. However, as the sample set sizes increase, the difference in performance between the two methods diminishes. In this case, for a sample set size of 80 the convergence of the two statistical methods is practically equal. In such cases SMC should be favoured over LHS for uncertainty quantification in the model output due to the capacity for quantified precision estimates.

The estimation of the sample size for which LHS ceases to be more efficient than SMC for a specific model schematization and for the assigned input distributions is a complex issue. Though SMC's convergence rate is related to the sample size and is known in literature ($\propto 1/\sqrt{n}$ for univariate sampling), the convergence rate of LHS is not known. However, based on the results we can assume that this convergence rate disparity diminishes faster with smaller uncertain input spaces, narrower output uncertainty ranges and more uniform uncertain input distributions. More specifically narrow uncertainty ranges in the inputs and outputs lead to faster convergence for both methods. This is illustrated in the cross-sections towards the center of the modelled domain for which both LHS and SMC converge rapidly. Lastly, the advantage of LHS lies in the guaranteed sampling from the tails of the distributions. However, when uniform distributions are assigned to the variables the model is most sensitive to, in this case k_b and θ, then there are no tails to sample from and the difference between the performance of LHS and SMC diminishes faster.

4.2 Uncertainty quantification for Delft3D

Due to the high computational cost of Delft3D simulations for the area of interest, the application of SMC sampling was considered inefficient at present. Only the application of Latin Hypercube Sampling was investigated further.

The sensitivity analysis on the D3D 3-year simulation of Anmok beach (paragraph 3.2.2) yielded three parameters to be included as stochastic in the uncertainty quantification process. The variables and their statistical characteristics are presented in Table 8 below.

Parameter	Description	Distribution
C [$m^{0.5}/s$]	bottom roughness coefficient	N (65, 3.33)
α_{Hs}	significant wave height amplification	N (1, 0.067)
d_{50} [µm]	median grain diameter	N (450, 50)

Table 8: Stochastic input variables for Delft3D

Similarly with the application of the statistical methods on UNIBEST-CL+, probability density plots as well as cumulative distribution plots of coastline change are presented for 9 different locations selected from a cross-sectional grid (Figure 4.16). Additionally, different percentiles of coastline change were calculated along the coastline and presented to provide an estimate of the location and dispersion of the model output sample.

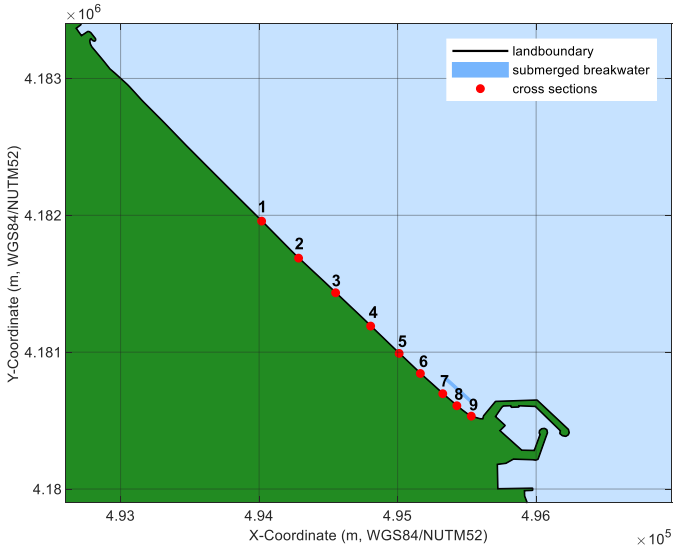

Figure 4.16: Spatial plot of Anmok beach. The red markings indicate the location of the cross-sections for which results of the LH Sampling application on the starting point D3D simulation will be presented.

4.2.1 Latin Hypercube Sampling

The application of Latin Hypercube Sampling on D3D simulations was made for four different sample sizes; n=10, n=20, n=40, n=80, with the smaller sample sets being subsets of the larger ones. The samples were selected from the 3D uncertain input space outlined by the ranges and distributions of the uncertain variables. In Figure 4.17 2D projections of the cloud of points sampled by Latin Hypercube can be seen for n=10. The projections for the different sample sizes can be found in Appendix E. All other variables/parameters were evaluated at a fixed, 'true' value.

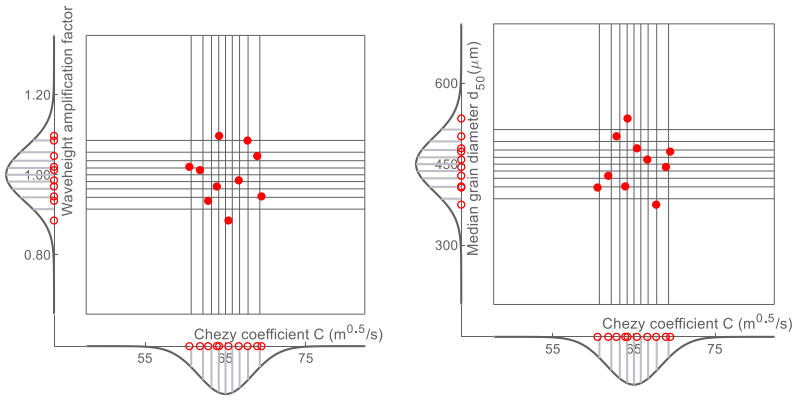

Figure 4.17: 2D projections of the sample vectors (red dots) generated by LHS for D3D, (n=10). The sampled probability distributions of the variables (waveheight amplification factor, Chezy coefficient, median grain diameter) have been plotted on the sides along with the sampled values for each variable (red circles).

Probability distribution plots and cumulative distribution plots of coastline change for different positions along the modelled stretch (as indicated in Figure 4.16) were computed based on the empirical distributions of the output for the different sample sizes used. Figure 4.18 below provides an overview of the general shape and position of the coastline change distributions generated using Delft3D at the selected cross-sections along the coast.

This time only a single LH sampling realisation was performed, rendering the quantification of the precision achieved per sample set size impossible. Taking that into account, in the following paragraphs we will aim to evaluate only the convergence of the different sample size distributions/quantiles to those of the largest sample set (n=80).

In comparison with the probability distribution plots from the UNIBEST-CL+ distributions (Figure 4.11) the range of coastline change obtained from the Delft3D probabilistic simulations is more uniform along the coast, and generally more restricted. A general tendency of coastline recession can be observed for the largest part of the modelled stretch.

The shape of the resulting distributions is an aspect of interest. Many of the distributions feature a few distinct peaks. For some of the points (e.g., point 4, point 1 left tail) as the sample set size increases, a grading of the peaks can be observed suggesting that a larger number of samples would result in a smoother distribution. In contrast the probability distribution estimates of coastline change at different points (e.g., point 8, point 2) seem to converge to the irregular shape for an increasing sample set size, suggesting different distinct modes of coastline change for variations in the stochastic parameters. This shape of the probability distributions of coastline change highlights the added value of using sampling techniques over using a traditional sensitivity analysis to estimate the range and fitting a distribution to that range. Further investigation of the shape could also provide insights to the system behaviour and response to variations in specific variables.

Different percentiles of interest as estimated from different LHS sample sizes along the coast are presented in Figure 4.19. The uneven dispersion of the quartiles around the mean suggests significant skewness or multiple peaks in the probability distributions. Median estimates from the different sample sizes seem to converge rapidly on the median estimates from the biggest sample size (n=80). Convergence can also be observed for the 25th, 75th, and 95th percentile estimates with the values resulting from the increasing sample sizes gradually approaching those of the biggest sample set. On the other hand, there is a wide dispersion of the 5th percentile estimates without a clear trend of convergence as the sample sizes increase.

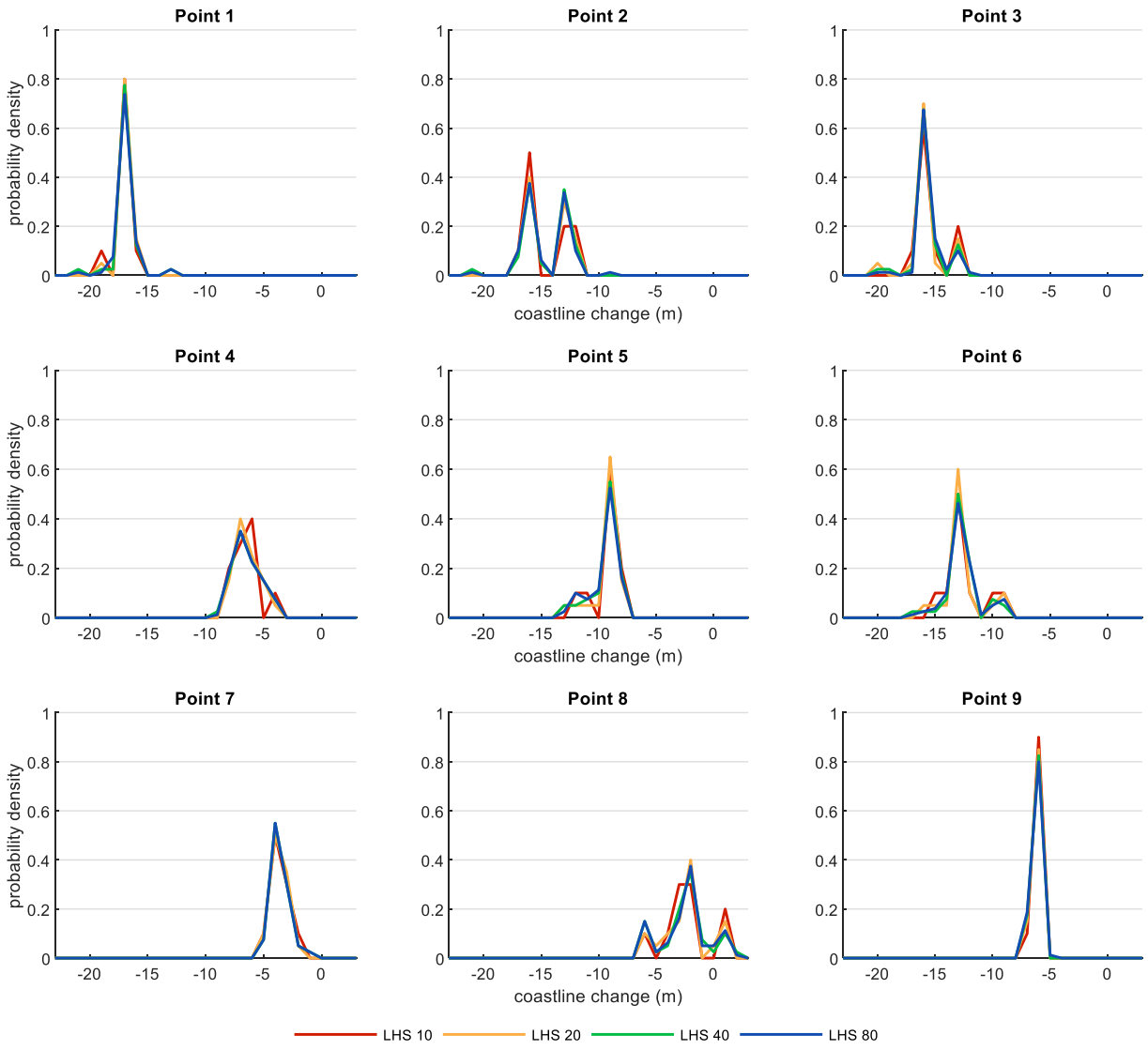

Figure 4.18: Probability density plots of coastline change at different cross-sections (defined in Figure 4.16) along the coast, estimated using different LH sample sizes (red: 10 samples, yellow: 20 samples, green: 40 samples and blue 80 samples). Positive coastline change indicates accretion. Bin resolution is 1m.

Considering more closely the convergence/scatter of the percentile estimates for the different LH sample set sizes, Figure 4.20 presents the deviations of the percentile estimates using smaller sample sizes (n=10, n=20, n=40) from the percentile estimates from the largest sample size (n=80). We can see that those deviations are negligible (<0.5m) for the median estimates along the modelled stretch and for all the different sample set sizes, implying that using 10 samples provides us with just as good an estimate of the coastline change median as using 80 samples. The same applies for the 25th, 75th and 95th percentile estimates with local exceptions at the areas where the variation of the distribution shape (and more specifically the emergence or smoothening of the peaks) causes the significant variations in the percentile estimates. It is surprising that the 5th percentile estimates resulting from 10 samples converge more towards the values of the LHS80 estimates than estimates coming from the larger sample sizes. Generally, the observed convergence patterns are not uniform along the coast; for some locations the percentiles converge rapidly and for some others we observe this irregular behaviour.

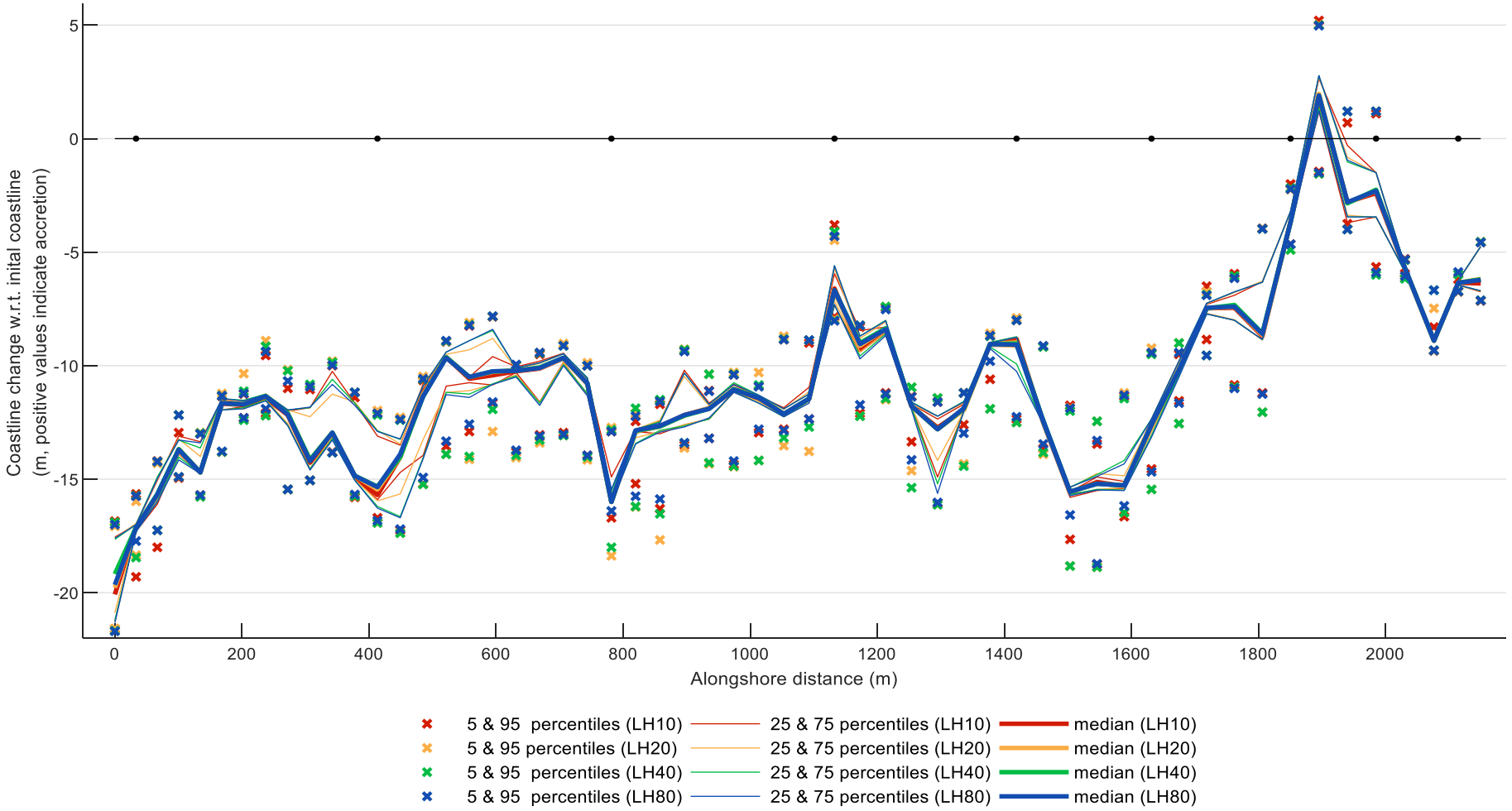

Figure 4.19: Percentile estimates for coastline change along Anmok beach for the different LH sample sizes (red: 10 samples, yellow: 20 samples, green: 40 samples, blue: 80 samples). Positive values of coastline change indicate accretion.

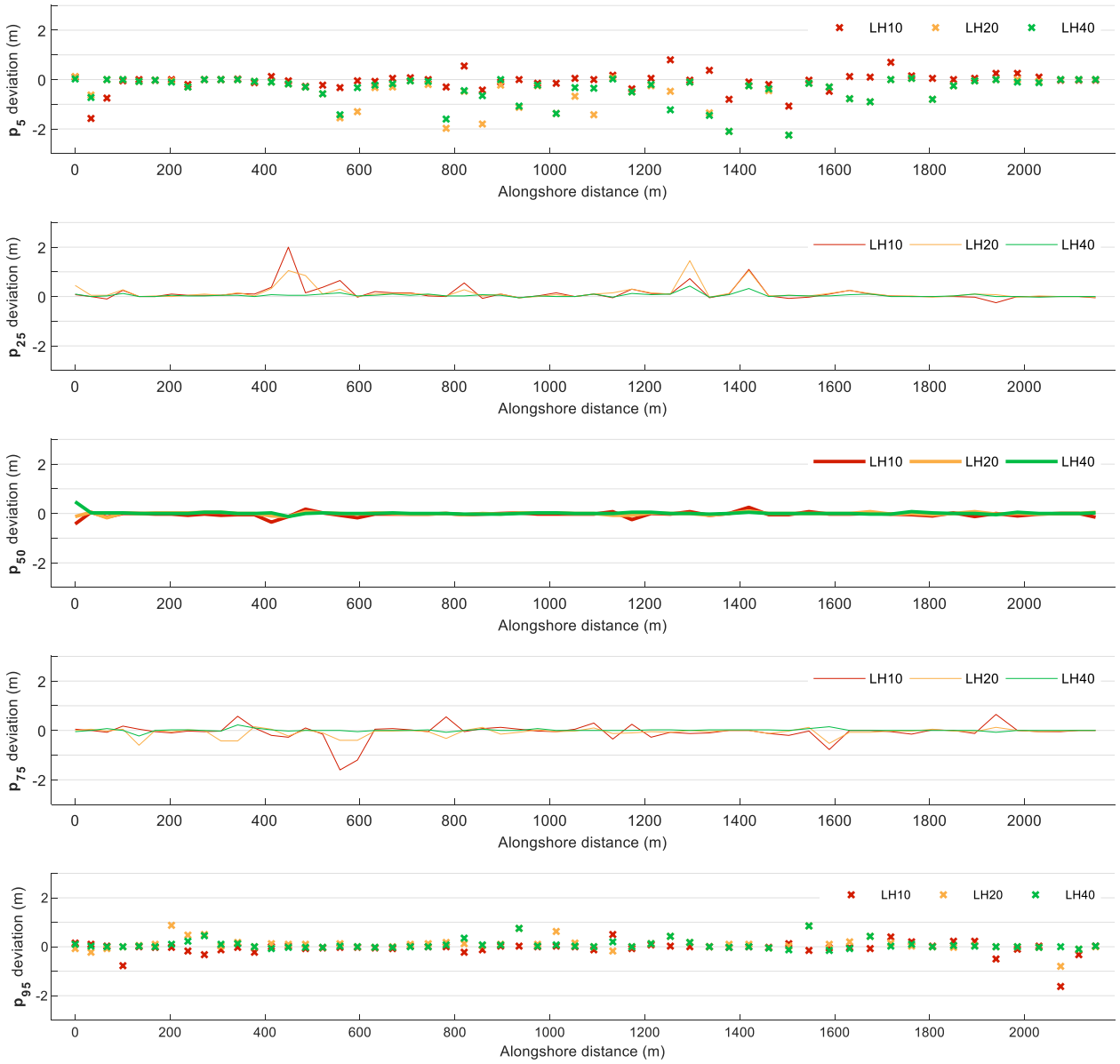

Figure 4.20: Deviations of coastline change percentile estimates using different sample sizes (red: 10 samples, yellow: 20 samples, green: 40 samples) from the percentile estimates estimated using the biggest sample size (n=80).

As mentioned before, the statistical formulas used to estimate the achieved precision for SMC results (Section 3.3.1) are not accurate for LHS due to the serial dependence of the samples of the latter. According to Morgan et al. (1992) application of these formulas on LHS results will typically result to lower precision estimates than those achieved. Nevertheless, these formulas were applied to the LHS estimated coastline change distributions to get a conservative estimate, of the precision achieved. Figure 4.21 presents the 95% confidence intervals around the different percentiles of coastline change estimated from LHS (n=80). The estimated values for the quartiles are for many cross-sections below 1m. For the extreme percentiles the estimated confidence intervals reach up to 4.5m.

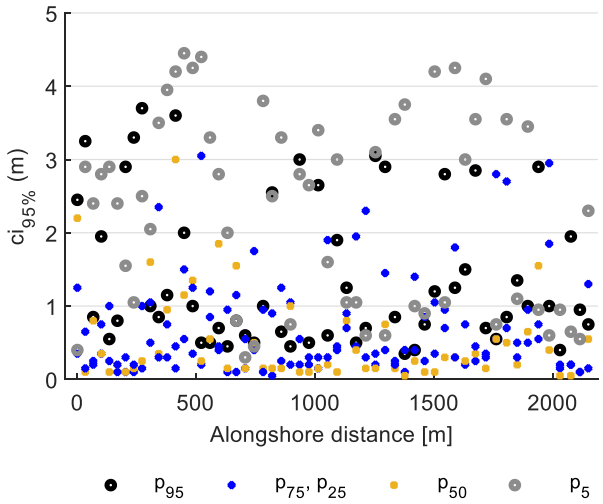

Figure 4.21: Alongshore distribution of the 95% confidence intervals (ci_{95}) around the percentiles of coastline change, derived using 80 LH samples. Range of $ci_{95\%}$ 1m around a percentile is equivalent to ±0.5m margin of error.

4.3 Multi-model coastline change uncertainty aggregation

The next paragraphs present the application of the uncertainty aggregation methodology as outlined in Section 3.4. The quantification of the uncertain effects of an intervention in the littoral zone on coastline position is carried out for a specific management horizon. Several interventions in the littoral zone are considered, including different breakwater designs and a small-scale nourishment. The effect of the large-scale wave climate variations and sandbar dynamics are incorporated in different parts of the aggregation process.

4.3.1 Submerged breakwater - nourishment

The first investigatory application refers to the already existing submerged breakwater in Anmok beach and the implemented small-scale nourishment behind it (Figure 3.2). We aim to assess the uncertain effect on the coastline position of different processes acting on the coast and evaluate the potential coastline position change in 2035 with respect to a reference coastline.

The formula that governs coastline change aggregation is presented below:

$$\mathbf{CC_{Cumulative}\,(m) = CC_{long\text{-}term} + CC_{intervention\ impact}} \quad (1)$$

$\mathbf{CC_{long\ term}}$ refers to the alongshore distribution of coastline change probability density functions under the effect of the long-term processes: autonomous evolution and wave climate variations. The UNIBEST-CL+ model schematization described in paragraph 3.1.1 forms the baseline simulation. It captures the autonomous evolution of the coastline in Anmok beach for the entire 20-year period, including any interventions present in the domain, apart from the Anmok beach submerged breakwater and nourishment, whose effect was simulated separately. The impact of climate change on the wave climate and in extent on the coastline evolution is incorporated during the probabilistic runs through the distributions assigned to the forcing conditions (H_s, dir). Additionally, 2 more variables were assigned distributions to address natural variability and parameter uncertainty in the simulations. Uncertainty quantification was performed using Latin Hypercube Sampling (n=80) and the distributions of coastline change for the cross-sections along the coast were derived directly from the model output (Table 9).

Process	Model	Simulated period	Uncertain Input	Uncertainty quantification method
Autonomous evolution Long-term wave climate variation	UNIBEST-CL+	2015-2035	H_s N (1, 0.067) θ U (-0.2, 0.2) d_{50} N (450, 50) k_b U (-0.02, 0.1)	LHS (n=80)

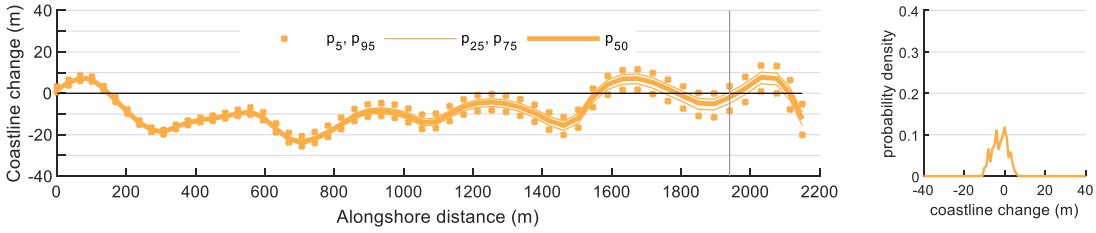

Table 9: Overview of the uncertainty quantification process for the baseline simulation including the effect of the long-term wave climate variations. The left graph presents the resulting alongshore distribution of different coastline change percentile estimates. Positive coastline change indicates accretion. On the right, the probability distribution plot of coastline change for one location (marked with a grey vertical line in the left graph) is presented.

For the uncertainty quantification of the considered intervention's net effect on coastline position, $\mathbf{CC_{intevention\ impact}}$, a set of Delft3D simulations were used: a simulation as described in paragraph 3.1.1 including the intervention, and an identical simulation without the intervention. The submerged breakwater and small-scale nourishment were assumed to be implemented at the start of the considered period (2015). Additionally, the morphodynamic response of the coast is expected to reach a steady state within a few years following the implementation of the intervention (Figure 4.22). Assuming that the coastline change realised by 2018 due to the presence of the intervention will remain unchanged until 2035, a 3-year simulation period was selected for the Delft3D model schematisations. Following the selection of the stochastic input, Latin Hypercube Sampling (n=80) together with the MCL approach were implemented to extract the coastline position change realisations from the model results, with and without the intervention. The differences in coastline change with and without the intervention were used to estimate the empirical distribution of the intervention impact on coastline change.

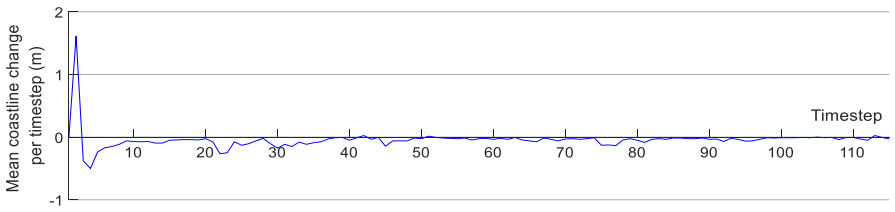

Figure 4.22: Coastline change per timestep averaged over the general area of the submerged breakwater (1700-2150m) for the Delft3D simulation including the submerged breakwater-nourishment intervention. The results show declining coastline changes per timestep indicating that the system approaches a morphodynamic equilibrium towards the end of the 3-year simulation.

In Table 10 the net effect of the intervention on the coastline position can be seen. The results show a net accretion for a 330m long stretch behind the breakwater at the end of the 3-year period. The interquartile range in the accretion area ranges from 1 to 3m. North of the submerged breakwater, for an area of approximately 200m coastline recession is the median effect with the quartiles and extreme percentiles located on the negative side. The rest of the coastal stretch is barely impacted by the intervention; the median coastline change is situated at zero and the 5th-95th percentile range takes a maximum value of 3m.

The accretion observed in the shadow zone of the breakwater is the combined effect of the artificial accretion by means of the implemented small-scale beach nourishment and the sheltering effect of the submerged breakwater. The nourishment is incorporated in the initial timesteps of the simulation and

causes a significant movement of the coastline seawards. The submerged breakwater creates a shadow zone, blocking a large part of the incident wave energy from reaching the coast and minimizing transport capacity. Depending on the mean direction of alongshore transport positive or negative gradients of sediment transport can be observed in the edges of the shadow zone leading to removal of nourishment material from the shadow zone or deposition of material respectively. Diffraction patterns can be observed at the edges of the submerged structure enhancing the accretion. For shore-normal or close to shore-normal wave incidence the onshore flow over the submerged breakwater deflects and returns offshore at the sides of the breakwater in a rip-current form removing a lot of sediment from the shadow zone. The interaction of these processes, as schematized in the model, results in the morphodynamic evolution of the coast during the simulation time and in extent to the general trends which we can discern in the probabilistic results.

Process	Model	Simulated period	Uncertain Input	Uncertainty quantification method
Intervention impact (submerged breakwater-nourishment)	Delft3D	2015-2018	H_s N (1, 0.067) d_{50} N (450, 50) C N (65, 3.33)	LHS (n=80)

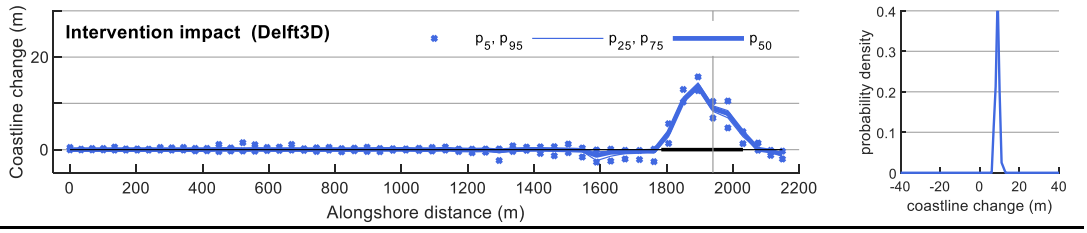

Table 10: Overview of the uncertainty quantification process for the Delft3D simulations used to assess the effect of the intervention (submerged breakwater and nourishment). On the left, the resulting alongshore distribution of different coastline change percentile estimates under the effect of the intervention is presented. Positive coastline change indicates accretion. The location of the intervention has been marked on the horizontal axis. On the right, a probability distribution plot of coastline change for one location (marked with a grey vertical line in the left graph) is presented.

The empirical coastline change distributions resulting from UNIBEST-CL+ and Delft3D models were evaluated at the same locations (56 cross-sections) along the coast with respect to a reference shoreline to overcome the differences in the spatial schematisation of the two models. In the end, although the coastline position definitions differ such that superposition of the coastline positions would be pointless, coastline change with respect to a reference coastline can be assumed 'independent' of the coastline definition and be aggregated irrespective of that.

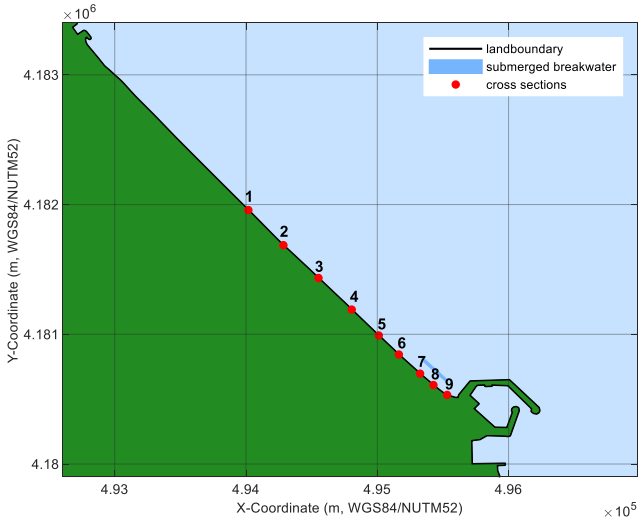

Figure 4.23: Spatial plot of Anmok beach. The markings show the location of the cross-sections for which probability density plots will be presented.

The next step includes the aggregation of the intervention impact, evaluated as described above (equation 1), with the effect of the long term processes (Figure 4.24 and Figure 4.25). A Monte Carlo approach with 10^6 samples was utilised in all the steps of the aggregation process with minimum computational time (2-3 minutes per aggregation). Similar to the previous sections, the results will be presented in the form of alongshore distributions of percentile estimates of coastline change. Additionally, the individual and cumulative probability density plots of coastline change will be presented for several cross-sections along the coast (Figure 4.23).

The results of the 20-year UNIBEST-CL+ simulation suggest shoreline recession under the effect of the long-term processes and the uncertainties included. The median projected coastline change varies on the alongshore with maximum values (-25m) at the north part of the area of interest. The dispersion of the percentiles around the median increases from north to south. Sparse areas with projected accretion can be observed, mainly towards the edges of the results area. When the effect of the intervention is superimposed on the aforementioned results, significant change can be observed concentrated at the south end of Anmok beach; an area earlier projected as erosive in the autonomous evolution simulation under the effect of long-term wave climate change, is now accretive under the impact of the submerged breakwater and nourishment. The projected accretion (median) reaches up to 8m, while there is 5% possibility that the shoreline propagates more than 12m at this area. The submerged breakwater and nourishment implementation does not achieve any reduction in the range of cumulative coastline change. On the contrary, the results indicate a slight increase in the 5-95 percentile range of 4% on average. For the cross-sections in the central and northern part of the coast, the characteristics of the cumulative coastline change distributions have been defined largely from the UNIBEST-CL+ derived distributions.

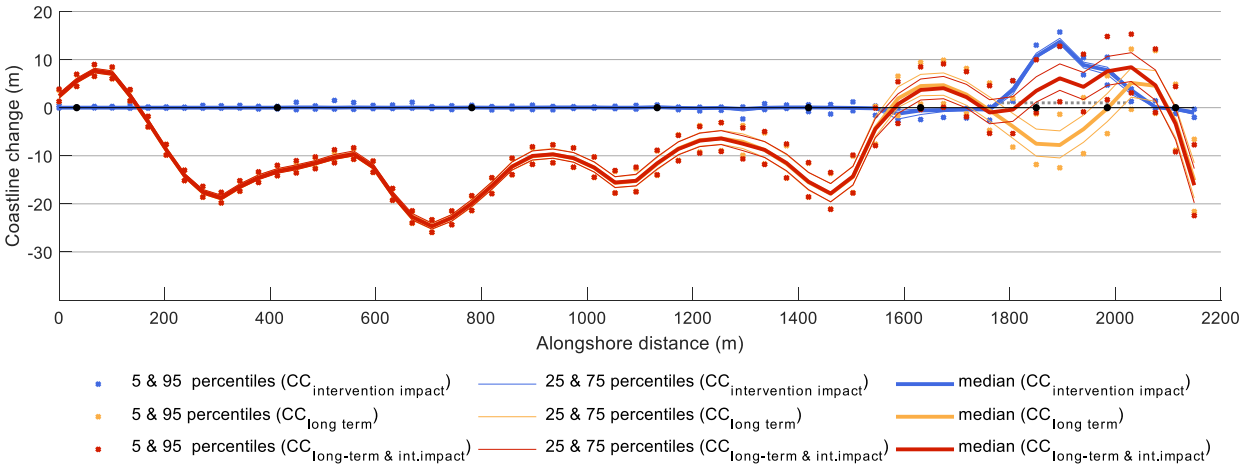

Figure 4.24: Overview of the coastline change percentile estimates for Anmok beach (blue: net intervention impact, yellow: climate change –wave climate variability, red: aggregated coastline change). The quartiles are shown with continuous lines, while the 5th and 95th percentile with x markings. Positive values of coastline change indicate accretion. The black markings on the horizontal axis indicate the location of different cross-sections (points 1 to 9) for which probability density plots are presented (Figure 4.23). The grey dotted line indicates the location of the intervention.

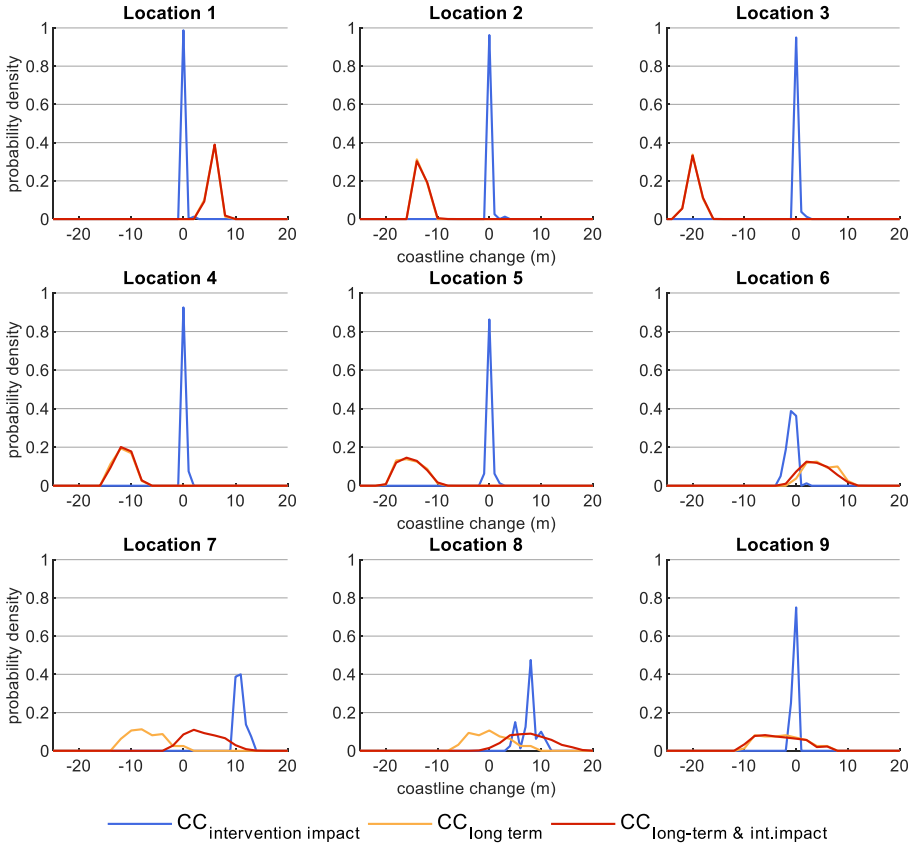

Figure 4.25: Probability density plots of coastline change (blue: net intervention impact, yellow: climate change –wave climate variability, red: aggregated coastline change) for different cross-sections along Anmok beach as defined in Figure 4.23.

Taking a closer look at the results of the aggregation steps carried out, a few points of interest relating to the convolution operation between probability distributions can be noted.

- Convolution is generally dominated by the component with the largest dispersion. The aggregated distribution is at least as wide and low as the component with the largest dispersion. The final shape also resembles that of the widest component, yet it tends to be smoother with lower/fewer peaks present.
- All the components contribute to the shifting of location of the aggregated distribution. The resulting distribution location is defined by a seemingly linear addition of the median locations of the components, resembling the linear superposition of normal distributions.

From the above, it is to be expected that in the coastline change aggregation process the probability distribution for the coastline change under the cumulative effect of the considered processes will be as wide as the widest contributing distribution. Depending on the aggregation context, and especially for aggregations on longer management horizons including long-term processes, these long-term processes are expected to define the shape and dispersion of the resulting distributions. For such aggregation processes we should not expect any reducing effect from the medium and small-scale processes/interventions on the aggregated coastline change range. The most important contribution of the net intervention impact lies in the shifting of the aggregated probability distribution function, preferably towards the positive side. From the aggregation procedure application above, when the net intervention impact pdf is located on the positive side, the aggregated probability is shifted towards the positive as well. This can help reduce or even practically eliminate the overall probability of erosion or the probability of erosion past a certain limit.

When a sufficiently large sample size is used, the Monte Carlo approach used for the aggregation of the individual probability distributions of coastline change has a minimal contribution to the uncertainty in the aggregated result. Figure 4.26 (a) indicates that the maximum margin of error around the aggregated coastline change percentiles due to the sampling uncertainty is ±6cm for a sample size of 10^6. The most important source of uncertainty for the aggregated coastline change estimates is in fact the imprecise statistical representation of the individual components of coastline change. Assuming that the individual components' errors (δc_1, δc_2, …., δc_n) are uncorrelated and random (normally distributed) and the combined uncertainty in the aggregated result (δc_{aggr}) can be calculated as follows (Palmer, 2003):

$$\text{if } c_{aggr}=c_1\pm c_2\pm\ldots\pm c_n \text{ then } \delta c_{aggr}=\sqrt{\delta c_1^2+\delta c_2^2+\ldots+\delta c_n^2} \quad (2)$$

The presented concept of uncertainty propagation through mathematical operations was used to quantify the uncertainty propagation through the applied aggregation equation (equation 1). The maximum margins of error around the percentile estimates of coastline change were used as standard uncertainty measures for the different aggregation components.

- $\delta c_{long\text{-}term} \approx \pm 2$m, derived from the 10 LHS realizations
- $\delta c_{intervention\ impact} \approx \pm 1.7$m estimated as described in Section 4.2.1 Figure 4.26 (b).

The total margin of error around the aggregated coastline change estimates is calculated, $\delta c_{aggr}=\pm 2.6$m. The aggregated error is always larger than that of any component and is dominated by the largest error source.

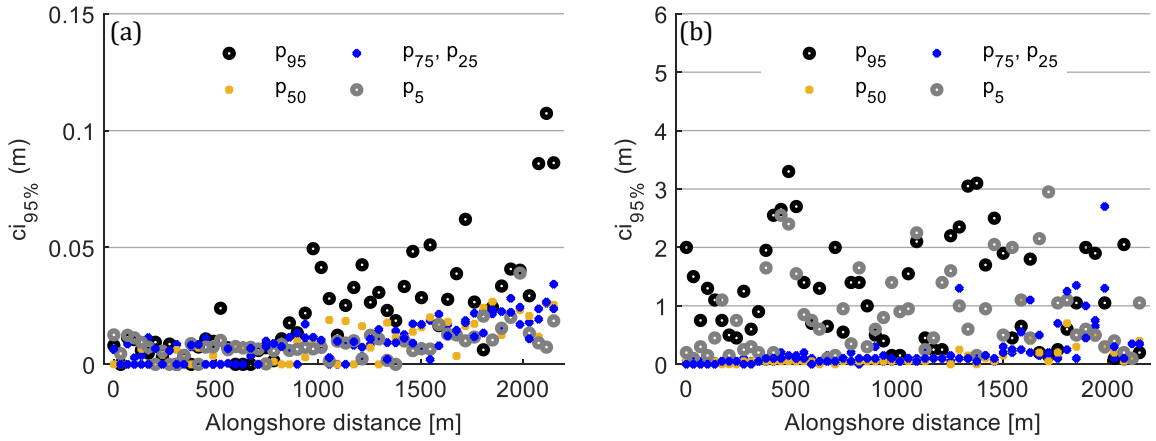

Figure 4.26: (a) alongshore distribution of the 95% confidence intervals (ci_{95}) around the percentiles of aggregated coastline change, derived using 10^6 SMC samples. (b) alongshore distribution of the 95% confidence intervals (ci_{95}) around the percentiles of coastline change under the effect of the intervention, derived using 80 LH samples.

4.3.2 Incorporating the effect of sandbar dynamics

Athanasiou (2017) showed that the alongshore migration of the crescentic sandbars present in Anmok beach is correlated with the existing medium-scale rhythmic shoreline patterns. UNIBEST-CL+ cannot reproduce these undulations while modelling attempts carried out during CoMIDAS research program showed that even state of the art process-based models like Delft3D are not able to simulate the relative processes (Athanasiou, 2017; Deltares, 2017). However, analysis of remote sensing and bathymetric survey data showed that sandbar migration can have an important effect on the instantaneous shoreline position causing undulations ranging from -20m (bays) to +30m (horns) from the mean shoreline position.

The analysis carried out during CoMIDAS program yielded mean and standard deviation estimates of the alongshore and time averaged coastline position with respect to a mean coastline, (μ, σ) = (1.2m, 9.4m). A normal distribution with the same characteristics was selected to quantify the uncertainty around the effect of the sandbar dynamics on the coastline position ($\mathbf{CC_{sandbars}}$). The distribution was

applied uniformly along the coast except for the area close to the submerged breakwater. Although there are no quantified results for this area, it is expected that uncertainty in the coastline position due to sandbar migration is lower close to the breakwater as the sandbar patterns merge with the effect of the submerged breakwater. Considering this stabilizing effect of the breakwater on the sandbar patterns and in extent the shoreline patterns, a linearly reducing standard deviation (to σ=1m) was assumed for the southern part of the coast (Table 11).

Process	Model	Simulated period	Uncertain Input	Uncertainty quantification method
Sandbar migration impact	Data Analysis	-	-	-

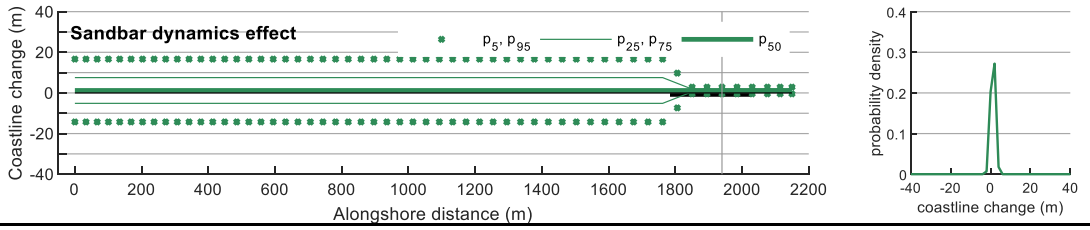

Table 11: Overview of the uncertainty quantification process for the assessment of the effect of the alongshore sand migration on the coastline position. On the left, the assumed alongshore distributions of different coastline change percentile estimates is presented. Positive coastline change indicates accretion. The location of the intervention has been marked on the horizontal axis. On the right, the probability distribution plot of coastline change for one location (marked with a grey vertical line in the left graph) is presented.

The parametric distributions ($CC_{sandbars}$) quantifying the sandbar migration effect on coastline change were included last in the aggregation process (equation 3) to yield the aggregated probability distributions of coastline change under the combined effect of the selected processes: autonomous evolution, long-term wave climate variation, intervention impact and sandbar dynamics effect.

$$\mathbf{CC_{Cumulative}\,(m) = CC_{long\ term\ +\ intervention\ impact} + CC_{sandbars}} \quad (3)$$

Figure 4.28 and Figure 4.27 present the contributing elements and the results of the last step in the aggregation process. The parametric distributions selected to represent the sandbar dynamics effect have median values close to zero indicating almost equal probabilities of erosion/ accretion. As a result, incorporating this effect does not vary the location of the median but affects significantly the range of the resulting distributions. A 350% alongshore averaged increase in the interquartile range (430% for the 5-95% percentile range) can be observed between the aggregated distributions with and without the sandbar dynamics effect on the coastline.

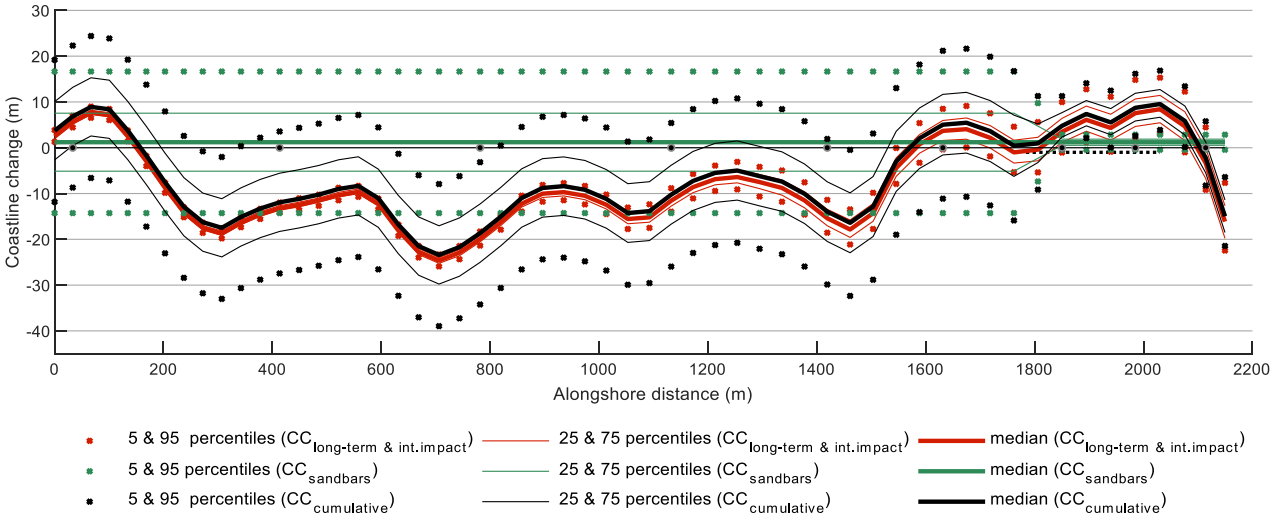

Figure 4.27: Overview of the coastline change percentile estimates for Anmok (red: climate change & intervention impact, green: sandbar dynamics, black: cumulative effect). The quartiles are shown with continuous lines, while the

5th and 95th percentile with x markings. Positive values of coastline change indicate accretion. The grey markings on the horizontal axis indicate the location of different cross-sections (points 1 to 9) for which probability density plots are presented (Figure 4.23). The black dotted line indicates the location of the intervention.

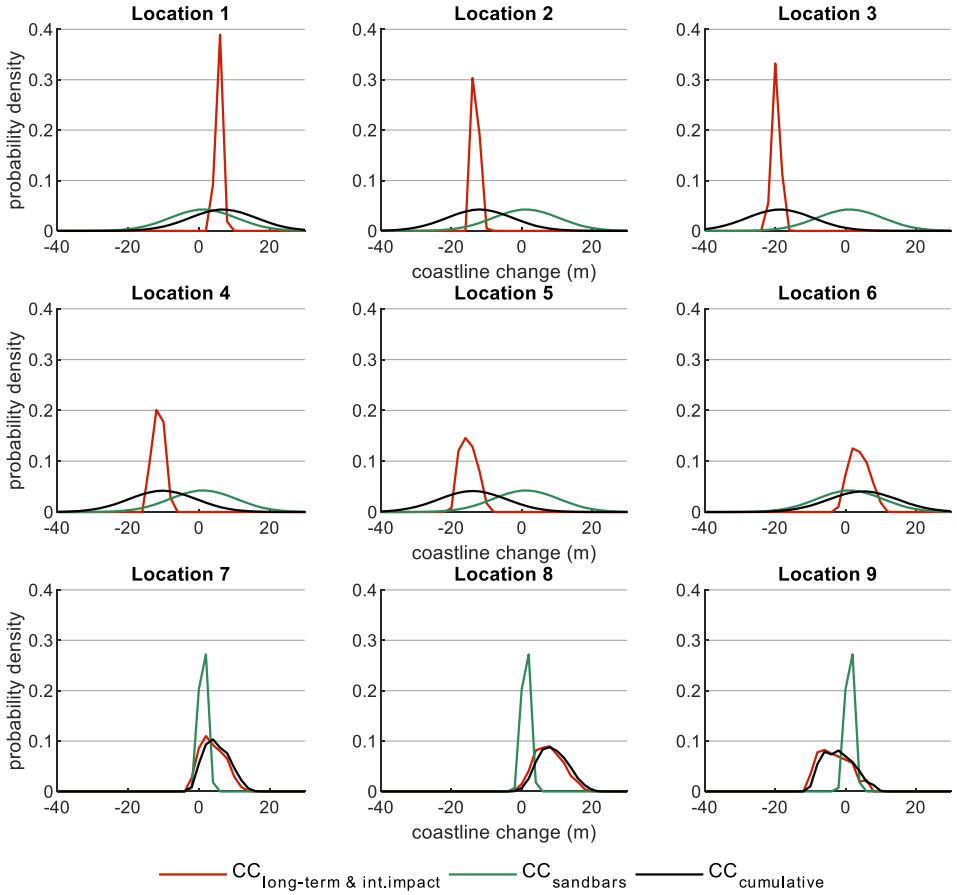

Figure 4.28: Probability density plots of coastline change (red: climate change & intervention impact, green: sandbar dynamics, black: cumulative effect) for different cross-sections along Anmok beach as defined in Figure 4.23.

The results show that the effect of the intervention is not fully quantified through the intervention net impact pdfs ($CC_{intervention\ impact}$) derived from the Delft3D simulations. Despite the assumption of independence between the processes, the influence of the submerged breakwater on the sandbar dynamics cannot be neglected. To accommodate this indirect effect of the intervention on the potential coastline change, an alongshore varying distribution was selected as described above. Consequently, the assessment of the overall intervention impact on the uncertainty of coastline change should be based not on the intermediate but on the final aggregation results incorporating the effects of all selected processes. To that end, Figure 4.29 is presented quantifying the uncertainty in the coastline change in 2035 under the cumulative effect of long-term processes and sandbar dynamics, with (black) and without (lilac) the effects of the submerged breakwater-nourishment. For the latter, the normal distribution (μ, σ) = (1.2m, 9.4m) was applied uniformly along the coast. In the area 1750m to 2150m both the direct and indirect impacts of the intervention can be observed: shift of the distributions towards the accretion side, by 6m on average over the shadow zone for the medians, and narrowing of the distributions, by 50% for 5-95 percentile ranges.

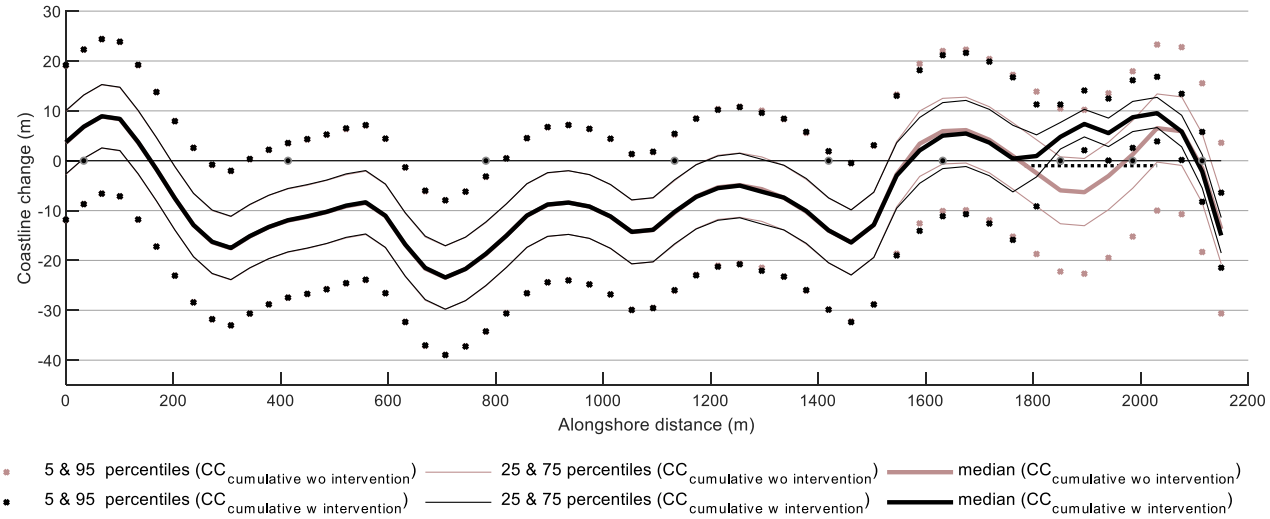

Figure 4.29: Alongshore distribution of coastline change percentile estimates under the cumulative effect of long-term processes and sandbar dynamics, with (black) and without (lilac) the effect of the considered intervention (SBW-nourishment). The quartiles are shown with continuous lines, while the 5th and 95th percentile with x markings. Positive values of coastline change indicate accretion. The grey markings on the horizontal axis indicate the location of different cross-sections (points 1 to 9) for which probability density plots are presented (Figure 4.23). The black dotted line indicates the location of the intervention.

The processes that govern the interaction of the crescentic sandbars and the coastline position are not very well understood until now. The distributions assumed to quantify the uncertainty of coastline position under the effect of sandbar migration with/without the presence of the submerged breakwater dominate the aggregated bandwidth and are characterised by significant statistical uncertainty. For this reason, this process is omitted from the aggregations carried out in the following sections.

4.3.3 Comparison with present framework

The uncertainty in the coastline change under the combined effect of long-term processes and the intervention (submerged breakwater-nourishment) evaluated probabilistically, as described in Section 4.3.1 was compared with the results of the scenario-based approach currently used in order to highlight the differences in the performance of the two approaches.

As mentioned in Section 3.4, in the currently used approach, the mean coastline change under the effect of different processes is selected as the output of the simulations with all variables evaluated at their mean values. Minimum/maximum coastline change estimates are evaluated using 'one-at-a-time' sensitivity simulations for the individual models. The total number of simulations implemented was 8 for UNIBEST-CL and 14 for Delft3D (7 including the intervention and 7 without it). To estimate the aggregated effect, a superposition of the mean coastline change estimates and minimum/maximum coastline change bandwidths was carried out.

The resulting mean, minimum and maximum coastline change estimates were visualised with the results of the fully probabilistic approach presented in this thesis; using LHS on the individual schematisations (80 simulations for UNIBEST-CL+ and 160 simulations for Delft3D in total) and a MC approach to convolute the resulting probability distributions. Figure 4.30 and Figure 4.31 feature the comparison of the aggregated uncertainty estimates of coastline change from the two methods. For comparisons on the intermediate results of the process the reader is referred to Appendix F.

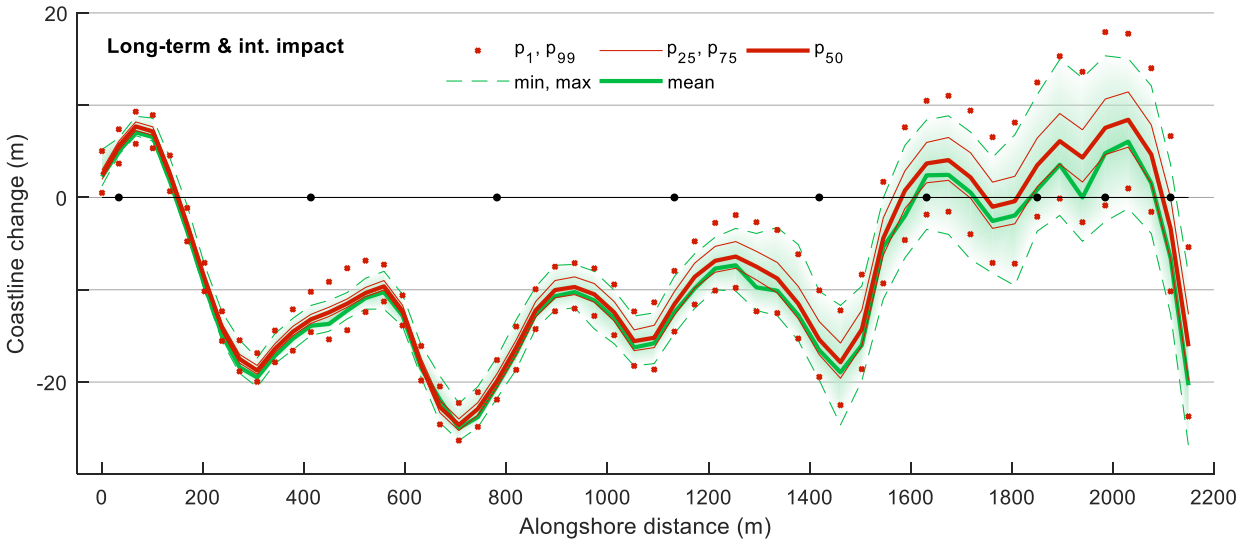

Figure 4.30: Overview of coastline change estimates under the combined effect of long-term processes and intervention for Anmok beach using two different approaches. Percentiles of coastline change (red) were estimated using LHS (n=80) on the individual model schematisations and convoluting the resulting probability distributions of coastline change using MC approach. Mean coastline change (green continuous line) was estimated by linear superposition of the model outputs with all variables evaluated at their mean values. Min/max coastline change (green dashed lines) were defined using linear superposition of uncertainty bandwidths estimated through sensitivity analysis. Positive values of coastline change indicate accretion. The black markings on the horizontal axis indicate the location of different cross-sections for which probability density plots are presented (Figure 4.23).

Mean coastline change was compared with the median and the mode, statistics that have a practical value for coastal zone managers. The median indicates the coastline change with equal probabilities of exceedance/non-exceedance (0.5) while the mode shows the coastline change with the highest density, the most probable result. The results show that the scenario-based mean coastline change does not correspond to the median coastline change. In fact, the deterministically defined median coastline change corresponds to 0.2/0.3 exceedance probabilities for the majority of cross-sections along the coast. Additionally, the mean coastline change estimates do not coincide with the mode of the probability densities.

The minimum and maximum estimates of coastline change were compared with the 1st and 99th percentiles of coastline change. Indeed, the sensitivity analysis sourced minimum and maximum coastline change estimates provide a rough approximation of the uncertainty present. However, they tend to overestimate the maximum erosion and at the same time underestimate the maximum accretion. The scenario-based approach leads to lower uncertainty ranges. The differences are larger for the south cross-sections considered where the characteristics of the intervention impact dominate and smaller, but still important for the norther cross-sections where the characteristics of the long-term processes impact dominate.

These differences stem from the incomplete estimation of the uncertainty present in the model output using a scenario-based approach and the invalid underlying assumption of model linearity. They can also be observed in the intermediate model results (Appendix F) and are transferred through the aggregation process to the aggregated result.

Figure 4.31 highlights the added value of the proposed framework. The scenario-based approach produces rough uncertainty estimates but is unsuited for any quantified results. The resulting coastline change estimates do not provide any information about the distribution of probabilities along this range. The full probabilistic approach applied in this thesis can provide this missing information. With adequate sampling, the shape of the probability distribution is acquired. The range of possible coastline change can be estimated in terms of different confidence intervals. Apart from the median and extreme percentiles, any percentile of interest can be calculated (along with a

quantified/qualitative precision level) or inversely, the likelihood of any realization of interest can be quantified.

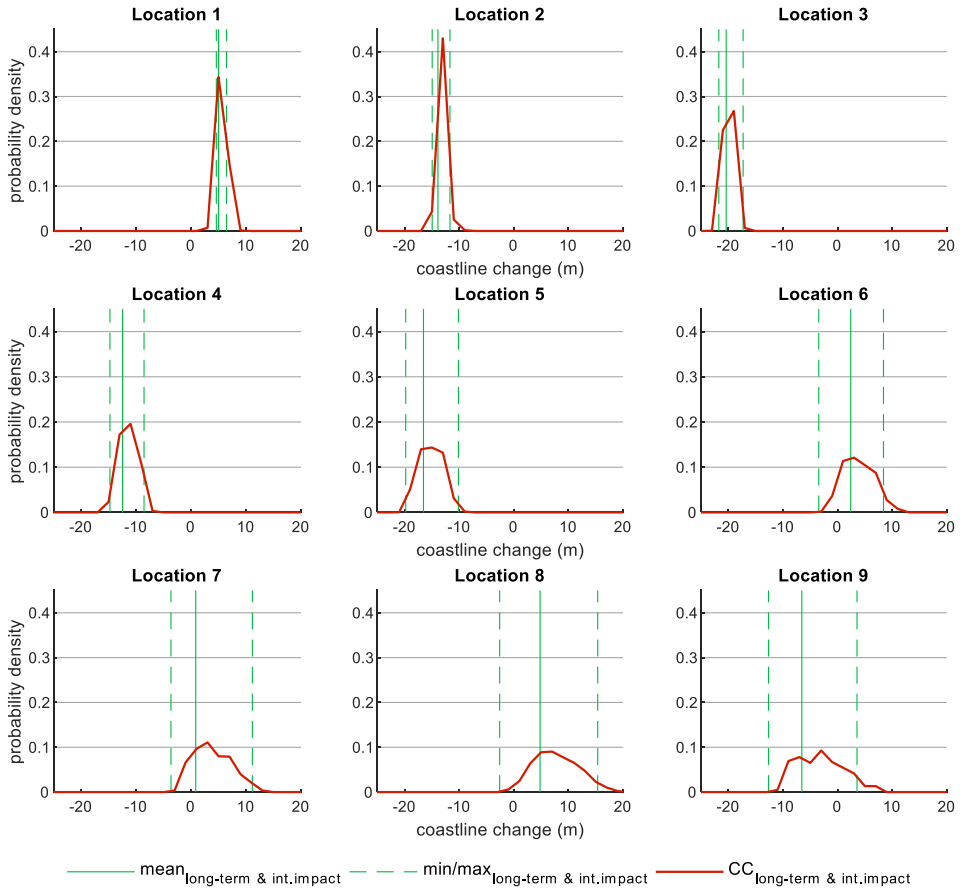

Figure 4.31: Coastline change estimates under the effect of long-term processes for different cross-sections along the coast (Figure 4.23) using two different approaches. Probability density plots (red) were estimated using LHS (n=80) on the individual model schematisations and convoluting the resulting probability distributions of coastline change using MC approach. Mean coastline change (green continuous line) was estimated by linear superposition of the model outputs with all variables evaluated at their mean values. Min/max coastline change (green dashed lines) were defined using linear superposition of uncertainty bandwidths estimated through sensitivity analysis. Positive values of coastline change indicate accretion. The black markings on the horizontal axis indicate the location of different cross-sections for which probability density plots are presented (Figure 4.23).

4.3.4 Uncertainty quantification for alternative interventions

Subsequently, the uncertainty around the coastline change estimates under the joint effect of the long-term processes and the impact of alternative interventions was quantified. Apart from the submerged breakwater-nourishment impact that was considered in the previous sections, the alternative interventions include a set of submerged breakwaters-nourishment (2SBW-nourishment, Figure 4.32-b) and an emerged breakwater-nourishment (EBW-nourishment, Figure 4.32-c).

The mechanisms that shape the coastline in the case of the 2SBW-nourishment are similar to those described for the submerged breakwater. The set of submerged breakwaters creates a more extensive shadow zone that is closed off on the south side from the Gangneung port breakwater. Diffraction, accretive or erosive alongshore sediment transport gradients and the horizontal compensation to the onshore flow over the submerged breakwaters impact mainly the coastline at the north end of the submerged breakwater. As for the last intervention considered, with minimal water level variations during the simulation, the breakwater with crest level at MSL practically eliminates the sediment transport capacity in the shadow zone as the incident waves break upon reaching the structure. Diffraction and accretive/erosive alongshore sediment gradients can be observed at both sides of the shadow zone.

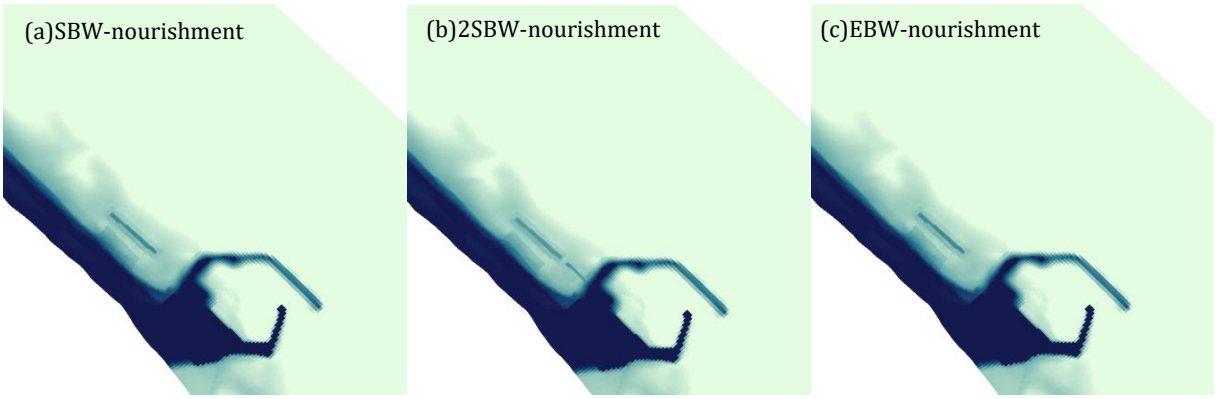

Figure 4.32: Schematisation of the interventions considered. (a) Submerged breakwater-nourishment: the submerged breakwater has dimensions 250m x15m and crest level at -0.5m MSL. (b) Set of submerged breakwaters-nourishment: the submerged breakwaters have dimensions 250m x15m and 110m x 12m, the crest level is at -0.5m MSL and the gap spans for 30m. (c) Emerged breakwater-nourishment: the emerged breakwater has dimensions 250m x15m and crest level at MSL. In all the figures the submerged nourishment (11000m^3) was simulated with the same characteristics.

For each of the alternative interventions a set of Delft3D simulations was used to evaluate the net impact of the interventions ($CC_{intervention\ impact}$). The resulting probability distributions were subsequently combined with the UNIBEST-CL+ derived probability distributions quantifying the uncertainty in the autonomous evolution and the effect of the long-term wave climate variations (equation 1). For more details on the application of the aggregation process on the alternative interventions the reader is referred to Appendix G.

Figure 4.33 presents the results of the aggregation process for the three interventions. Alongshore distributions of coastline change percentile estimates under the cumulative effects of the long-term processes and the net intervention impact (red) as well as only for the effects of long-term processes (yellow) are presented. This allows for the comparison of the intervention alternatives effect in terms of the change induced by their inclusion/exclusion from the aggregation process.

In the alongshore distribution graphs 4 regions can be discerned. Along the first area, spanning from 0 to 1500m, the median effect of all interventions has been estimated at or close to zero and the dispersion of the intervention impact probability distributions is for the most part smaller than the dispersion of the other aggregation component. As a result, the aggregated distributions resemble the long-term distributions very closely in terms of location, shape and dispersion. For this coastline part the interventions have minimal effect on the cumulative probability distributions of coastline change which are identical for all three interventions. From 1500m to 1700m (as well as for 2100-2150m) the long-term percentile estimates are shifted downwards when the net intervention impact is aggregated. This downward shift is in the order of 1-2m for the medians, for all different interventions. It is due to the high probabilities of negative coastline change under the net effect of the intervention for the area downdrift of shadow zone.

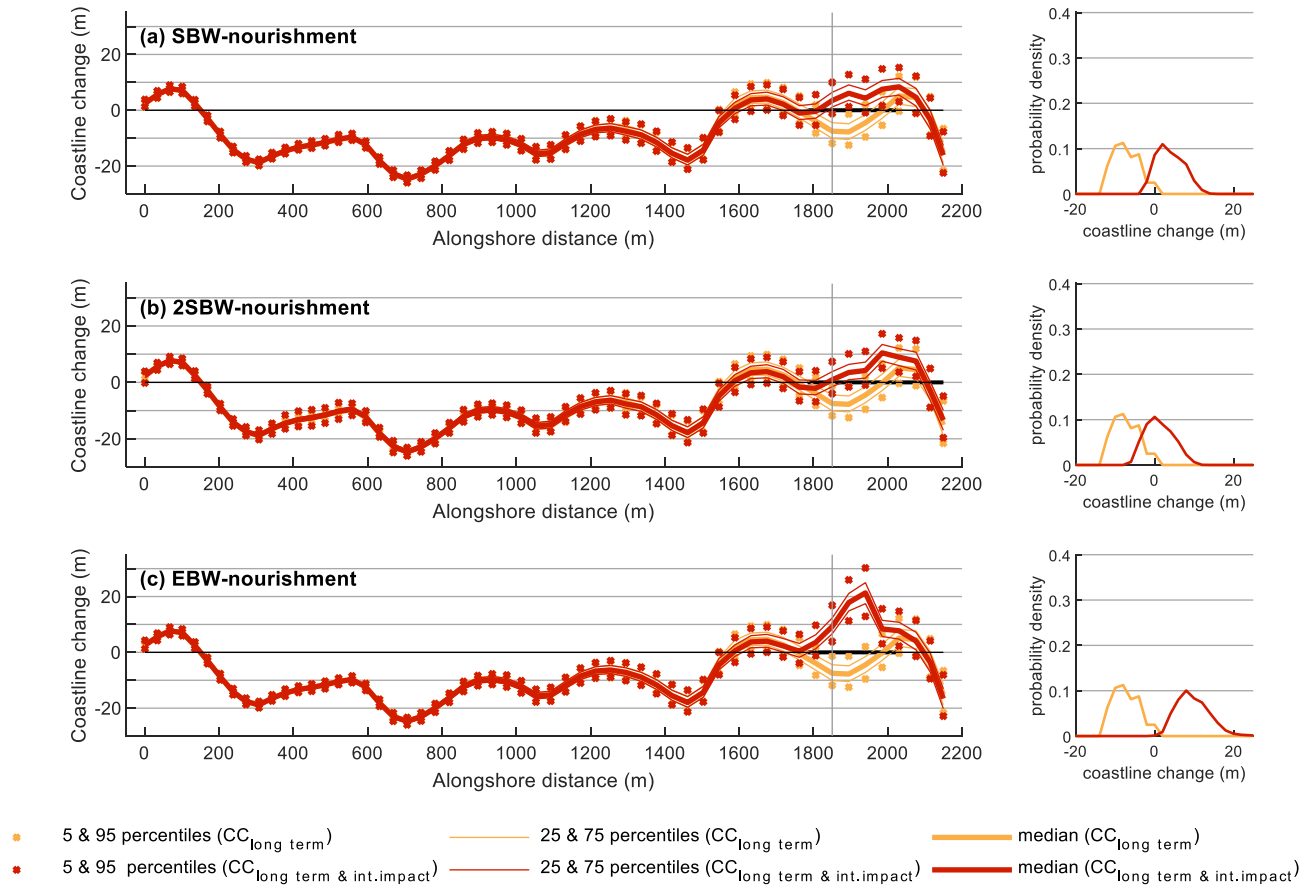

Figure 4.33: Alongshore distribution functions of different coastline change percentile estimates for the different interventions considered (left) and probability distribution plots of coastline change (right) for one location, marked with a grey vertical line in the left graphs. Yellow colour is used for the probability density plots/ percentile estimates quantifying the uncertainty in the autonomous evolution and the effect of long-term wave climate variations (same in all the graphs). Red colour is used for the probability density plots/ percentile estimates quantifying the aggregated effect of the long-term processes and the net intervention impact.

The zone 1700m to 2150m is the area for which the effect of the different interventions is most obvious on the aggregated results. The common trend that can be observed for all interventions is a lift of all probability distributions in this zone towards the accretion region. However, the magnitude and the stretch of this effect varies. As mentioned in Section 4.3.1 when the effect of the SBW-nourishment is included in the aggregation the projected accretion (median) reaches up to 8m, while there is 5% possibility that the shoreline propagates more than 10m in this area. A slight increase (4%) in the 5-95 percentile range averaged for the shadow zone of the intervention can be observed. The spatial range of the SBW-nourishment accretion effect, measured as the alongshore distance along which the median of the net intervention impact ($CC_{\text{intervention impact}}$, graphs in Appendix G) is greater than zero, is ~330m. When the second intervention (2SBW-nourishment) is considered, under the cumulative effect of all the considered processes the expected coastline change in the area reaches up to 10m, the 5-95 percentile range increased by 3.6% on average, compared to the respective range when the intervention impact is not considered. The spatial range of the accretive effect for this intervention is ~340m. Lastly, in the shadow zone of the emerged breakwater the projected accretion (median) reaches up to 21m locally in contrast to the expected 8m of erosion when the emerged intervention is not considered. Behind the emerged breakwater a 17% increase in the 5-95 percentile range can be observed with respect to the respective range without the intervention impact. The length of the accretive effect is ~340m.

Apart from the position of the mean and extreme percentiles, various other indicators of the performance of the different intervention designs can be derived from the probability distribution

functions that are now available. These indicators may differ according to the aim of the intervention design and the demands of the coastal zone managers/stakeholders. Figure 4.34 features some of these indicators. For an intervention aiming to reduce/prevent erosion locally, the probabilities of erosion or erosion past a specific threshold in a specific time horizon and under the cumulative effect of different processes can be assessed. Figure 4.34 (a) and (b) showcase that the implementation of one of the considered interventions can significantly decrease the probabilities of erosion and erosion exceeding 5m locally. Clearly, the intervention design including the two submerged breakwaters and nourishment is the least effective in reducing the probabilities of erosion and erosion exceeding 5m, while the emerged breakwater nourishment design is the most effective. For interventions aiming to induce accretion the probability of different accretion levels along the coastline can be evaluated to assess the level of success of the designs. When the probability of accretion exceeding the 5m threshold is considered (Figure 4.34 (c)), the intervention design including the emerged breakwater gives the higher probabilities for the majority of cross-sections considered.

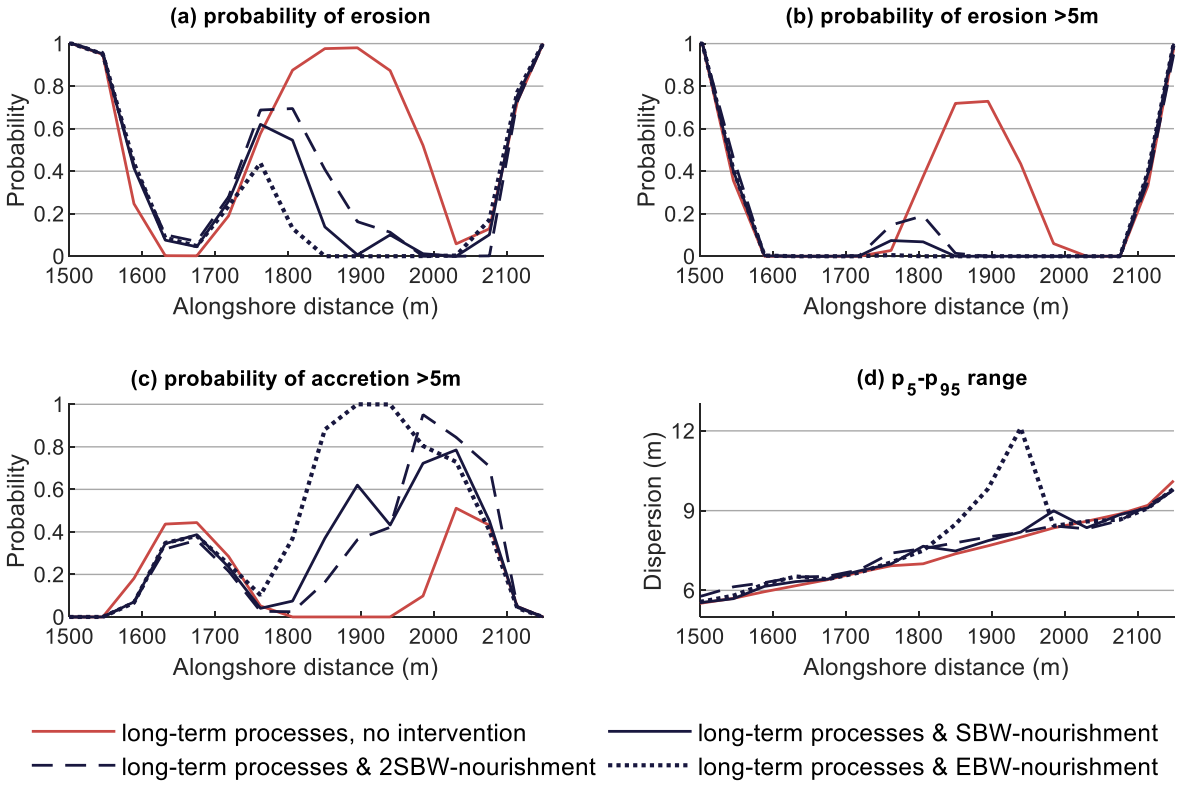

Figure 4.34: Various indicators of performance for the different intervention designs and the absence of interventions: (a) alongshore distribution of probabilities of erosion, (b) alongshore distribution of probabilities of erosion exceeding 5m, (c) alongshore distribution of probabilities of accretion exceeding 5m, (d) alongshore distribution of the p_5, p_{95} range as a measure of dispersion of the probability distributions of coastline change.

Lastly, an indication about the robustness of the proposed interventions can be obtained by assessing the dispersion of the aggregated distributions. The narrower the resulting distributions of coastline change, the less responsive the intervention is to uncertainty. Interventions that yield narrower distributions may appeal better to risk-averse coastal zone managers even when the expected coastline change is not the optimal. Figure 4.34 (d) features the alongshore distribution of 5^{th}-95^{th} percentile range, as a measure of the coastline change dispersion, under the effect of long-term processes with/without the intervention impact. For all the cases examined, the dispersion of the coastline change distribution increases from the north end towards the south end of the considered domain. This trend originates from the forcing uncertainty in the long-term processes acting on the coast, manifested in the varying rotation of the final coastline, affecting more the cross-sections closer to the edges of the coastal cell. Generally, the different interventions result in an incremental increase of the dispersion of the coastline change probability distributions. At the location of the intervention a

local increase in the distribution dispersion can be observed for the emerged breakwater-nourishment design. Although this design yields the best results in terms of median coastline change and probabilities of erosion/accretion, the higher range of uncertainty in the intervention's effect in the area of interest could lead the selection towards another design.

5 Discussion

The previous chapters presented the methods implemented and the results used to address the research questions of Section 1.3. In this chapter we discuss the main assumptions made that shaped the research, the restrictions of the methods as well as any points of interest and opportunities that appeared during the process and have not been elaborated previously.

5.1 Selection of the uncertain variables

The work carried out in this thesis provided a framework for uncertainty propagation through the morphodynamic simulations and the aggregation process in order to obtain quantified estimates of the uncertainty around the coastline change projections under the effect of multiple processes. However, the meaningful and successful implementation of this framework relies on the assumption that the input uncertainties selected capture the uncertainties in the system. This refers not only to the identification of the input variables that account for most of the variation of the output, but also to the ranges selected. Assigning too small ranges will lead to results that do not represent the full uncertainty present. On the other hand, by including larger ranges we may stand on the safe side (as extreme events will be included in the analysis) but that would most probably lead to an unnecessary increase in the computational load to get an estimate of the probability density function. Additionally, larger input uncertainties are expected to lead to larger output uncertainties and contaminate the aggregation results.

In this study knowledge on the specifics of the case study, the model schematizations, the aggregation timescale and variable of interest was available to guide the selection of the uncertain variables and the selected ranges. This creates confidence in the selection of the input uncertainties carried out by means of expert consultation, literature review and sensitivity analysis on the model schematizations. This selection is very much dependent on the model structure and the formulas used, the processes modelled, the target output and the relevant timescales. That means that the relative importance of variables can change when there is a change in one of the above-mentioned factors. In an aggregation context, where multiple schematizations of a single model may be used, the selection of uncertain variables should consider the differences per model schematization. A more complete and comprehensive approach would include cataloguing the variables and parameters used in each model and the appropriate ranges for each model schematization, and conducting a wider sensitivity analysis using the parameters/variables that fall under the uncertainty categories considered.

For the two methods of uncertainty quantification applied in this study (i.e., SMC and LHS) the number of variables to which probability distributions are assigned is not restricted. In practice, if extra input uncertainties are included in the analysis increasing the output variance, more samples will be required for both methods to reach a certain precision level. Most importantly, as the number of input variables increases the relative efficiency of LHS over SMC is expected to reduce as the same number of randomly selected input sample sets is used to cover an input space with additional dimensions. Although in literature there are no conclusive results as to the maximum number of variables for which LHS converges faster than SMC, the use of LHS with computationally expensive coastal

morphodynamic models leads to a more restricted selection of input uncertainties in order to maintain the relative advantage of the statistical method.

Lastly, the aggregation process should not influence the selection of the uncertain inputs. The resulting coastline change probability distributions are combined independently from the uncertainty sources that led to those probability distributions. As mentioned before, the selected variables reflect the model structure and the simulated processes which may differ significantly across the different models or model schematizations used. Introducing new features (e.g., an intervention) in a model schematization may also lead to differentiation to the relative significance of different variables. Even for variables that are expected to introduce significant uncertainty in different models (e.g., significant wave height), the ranges assigned should be selected according to the relevant processes and timescales. In conclusion, a critical selection of the input uncertainties and awareness about the uncertainties quantified in the model results is more important than uniformity of the uncertain inputs across the different models.

5.2 Uncertainty quantification

Both sampling techniques used in this study can deal with correlations between variables (Iman et al., 1982; Morgan et al., 1992). Nevertheless, in this study the sampling from the uncertain input distributions took place under the assumption of no dependence/no correlation of the individual distributions. However, this assumption is not generally applicable. As mentioned in Section 3.3, H_s and incident wave direction are generally correlated for every coastal region. However, for the small values of directional variance considered in this study this dependence can be safely omitted. At the same time, independence was assumed between H_s and T_p in the spectral boundary conditions of the UNIBEST-CL+ and Delft3D model schematisations. In this study, the significant wave height was varied using sampled values of an amplification factor, while T_p was kept constant. Although the effect of this assumption has not been investigated further, it would be recommended for further investigations to incorporate this dependence by applying correlated statistics.

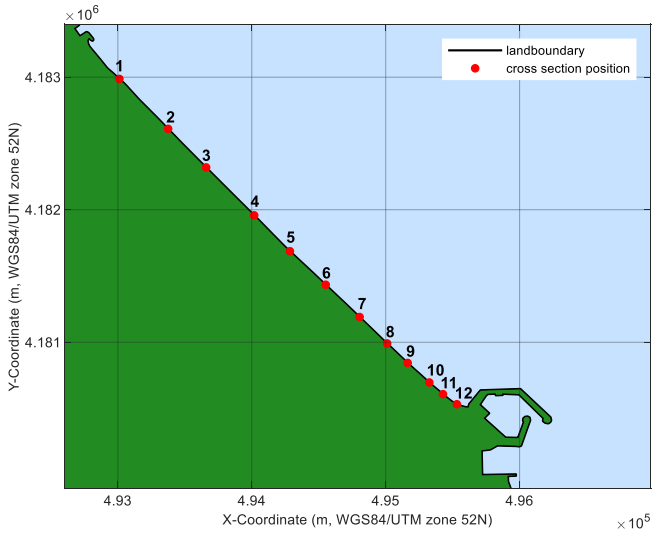

Figure 5.1: Spatial plot of Anmok beach. The markings show the location of the cross-sections for which probability density functions of coastline change will be presented.

The procedure of uncertainty quantification offers the opportunity of investigating the uncertainty evolution in time. Figure 5.2 presents the time evolution of the probability distributions of coastline change estimated using the UNIBEST-CL+ simulation and LHS method (n=80) as described in Section 4.1.1 . The cross-sections located at the centre of the coastal cell are only minimally affected by the uncertainty relevant to the reorientation of the coast. As a result, after the changes in the first 5 years creating the initial probability density function, this initial pdf does not change a lot in terms of location/dispersion. On the other hand, for cross-sections towards the edges of the coastal cell, there

is significant change in the coastline change uncertainty between the timepoints considered. The location of the distribution changes through time showing the progression of erosion/accretion at the edges of the coastal cell. Additionally, the dispersion of the distributions increases indicating increasing uncertainty in time. The rate of change in the location and dispersion of the distributions is higher towards the start of the simulation and subsequently decreases as the coast approaches the equilibrium orientation.

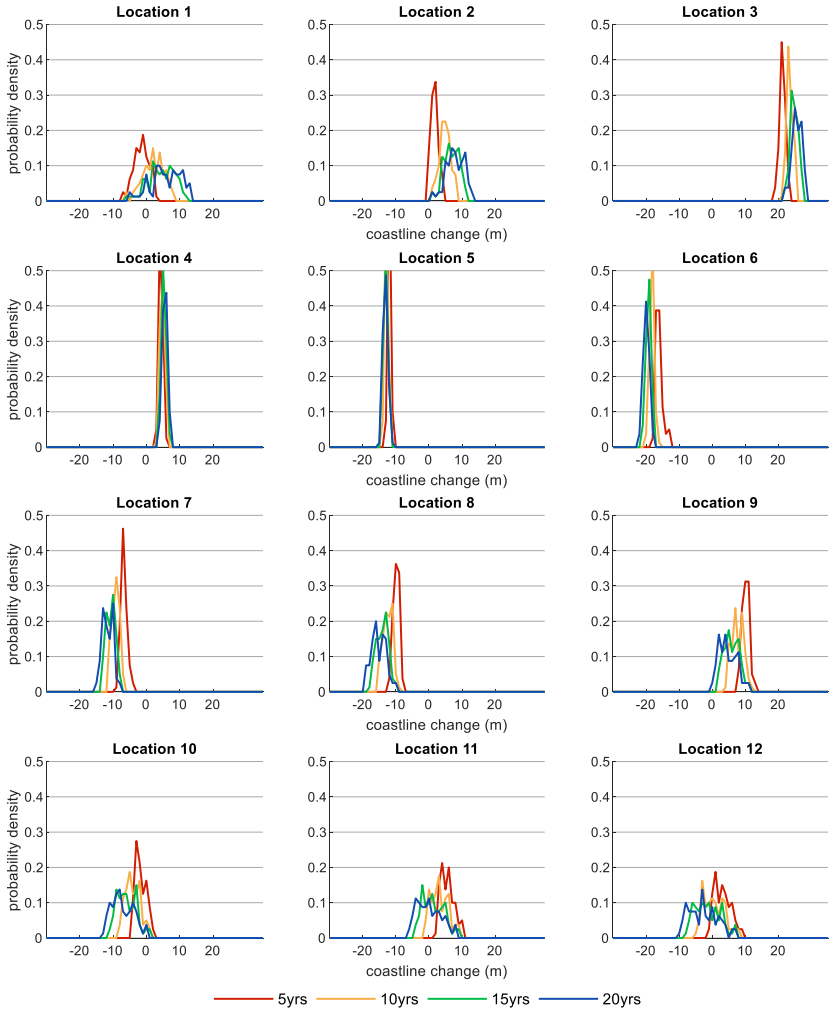

Figure 5.2: Probability density plots of coastline change at different cross-sections (as marked in Figure 5.1) along the coast for different timesteps (red: 5years, yellow: 10 years, green: 15 years and blue: 20 years). Positive coastline change indicates accretion. The probability density plots have been derived using Latin Hypercube Sampling (n=80) on the UNIBEST-CL+ simulation varying the uncertain parameters as described in Section 4.1.1 .

The concept of precision used to evaluate and compare the performance of the different methods describes the sampling error, the fact that a sample will be inevitably different from the population. Sampling precision indicates the variation in repeated estimates of the response (e.g., for different percentiles) and is in this thesis quantified using statistics such as the confidence intervals and standard error. Wide confidence intervals/large standard errors indicate high variability in the repeated response, low precision and thus unreliable results. Accuracy describes systematic errors that can introduce bias in the estimators used. When sampling is used to estimate an unknown probability distribution function, bias in the statistical estimators could be introduced from the assumption of a specific distribution. According to Helton et al. (2003) both SMC and LHS give unbiased estimates of the distribution when percentile estimates are used.

Most importantly, in the context of simulating the uncertain coastline change under the effect of different processes, accuracy relates to the performance of the model itself and its capacity to simulate

the relevant processes and the response. Governing equations and modelling assumptions impose restrictions on model applicability. Disregarding or misinterpreting these restrictions can lead to unrealistic outputs. For process-based morphodynamic models, modelling choices such as the use of upscaling factors, the timestep, or sediment transport formula may influence the accuracy of the modelled response while frequently, improvements in model accuracy come at a computational cost. Processes such as calibration and verification are used to enhance and measure the model's capacity to reproduce the response for a specific case study. In case studies where modelled bathymetry has been verified against measurements, the model skill in reproducing measured bathymetry is either judged qualitatively or quantified using indicators such as the Root Mean Square Error or the Brier Skill Score, with mixed results (Judith Bosboom et al., 2014; J Bosboom et al., 2014; G. Lesser et al., 2004; G. R. Lesser, 2009; A. P. Luijendijk et al., 2017; Sutherland et al., 2004). For the utilisation of model coastline change estimates in thein real-world applications, in a deterministic or probabilistic context, an absolute measure of the model accuracy or the model uncertainty as demonstrated in the output of interest would be useful. Minimizing model uncertainties is not a first priority when model outputs are used for comparison among different management alternatives. Nevertheless, model uncertainties should be smaller than the difference in the management alternatives' performance for a valid comparison.

In this study, we estimated the precision achieved with different sample sizes using SMC and LHS on the Delft3D and UNIBEST-CL+ schematisations for the selected uncertain inputs. We showed that for the UNIBEST-CL+ schematisation and small sample sizes LHS gave higher precision estimates than SMC. In different applications with different model schematisations and uncertain variables/ranges, the convergence rates and precisions for the two methods and selected sample sizes can be different than the ones observed in this study. Nevertheless, the approach presented and applied in this study for uncertainty quantification in the model output remains valid.

5.3 Multi-model coastline change uncertainty aggregation

The numerical convolution approach suggested, using MC sampling, allows for the propagation of the quantified uncertainties through the aggregation process to the aggregated coastline change estimates. The presented framework provides insight about the uncertainty around the expected morphodynamic response that is not available from the currently used scenario-based approach. It enables the probabilistic assessment of intervention performance under the effect of different processes in terms of the likely coastline change realisations and the induced coastline change variability.

Inclusion of storm impacts on coastline change in the aggregation process would make the probabilistic coastline change assessment more meaningful. The inclusion of short-scale processes' impact could be achieved using one of two different approaches that will be discussed briefly in this paragraph. During the management horizon considered, storms of different magnitudes are expected to hit the coast at various points in time. After a storm, the coast is able to recover partially or completely from the storm erosion until the next storm hits. As a result, storm impact cannot be included in the aggregation in the same way that the structure impact was considered, assuming that the coastline change reaches a steady state and remains unchanged afterwards. An approach that would account for the stochastic sequencing of storm events and the recovery processes, not omitting the effect of interventions on storm impact would be more appropriate. Such approaches have been developed and presented by Callaghan et al. (2008) and Ranasinghe et al. (2009). An alternative approach would be to incorporate the storm impact as an 'envelope' effect assuming that a storm of defined return period hits the coast towards the end of the management horizon defined, such that no recovery has taken place. Assuming a distribution of storm induced coastline change the effect could then be aggregated with the effects of the other processes in a manner similar to the inclusion of sandbar dynamics effects.

The probabilistic investigation of coastline evolution with the framework presented in this thesis provides extra value for coastal zone managers and decision makers. Not only does it highlight the uncertainty around the deterministic morphological response, it provides quantified estimates of this uncertainty, information that was not available through the currently applied approach. It enables the comparison of alternative interventions based on the full range of possible results and their probabilities and lays the foundation for coastline recession risk reduction quantification. Undoubtedly, a probabilistic investigation of coastline evolution is a complex process. The uncertainty quantification part can increase significantly the computational costs compared to a sensitivity analysis. Adding to that, extra time and research need to be allotted to obtain the extra information needed to complete the process. The large amount of already available knowledge and data for this specific coast made the application of the presented methods in this study feasible. The application of the methods provided insight for the expected results, intuitive knowledge about the aggregation mechanisms and leads for future research. Whether the presented framework is applicable for other case studies depends on the case-specific balance between added value and the available resources.

6

Conclusions & Recommendations

This study examines the use of statistical methods to quantify and aggregate uncertainty in coastline evolution based on multiple process-based models. To this end we investigate the application of two sampling techniques (i.e., Standard Monte Carlo -SMC and Latin Hypercube Sampling -LHS) on two types of numerical models (i.e., Delft3D and UNIBEST-CL+). Subsequently, a Monte Carlo sampling technique was suggested as a method to combine probabilistic coastline change estimates from individual processes/models into aggregated coastline change distributions. Lastly, the statistical methods and aggregation framework are applied on Anmok beach, South Korea, to assess the impact of alternative interventions on the coastline change uncertainty under the cumulative effect of different processes in a 20-year management horizon.

This chapter exhibits the outcome of this study, in the context of answers to the research questions of Section 1.3. Additionally, recommendations for future research are outlined.

6.1 Conclusions

1. Which statistical methods can be used with process-based morphodynamic models (such as Delft3D, Unibest-CL+) to provide precise probabilistic estimates of coastline recession on varying timescales in a computationally efficient way?

From the statistical methods initially reviewed in this study, Standard Monte Carlo (SMC) and Latin Hypercube Sampling (LHS) were found to satisfy the applicability criteria for uncertainty quantification in coastline change estimates from process-based models. Both methods are able to deal with the non-linearity and complexity of coastal morphodynamic models, the large input uncertainty ranges expected, and yield estimates of the full probability density functions of coastline change.

The results of SMC and LHS application on UNIBEST-CL+ and Delft3D model schematizations showed that both methods with adequate sampling can produce probability distribution outputs for coastline change when applied to the morphodynamic models. Evaluation of SMC and LHS relative performance highlighted the methods' advantages and drawbacks and the implications for coastal engineering studies.

SMC remains the most suitable method for coastline change uncertainty quantification for models such as UNIBEST-CL+ with small simulation durations. The method yields results of readily quantifiable precision and the rate of convergence can be explicitly expressed as a function of the sample size used, enabling engineers to meet potential strict precision requirements of the analysis. The observed faster convergence of LHS for small sample sizes supports the selection of this method with process-based models whose large computational requirements restrict the number of simulations. The capacity of the method for faster convergence is highlighted for larger uncertainty ranges and non-uniform input distributions. On the downside, there is no formula available relating the sample size with a target precision and for a given sample size, only conservative/upper estimates of the achieved precision can be obtained.

2. How can the probabilistic model results of the individual timescales be integrated to assess the impact of the selected mitigation/adaptation measures?

The second research question is addressed through the answers to the following two subquestions.

a. What are the steps in a generic approach for the aggregation of probabilistic model outputs to arrive to one probability distribution function of coastal recession?

A multi-model coastline change aggregation approach is frequently used when the driving morphodynamic processes transcend the applicability limits of individual process-based models or the possibilities for model coupling. In this thesis, the scenario-based aggregation approach developed by Deltares was extended to accommodate the synthesis of probabilistic coastline change estimates. A numerical convolution approach involving Monte Carlo (MC) sampling was suggested for the linear superposition (i.e., aggregation) of the individual coastline change probability distributions. The advantages of the MC approach over alternative analytical/numerical convolution methods include speed, ease of implementation and comprehensibility. With sufficient sampling the method itself does not contribute extra imprecision to the aggregated distribution; the imprecision of the aggregated probability distribution is dominated by the lowest precision component.

Comparison of the probabilistic and scenario-based aggregation framework outcomes illustrates the incomplete picture of uncertainty captured from the latter and the added value from the application of the first. Application of the scenario-based framework yielded more conservative coastline change estimates and underestimated the uncertainty range. By contrast, the presented probabilistic framework allows for quantified coastline change uncertainty estimates. The framework provides additional information concerning the precision of the aggregated uncertainty estimates and the distribution of uncertainty across its range. Additionally, it enables the evaluation of various coastline change percentiles, confidence intervals and probabilities of any coastline change realisation of interest.

b. What is the impact of the considered measures on the uncertainty of the coastline position for the case study of Anmok beach?

For a 20-year management horizon, the autonomous evolution of Anmok beach, the effects of long-term processes and the net impact of three alternative detached breakwater-nourishment designs were evaluated, using Latin Hypercube Sampling, and subsequently aggregated to estimate the cumulative uncertainty in coastline change. The use of the probabilistic uncertainty quantification and aggregation framework allowed for the definition of various indicators to assess the performance of the considered interventions. Percentile estimates of coastline change, the probabilities of exceeding defined erosion/accretion thresholds and the uncertainty range assigned to a confidence interval as an indication of intervention robustness were evaluated. From the designs considered, the emerged breakwater-nourishment yielded the best results in terms of erosion/accretion probabilities. However, the intervention lead to a significant increase of the uncertainty range in the predicted coastline change locally. When included in the aggregation process, the effect of sandbar dynamics dominated over the other contributing processes due to the high variance in the selected distributions.

6.2 Recommendations

Points of interest for further research and practical applications have been identified during the course of the present research topic. They are briefly presented in the next paragraphs.

Storms are short-term processes that affect coastal morphology and coastline position on coastal stretches worldwide. The joint effect of storms and longer-term processes such as climate change or intervention impacts is defining for many management practices in the coastal zone, most importantly for the creation of setback lines or zoning restrictions. As discussed in Section 5.3, the recurring

character of storms and the relevant recovery processes do not allow the direct inclusion of storm impacts in the presented aggregation framework. Future research should focus on the simulation of the cumulative storm impact on coastline position incorporating the recovery processes' effect. Statistical methods as the ones presented in this thesis could then be used for the quantification of uncertainties around the coastline position estimates and the inclusion of this component in the aggregation process.

The applicability of the presented framework in real-world coastal management studies requires confidence in the capacity of models to successfully simulate the system response under the effect of the relevant processes. Extra research on the relative importance and quantification of model uncertainty is therefore recommended. Coastline change verification against bathymetry measurements or remote sensing extracted coastline positions can provide quantified estimates of the model accuracy on the output of interest (e.g., coastline change error bandwidth). Sensitivity analysis on the effect of different transport formulations on the resulting coastline change or output comparison from different models applied on the same case study could provide an indication/quantification of the uncertainty manifested in the model output due to model structure and modelling assumptions.

A comparison between the performance of the two considered uncertainty quantification methods (i.e., SMC and LHS) for a Delft3D schematisation and/or other model schematisations would be advisable. Such an analysis could not lead to generally applicable conclusions about the sample size required for specific precision targets. Nevertheless, it would lead to more clear conclusions about the relative performance of the statistical methods on the different models and could be used as validation of the conclusion of this thesis that LHS is generally preferable to SMC in terms of the achieved precision for computationally expensive models when only small sample sizes are feasible.

The results of uncertainty quantification can be used to obtain more information on the response of the models to parameter variations than could be obtained from the results of the OAT sensitivity analysis conducted. The use of scatter plots of input and output values, correlation coefficients or regression analysis expected to define the degree of linearity of the relations between each input variable and the output as well as the relevant importance of these input variables. Especially for Delft3D, it could be used to explain the patterns of bimodal model behaviour observed in the resulting coastline change probability distributions.

The assumption of negligible interdependences between the long-term processes and the intervention impact is generally valid for the specific case study. However, for large coastline change uncertainties or different implementation times of the interventions the effect of the long-term processes on the intervention impact may be important. Additionally, for studies evaluating large-scale interventions, the potential effect on the long-term processes should not be omitted. Inclusion of some aspects of the interdependencies could be achieved by a suitable selection of the simulation plan: selection of suitable initial bathymetries/coastline positions for the simulations of the intervention impacts or inclusion of simulations of the long-term processes incorporating the large-scale interventions respectively. Utilisation of the presented uncertainty aggregation framework in additional case studies will help define its applicability limits and explore ways to possibly extend them. However, when the coupled behaviour cannot be sufficiently captured by the composite approach used in this study, the use of coupled models or models that cover multiple timescales should be considered.

Uncertainty quantification for coastline change estimates under the combined effect of different processes is the first step towards a risk-informed coastal zone management and risk-based evaluation of coastal interventions. Risk is commonly defined as the product of the probability of an event and the consequence of the same event. Combining the coastline change probability distributions with quantified estimates of coastline change consequences (e.g., economic, environmental, safety related)

would lead to risk probability distributions under the effect of different coastal processes and in extent to the evaluation of risk reduction/increase expected due to intervention implementation.

Additionally, the aggregation framework could be used to investigate the combined uncertainty evolution through time. Defining several timesteps, selecting accordingly the simulation plan and accounting for the potential interdependencies between processes could provide insight into the evolution of the compound uncertainty through time and the derivation of the initial and longer-term probabilistic impact of interventions. Investigation of such an application of the framework presented in the present study could be applied for the design/assessment of interventions with adaptive character. Nourishments are an example of a flexible mitigation measure of coastal recession that can facilitate adaptive planning. Nourishment plans can be designed based on the uncertainty calculated at the start of their lifetime, implemented and monitored. As the coast evolves over time, new information will be collected that will potentially reduce the uncertainty. This information can be used to reassess the maintenance of the measure and scale up or down the future nourishment according to the changing conditions. It would be useful to explore the capabilities of quantifying the evolution in the coastline recession probabilities through the lifetime of a proposed measure with the aim of supporting the decision between stiff and flexible/adaptive solutions.

The application of the uncertainty quantification and aggregation framework for different target variables beyond coastline change could also be investigated as long as the total effect can be estimated as the superposition of the different driving processes effect.

References

Athanasiou, P. (2017). Understanding the interactions between crescentic bars, human interventions and coastline dynamics at the East coast of South Korea.

Beckers, F., Noack, M., & Wieprecht, S. (2017). Uncertainty analysis of a 2D sediment transport model: an example of the Lower River Salzach. *Journal of Soils and Sediments*, 1-12.

Bjerager, P. (1988). Probability integration by directional simulation. *Journal of Engineering Mechanics, 114*(8), 1285-1302.

Bosboom, J., & Reniers, A. (2014). Scale-selective validation of morphodynamic models. *Coastal Engineering Proceedings, 1*(34), 75.

Bosboom, J., Reniers, A., & Luijendijk, A. (2014). On the perception of morphodynamic model skill. *Coastal Engineering, 94*, 112-125.

Callaghan, D., Nielsen, P., Short, A., & Ranasinghe, R. (2008). Statistical simulation of wave climate and extreme beach erosion. *Coastal Engineering, 55*(5), 375-390.

de Bruijn, F. (2005). Application of Unibest to model White Lagoon beach enhancement.

de Queiroz, B. (2017). Input Reduction Analysis for Long-term Morphodynamic Simulations.

Deltares. (2011). UNIBEST-CL+ Manual, Manual for Version 7.1 of the Shoreline Model UNIBEST-CL+. In.

Deltares. (2016). CoMIDAS - East Coast Case, Numerical model study for Anmok beach. In.

Deltares. (2017). Modeling framework for the Korean East coast, Progress report CoMIDAS 2017 (draft). In.

den Heijer, C. K., Baart, F., & van Koningsveld, M. (2012). Assessment of dune failure along the Dutch coast using a fully probabilistic approach. *Geomorphology, 143*, 95-103.

Eamon, C. D., Thompson, M., & Liu, Z. (2005). Evaluation of accuracy and efficiency of some simulation and sampling methods in structural reliability analysis. *Structural safety, 27*(4), 356-392.

Fortunato, A., Bertin, X., & Oliveira, A. (2009). Space and time variability of uncertainty in morphodynamic simulations. *Coastal Engineering, 56*(8), 886-894.

Fullwood, R. (1999). *Probabilistic safety assessment in the chemical and nuclear industries*: Elsevier.

Hamby, D. (1994). A review of techniques for parameter sensitivity analysis of environmental models. *Environmental monitoring and assessment, 32*(2), 135-154.

Helton, J. C., & Davis, F. J. (2003). Latin hypercube sampling and the propagation of uncertainty in analyses of complex systems. *Reliability Engineering & System Safety, 81*(1), 23-69.

Hurtado, J., & Barbat, A. H. (1998). Monte Carlo techniques in computational stochastic mechanics. *Archives of Computational Methods in Engineering, 5*(1), 3.

Iman, R. L., & Conover, W.-J. (1982). A distribution-free approach to inducing rank correlation among input variables. *Communications in Statistics-Simulation and Computation, 11*(3), 311-334.

Iman, R. L., & Helton, J. C. (1988). An investigation of uncertainty and sensitivity analysis techniques for computer models. *Risk analysis, 8*(1), 71-90.

IPCC. (2014). *Summary for Policymakers*. Climate Change 2014: Mitigation of Climate Change. Contribution of Working Group III to the Fifth Assessment Report of the Intergovernmental Panel on Climate Change. Cambridge University Press, NY, USA.

Jongejan, R., Ranasinghe, R., Wainwright, D., Callaghan, D. P., & Reyns, J. (2016). Drawing the line on coastline recession risk. *Ocean & coastal management, 122*, 87-94.

Klis, H. (2003). *Uncertainty analysis applied to numerical models of river bed morphology*: DUP Science.

Kroon, A., de Schipper, M., den Heijer, K., Aarninkhof, S., & van Gelder, P. (2017). Uncertainty assessment in coastal morphology prediction with a bayesian network.

Kurowicka, D., & Cooke, R. M. (2006). *Uncertainty analysis with high dimensional dependence modelling*: John Wiley & Sons.

Larson, M., Erikson, L., & Hanson, H. (2004). An analytical model to predict dune erosion due to wave impact. *Coastal Engineering, 51*(8-9), 675-696.

Lesser, G., Roelvink, J. v., Van Kester, J., & Stelling, G. (2004). Development and validation of a three-dimensional morphological model. *Coastal Engineering, 51*(8-9), 883-915.

Lesser, G. R. (2009). *An approach to medium-term coastal morphological modelling*: IHE Delft Institute for Water Education.

Loucks, D. P., & Van Beek, E. (2017). *Water resource systems planning and management: An introduction to methods, models, and applications*: Springer.
Luijendijk, A., de Vroeg, H., Swinkels, C., & Walstra, D.-J. (2011). Coastal response on multiple scales: a pilot study on the IJmuiden port. In *The Proceedings of the Coastal Sediments 2011: In 3 Volumes* (pp. 602-615): World Scientific.
Luijendijk, A., Hagenaars, G., Ranasinghe, R., Baart, F., Donchyts, G., & Aarninkhof, S. (2018). The State of the World's Beaches. *Scientific reports, 8*.
Luijendijk, A. P., Ranasinghe, R., de Schipper, M. A., Huisman, B. A., Swinkels, C. M., Walstra, D. J., & Stive, M. J. (2017). The initial morphological response of the Sand Engine: A process-based modelling study. *Coastal Engineering, 119*, 1-14.
Manache, G., & Melching, C. (2007). *Sensitivity of Latin hypercube sampling to sample size and distributional assumptions.* Paper presented at the Proceedings of the 32nd Congress of the International Association of Hydraulic Engineering and Research, 1–6 July 2007, Venice, Italy.
McKay, J. (1988). Sensitivity and uncertainty analysis using a statistical sample of input values. *Uncertainty analysis*.
McKay, M. D., Beckman, R. J., & Conover, W. J. (1979). Comparison of three methods for selecting values of input variables in the analysis of output from a computer code. *Technometrics, 21*(2), 239-245.
McNamara, D. E., & Keeler, A. (2013). A coupled physical and economic model of the response of coastal real estate to climate risk. *Nature Climate Change, 3*(6), 559.
Morgan, M. G., Henrion, M., & Small, M. (1992). *Uncertainty: a guide to dealing with uncertainty in quantitative risk and policy analysis*: Cambridge university press.
Nicholls, R. J., & Cazenave, A. (2010). Sea-level rise and its impact on coastal zones. *science, 328*(5985), 1517-1520.
Nielsen, T. D., & Jensen, F. V. (2009). *Bayesian networks and decision graphs*: Springer Science & Business Media.
Palmer, M. (2003). Propagation of uncertainty through mathematical operations. *Massachusetts Institute of*.
Plant, N. G., & Holland, K. T. (2011). Prediction and assimilation of surf-zone processes using a Bayesian network: Part I: Forward models. *Coastal Engineering, 58*(1), 119-130.
Ranasinghe, R. (2016). Assessing climate change impacts on open sandy coasts: A review. *Earth-science reviews, 160*, 320-332.
Ranasinghe, R., Callaghan, D., & Stive, M. J. (2009). A process based approach to derive probabilistic estimates of coastal recession due to sea level rise. In *Proceedings Of Coastal Dynamics 2009: Impacts of Human Activities on Dynamic Coastal Processes (With CD-ROM)* (pp. 1-9): World Scientific.
Ranasinghe, R., Callaghan, D., & Stive, M. J. (2012). Estimating coastal recession due to sea level rise: beyond the Bruun rule. *Climatic Change, 110*(3-4), 561-574.
Regan, H. M., Ferson, S., & Berleant, D. (2004). Equivalence of methods for uncertainty propagation of real-valued random variables. *International journal of approximate reasoning, 36*(1), 1-30.
Rijkswaterstraat. (2018). Beheerbibliotheek Schiermonnikoog. In *Beschrijvingen van het kustvak ter ondersteuning van het beheer en onderhoud van de kust*.
Ruggiero, P., List, J., Hanes, D., & Eshleman, J. (2007). Probabilistic shoreline change modeling. In *Coastal Engineering 2006: (In 5 Volumes)* (pp. 3417-3429): World Scientific.
Saltelli, A. (1999). Sensitivity analysis: Could better methods be used? *Journal of Geophysical Research: Atmospheres, 104*(D3), 3789-3793.
Scheel, F., de Boer, W. P., Brinkman, R., Luijendijk, A. P., & Ranasinghe, R. (2014). On the Generic Utilization of Probabilistic Methods for Quantification of Uncertainty in Process-Based Morphodynamic Model Applications. *Coastal Engineering Proceedings, 1*(34), 88.
Sutherland, J., Peet, A., & Soulsby, R. (2004). Evaluating the performance of morphological models. *Coastal Engineering, 51*(8-9), 917-939.
Uusitalo, L., Lehikoinen, A., Helle, I., & Myrberg, K. (2015). An overview of methods to evaluate uncertainty of deterministic models in decision support. *Environmental Modelling & Software, 63*, 24-31.
Villaret, C., Kopmann, R., Wyncoll, D., Riehme, J., Merkel, U., & Naumann, U. (2016). First-order uncertainty analysis using Algorithmic Differentiation of morphodynamic models. *Computers & Geosciences, 90*, 144-151.

Vousdoukas, M. I., Mentaschi, L., Voukouvalas, E., Verlaan, M., Jevrejeva, S., Jackson, L. P., & Feyen, L. (2018). Global probabilistic projections of extreme sea levels show intensification of coastal flood hazard. *Nature communications, 9*(1), 2360.

Vrijling, J., & Meijer, G. (1992). Probabilistic coastline position computations. *Coastal Engineering, 17*(1-2), 1-23.

Wainwright, D. J., Ranasinghe, R., Callaghan, D. P., Woodroffe, C. D., Jongejan, R., Dougherty, A. J., . . . Cowell, P. (2015). Moving from deterministic towards probabilistic coastal hazard and risk assessment: Development of a modelling framework and application to Narrabeen Beach, New South Wales, Australia. *Coastal Engineering, 96*, 92-99.

Walstra, D., Hoekstra, R., Tonnon, P., & Ruessink, B. (2013). Input reduction for long-term morphodynamic simulations in wave-dominated coastal settings. *Coastal Engineering, 77*, 57-70.

Appendix A: Input reduction for Delft3D model schematisation

Specifically for the Delft3D model, frequent instabilities in the model domain hindered the completion of the probabilistic simulations. To guarantee the stability of the model under the uncertain forcing conditions, a smaller Courant number (<10 for free surface waves) and thus a smaller timestep had to be applied. Considering the high initial run duration of the Anmok beach model (~160hrs), the need for input reduction was created.

Input reduction aims to describe the original dataset of forcing conditions using a reconstructed or synthetic timeseries of fewer representative conditions, consequently reducing the computational effort, without affecting significantly the morphological prediction (de Queiroz, 2017; Walstra et al., 2013). The east South Korean coast is wave dominated (de Queiroz, 2017; Deltares, 2017) and thus the input reduction focuses solely on the wave forcing. In this study the Input Reduction Tool, developed by F. Scheel as a tool to assist wave input reduction, available in OET, was used. The main steps followed are described in the following paragraphs and presented in Figure A.1.

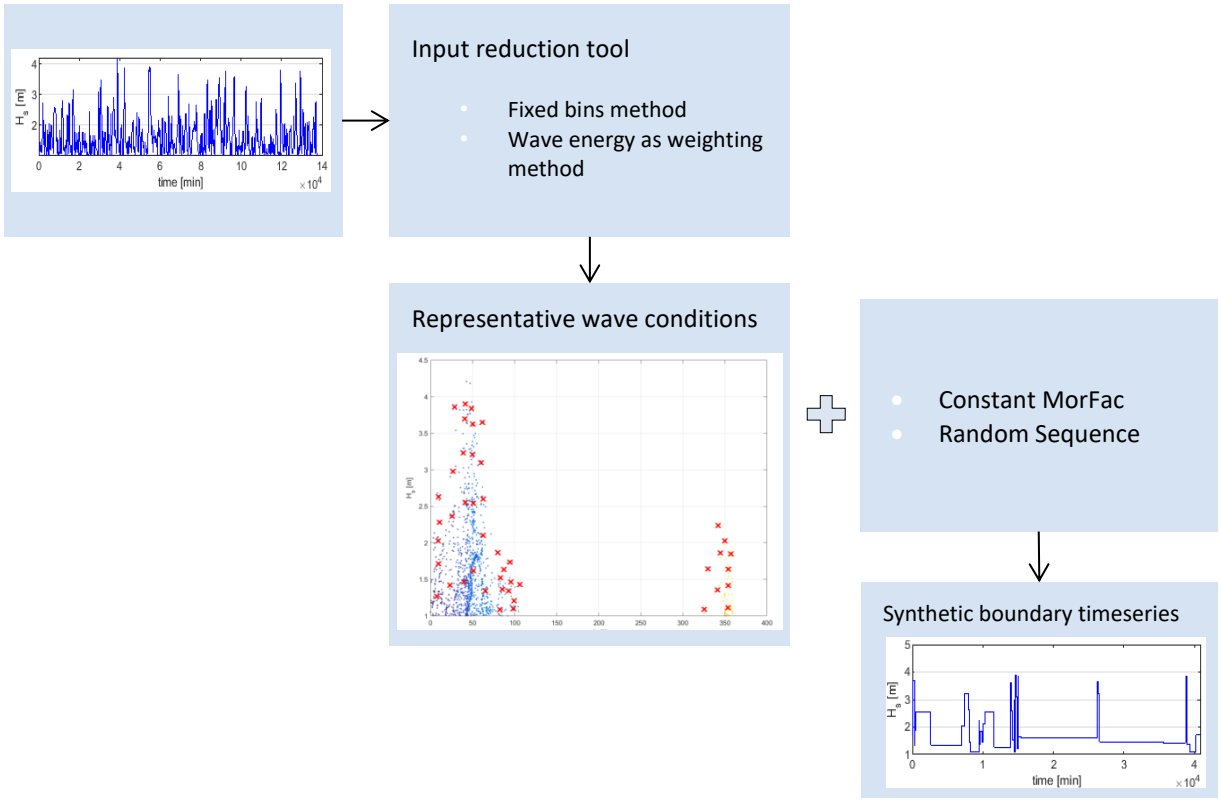

A.1: Flowchart of the steps followed to define the reduced synthetic timeseries for D3D

The representative wave conditions were selected using the fixed bins method, with wave energy ($E=c_g*H_s^2*g*\rho/8$) as a weighting method. The original wave conditions were distributed over a user defined number of directional bins. Each directional bin was subsequently divided in the user defined number of wave height bins. The representaA.1tive wave conditions (H_s, dir.) were determined as the average wave conditions within the bins. A peak period (T_p) was assigned to each of the representative wave conditions using the nearest neighbour interpolation method.

As in the original model schematisation, the 'MorFac' approach was applied. The use of a constant over a varying morphological time scale factor was chosen for more efficient computations. Given the value

of the MorFac and the original simulation period, the new simulated period was calculated. Lastly, the selected representative wave conditions were combined in random sequence, not maintaining any chronology patterns, into the synthetic timeseries of boundary conditions.

The procedure described above was repeated several times with different bin schematisations and MorFac values (Table 12). The resultant synthetic timeseries were applied as boundary conditions in the model for Anmok beach. Synthetic timeseries including wave conditions with duration shorter than the WAVE-FLOW communication file writing interval (20min) were not considered further. Table 13 includes the timescales of the original model schematisation and the alternative values used. Schematisations with hydrodynamic simulation periods shorter than the spring-neap tidal cycle were not excluded from the analysis as the microtidal forcing at the boundaries of the domain is not expected to affect the morphodynamic evolution in the domain significantly.

dir. bins * H_s bins	MF=10	MF=20	MF=30	MF=50
05 x 04	✓	✓	✓	✓
05 x 05	✓	✓	✓	✓
05 x 10	✓			
10 x 05	✓			
10 x 10	✓	✗ too short wave conditions		
15 x 05	✓			
24 x 05	✓			

Table 12: Combinations of bin discretisation and MorFac values applied to reduce the computational effort for D3D simulations of Anmok beach.

MorFac	3	10	20	30	50
Simulated period (hydrodynamics)	95.6 days	28.7 days	14.4 days	9.6 days	5.8 days
Simulated period (morphodynamics)	~9.6 months				
Run duration	160 hrs	96 hrs	48 hrs	32 hrs	20 hrs
Timestep	6 s	1.5 s	1.5 s	1.5 s	1.5 s

Table 13: Different values of MorFac applied in the input reduction process, and the relevant resulting timescales. The first column (MF=3) corresponds to the original model schematisation.

Subsequently, simulations were run using the different synthetic boundary timeseries and the success of the input reduction was reviewed. In this case, the variable of interest was the morphology at the end of the simulation and more specifically, the coastline position as defined using the MCL approach. In Figure A.2 the change of the coastline position along the Anmok beach at the end of the reference and reduced-input simulations is presented. Figure A.3 shows the difference of coastline position (change) between the reduced-input simulations and the reference simulation with the original schematisation. Both figures indicate that the combinations of smaller MorFac values and higher directional bin discretisation (red lines) give results closer to those of the original schematisation.

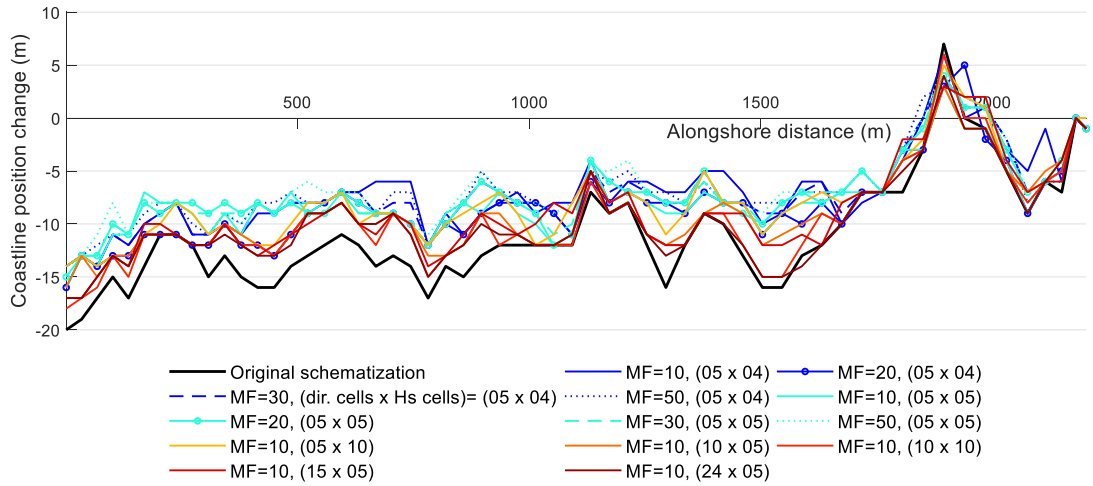

A.2: Coastline change at the end of the original and input-reduction simulations. Positive values indicate accretion. The coastline position was defined using the MCL approach between levels MSL [-1 1]m.

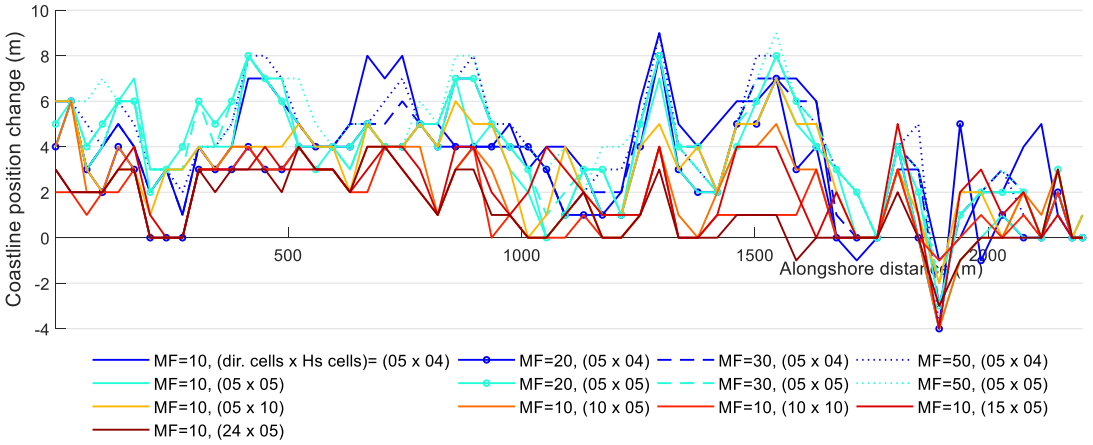

A.3: Coastline change at the end of the input reduction simulations relative to the coastline change of the reference simulation (original schematisation). Positive values indicate accretion. The coastline position was defined using the MCL approach between levels MSL [-1 1] m.

Two quantitative performance indicators (Root Mean Square Error & Absolute Mean Square Error) were used to evaluate the ability of the reduced input model to approximate closely the final coastline position of the original model. Figure A.4 illustrates once more that higher directional bin discretisation yields lower deviations from the final coastline position of the reference simulation which is in agreement with the findings of de Queiroz (2017).

Subsequently, the success ability of the model to produce a final morphology in the domain similar to that of the original model was assessed qualitatively. Figure A.5 shows that the reduced input simulation 'MF=20, (05 x 04)' results in pronounced erosion and accretion features in the middle and south part of the domain which are not present in the reference simulation results, suggesting that the bin resolution and the MorFac value choices are suboptimal. In contrast, the morphodynamic conditions at the end of the 'MF=10, (24 x 05)' simulation are very similar to the target conditions.

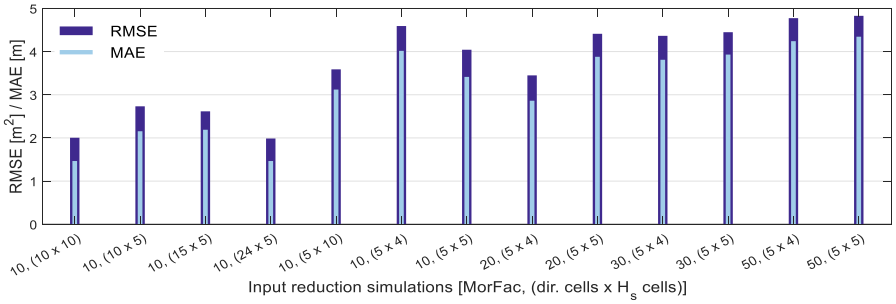

A.4: Root Mean Square Error and Mean Average Error scores of the coastline position predictions of the reduced input models.

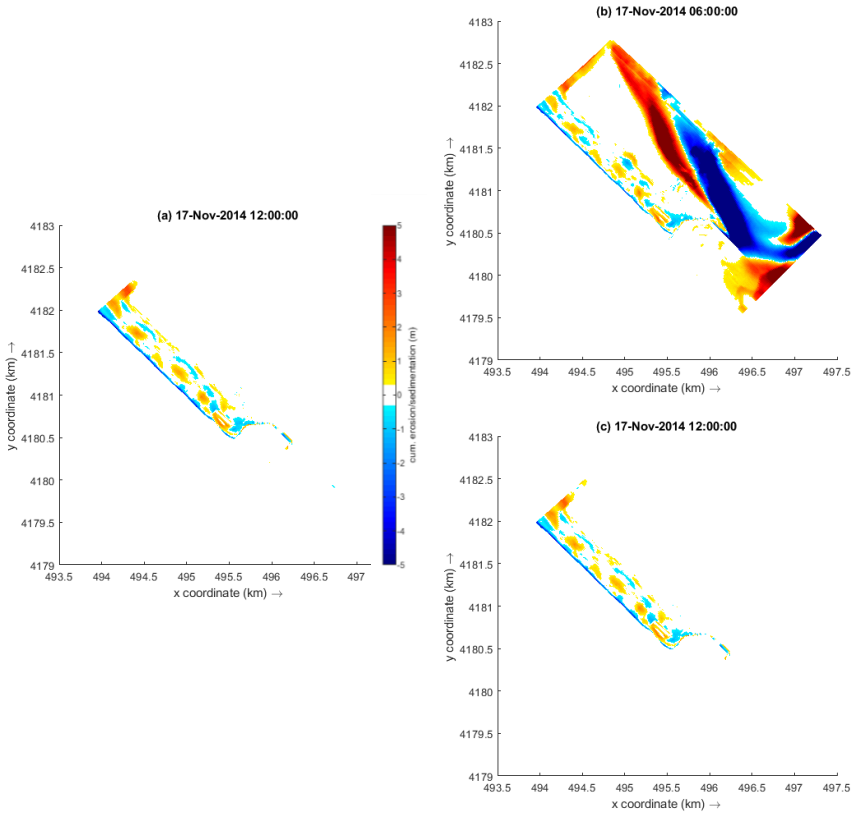

A.5: Cumulative erosion/sedimentation at the final timestep of the simulation for (a) the original model schematisation (MF=3) , (b) MorFac=20 , 05(dir. bins) * 04(H$_s$ bins) and (c) MorFac=10 , 24(dir. bins) * 05(H$_s$ bins).

The process of input reduction as applied in this project gives sufficiently good results, yet there are aspects that could be improved. These relate mainly to the application of different and potentially more suitable methods of selecting the representative conditions, taking into account the chronology effect, considering the application of varying MorFac and assessing the success of the input reduction based on more than the last timestep. However, the optimisation of the input reduction performance is not an objective by itself, but a means of ensuring that the objectives of this project as defined in paragraph 1.3 would be feasible in the given timeframe. With that in mind, the input reduction process was discontinued as soon as a sufficiently good approximation of the reference target output was obtained with the given assumptions.

Appendix B: Alternative coastline definitions for Delft3D sensitivity analysis

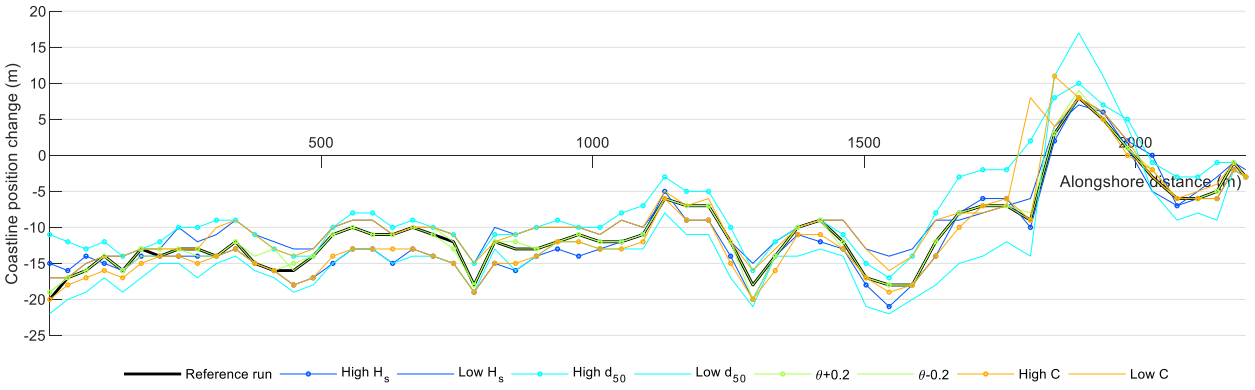

B.1: Coastline change with respect to initial coastline for the different sensitivity runs. The MCL approach is used between MSL-2m and MSL+2m. Positive coastline change indicates accretion.

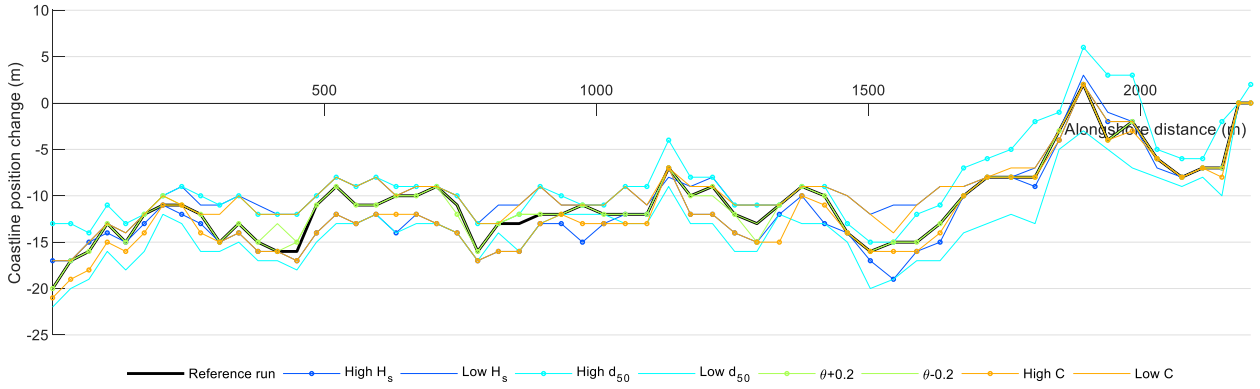

B.2: Coastline change with respect to initial coastline for the different sensitivity runs. The coastline is defined using the MSL+0m contourline. Positive coastline change indicates accretion.

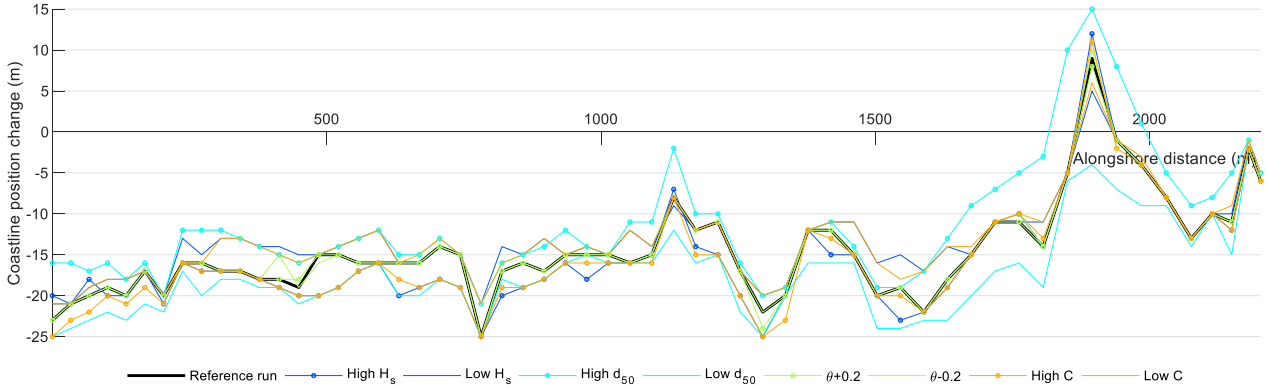

B.3: Coastline change with respect to initial coastline for the different sensitivity runs. The coastline is defined using the MSL-1m contourline. Positive coastline change indicates accretion.

Appendix C: Uncertainty quantification, Unibest-CL+ -supportive figures

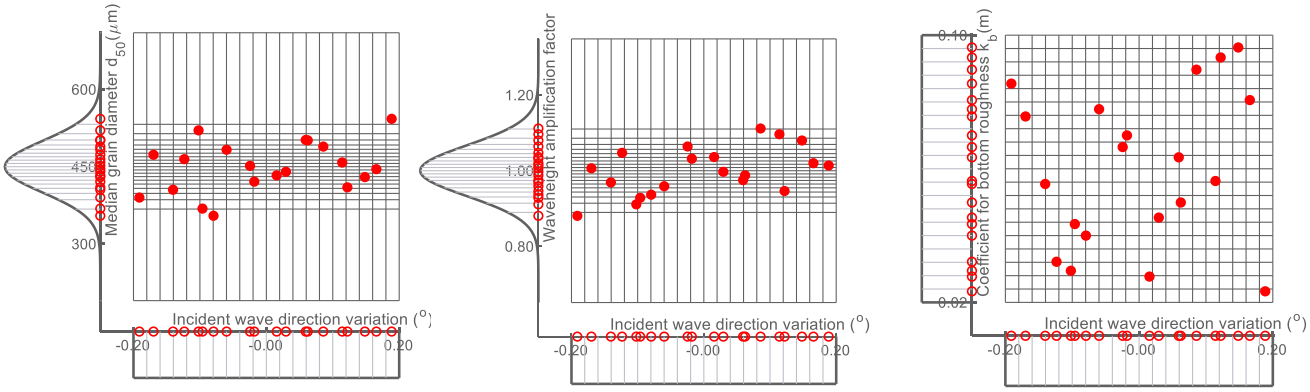

C.1: 2D projections of the cloud of sample vectors (red filled dots) generated by LHS for Unibest, (n=20). The sampled probability distributions of the variables (median grain diameter, waveheight amplification factor, coefficient for bottom roughness) have been plotted on the sides along with the sampled values from each variable (red circles).

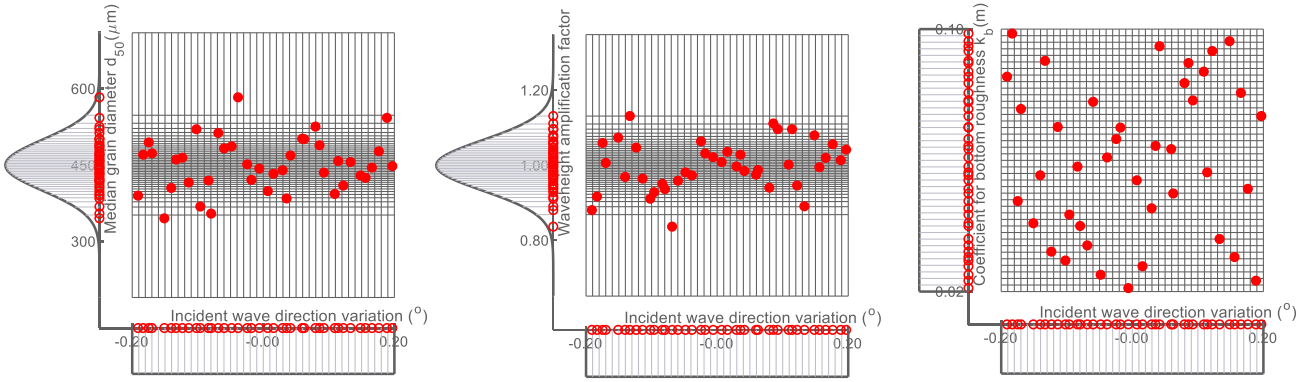

C.2: 2D projections of the cloud of sample vectors (red filled dots) generated by LHS for Unibest, (n=40). The sampled probability distributions of the variables (median grain diameter, waveheight amplification factor, coefficient for bottom roughness) have been plotted on the sides along with the sampled values from each variable (red circles).

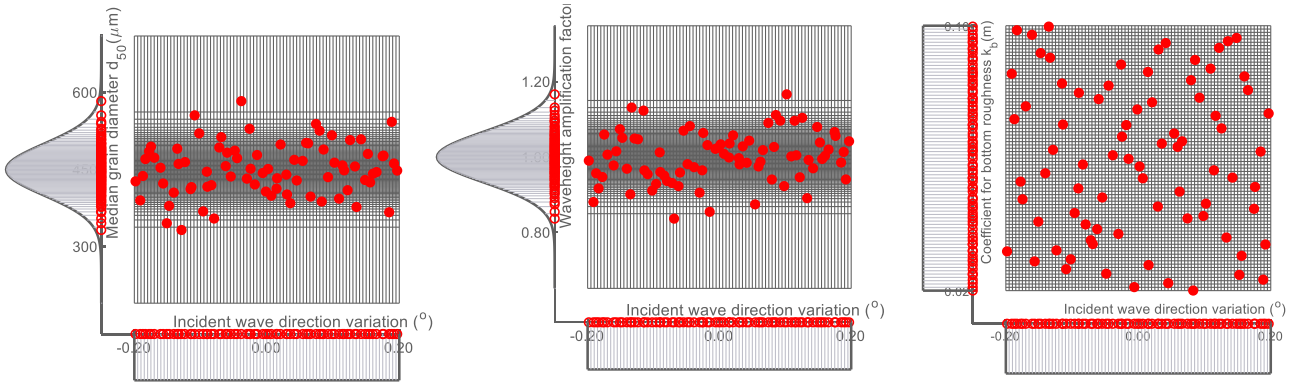

C.3: 2D projections of the cloud of sample vectors (red filled dots) generated by LHS for Unibest, (n=80). The sampled probability distributions of the variables (median grain diameter, waveheight amplification factor, coefficient for bottom roughness) have been plotted on the sides along with the sampled values from each variable (red circles).

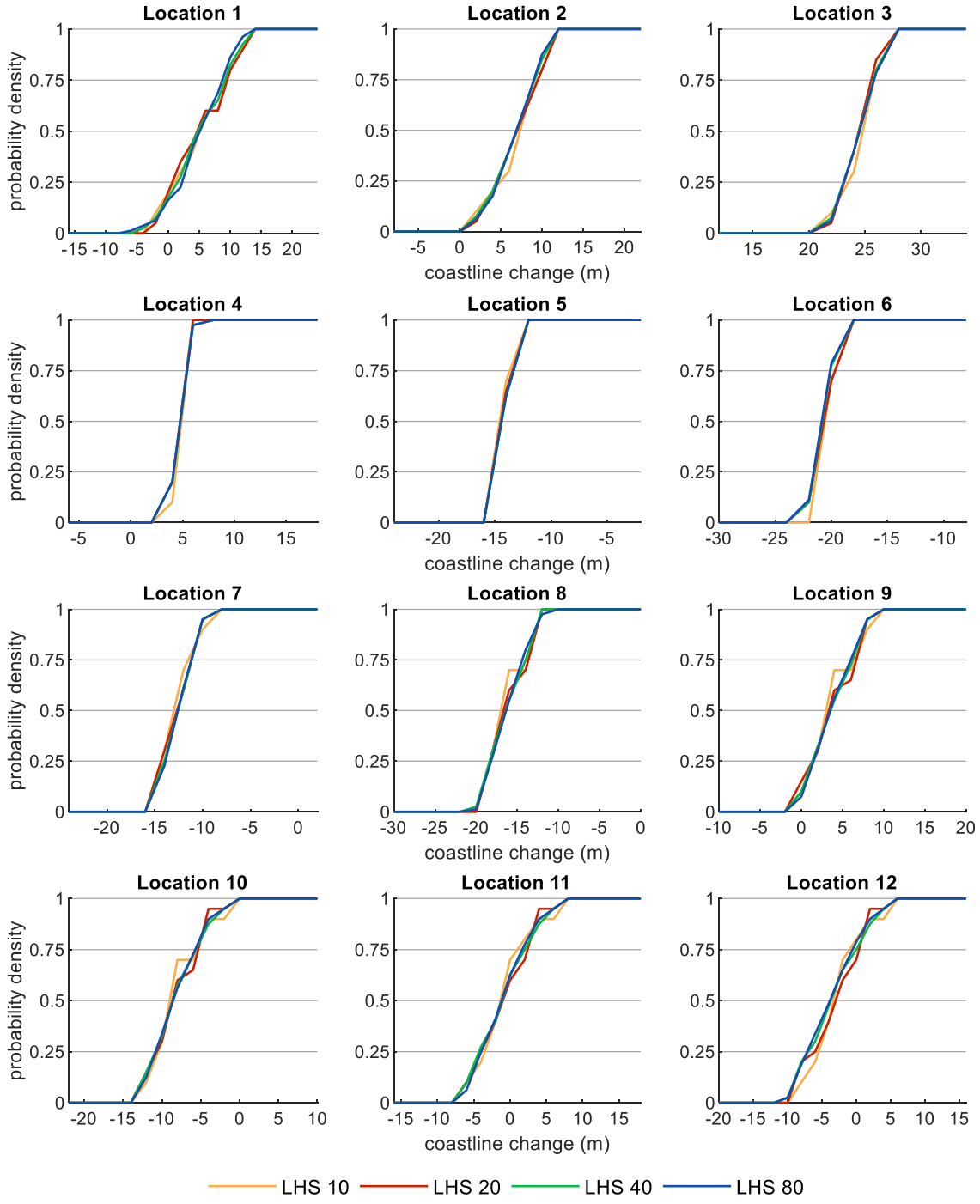

C.4: Cumulative distribution plots of coastline change at different cross-sections (as marked in Figure 4.7) along the coast for the different LH sample sizes (red: 10 samples, yellow: 20 samples, green: 40 samples and blue: 80 samples). Positive coastline change indicates accretion.

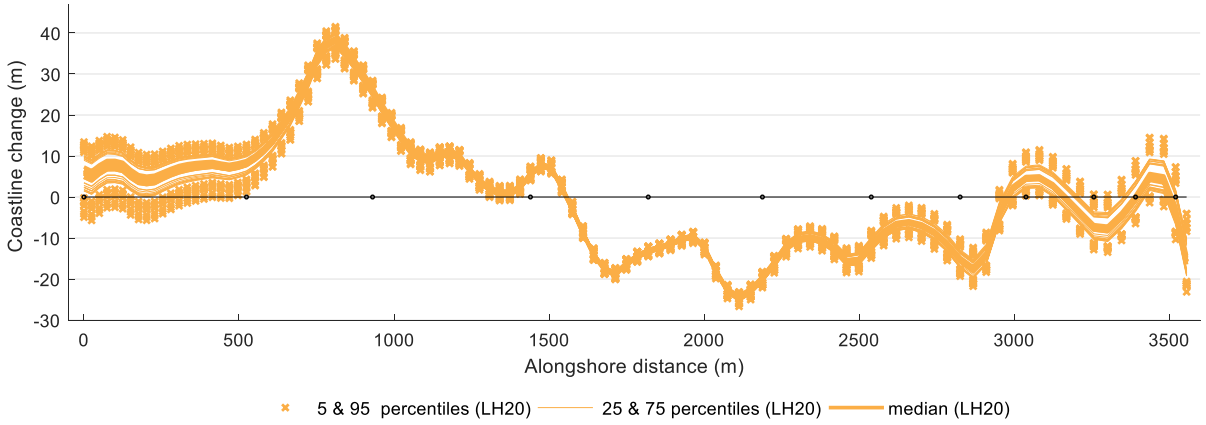

C.5: Percentiles of coastline change along the coast as estimated using 10 LH sets of 20 samples each. Positive values of coastline change indicate accretion. The black markings on the horizontal axis indicate the location of different cross-sections presented in Figure 4.3.

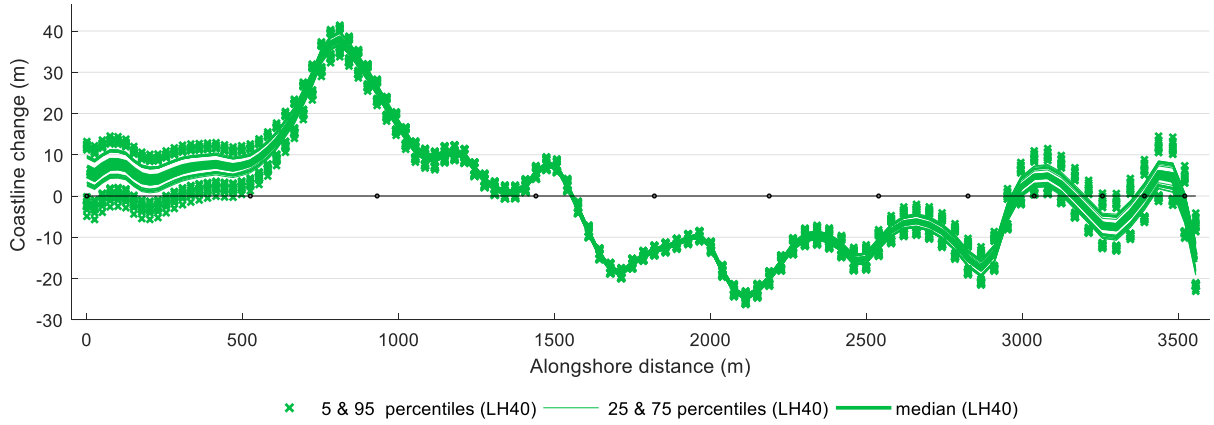

C.6: Percentiles of coastline change along the coast as estimated using 10 LH sets of 20 samples each. Positive values of coastline change indicate accretion. The black markings on the horizontal axis indicate the location of different cross-sections presented in Figure 4.3.

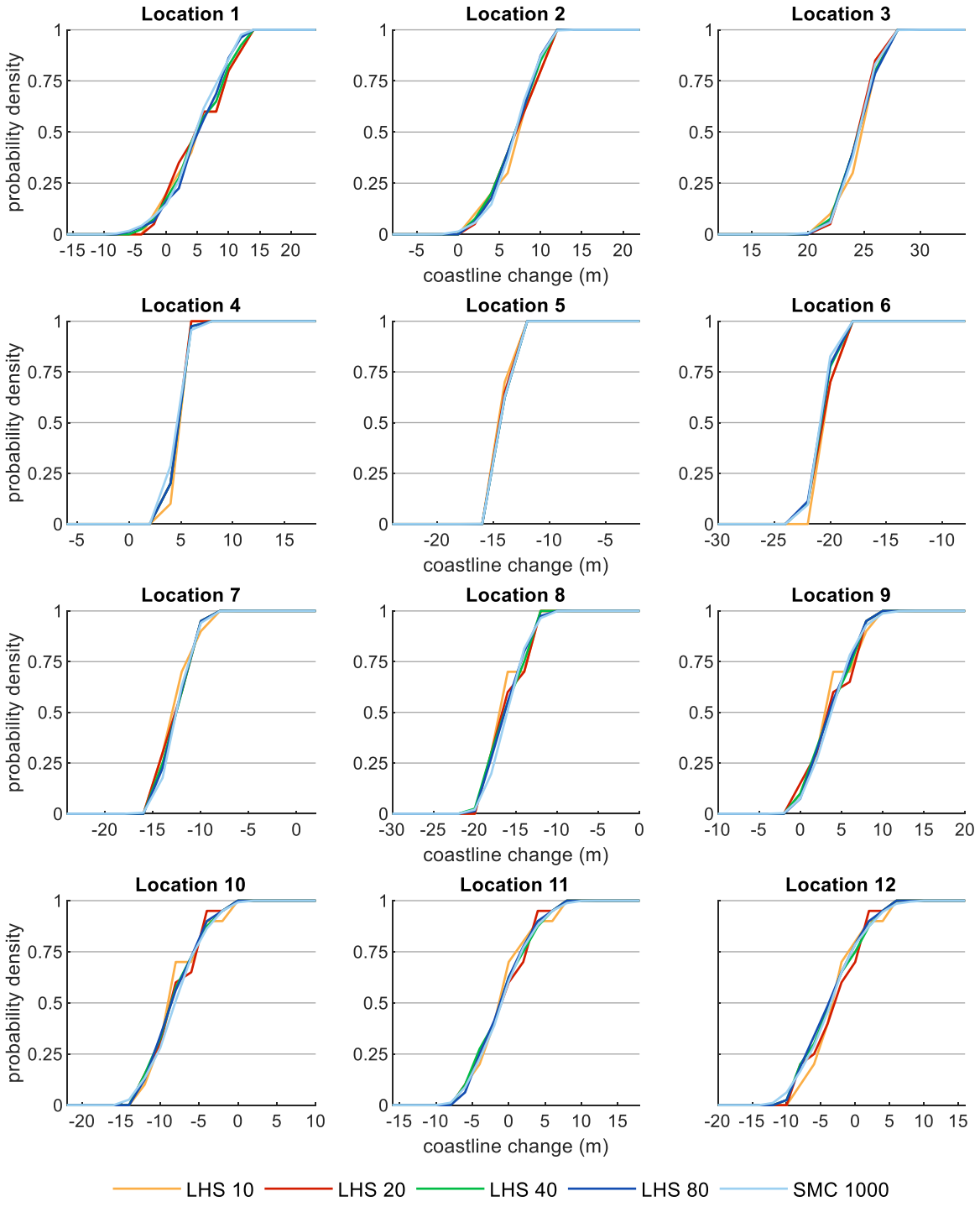

C.7: Cumulative probability plots of coastline change at different cross-sections (as marked in Figure 4.1) along the coast for the different LH sample (red: 10 samples, yellow: 20 samples, green: 40 samples, blue: 80 samples) and SMC (light blue: 1000 samples). Positive values of coastline change indicate accretion.

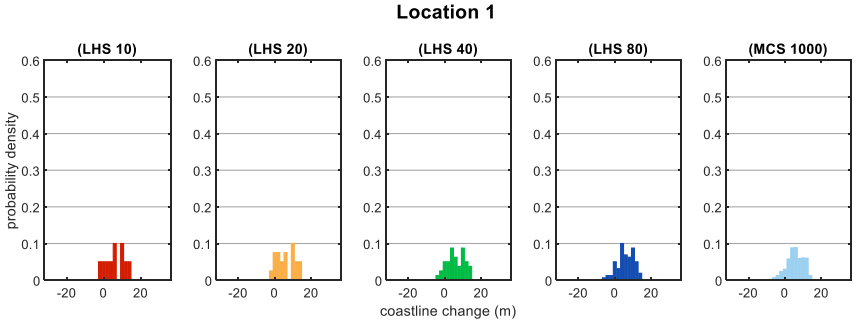
Location 1
(LHS 10)
(LHS 20)
(LHS 40)
(LHS 80)
(MCS 1000)
probability density
coastline change (m)

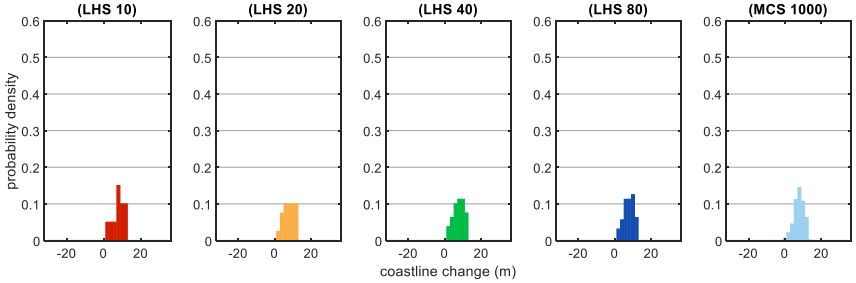
Location 2
(LHS 10)
(LHS 20)
(LHS 40)
(LHS 80)
(MCS 1000)
probability density
coastline change (m)

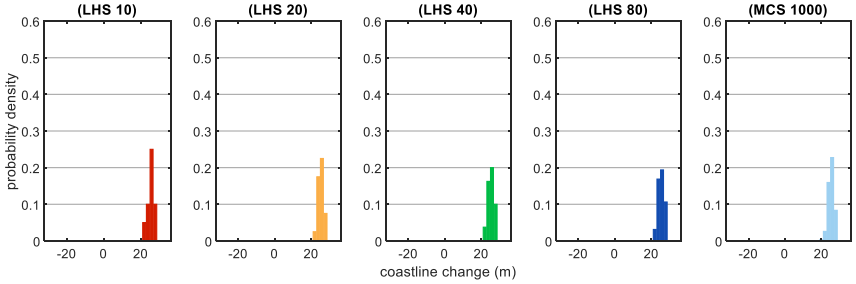
Location 3
(LHS 10)
(LHS 20)
(LHS 40)
(LHS 80)
(MCS 1000)
probability density
coastline change (m)

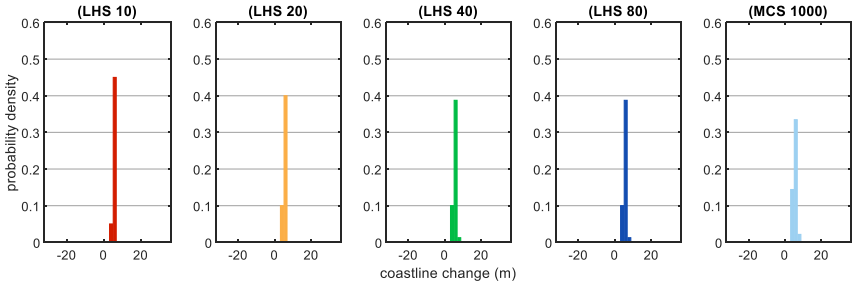
Location 4
(LHS 10)
(LHS 20)
(LHS 40)
(LHS 80)
(MCS 1000)
probability density
coastline change (m)

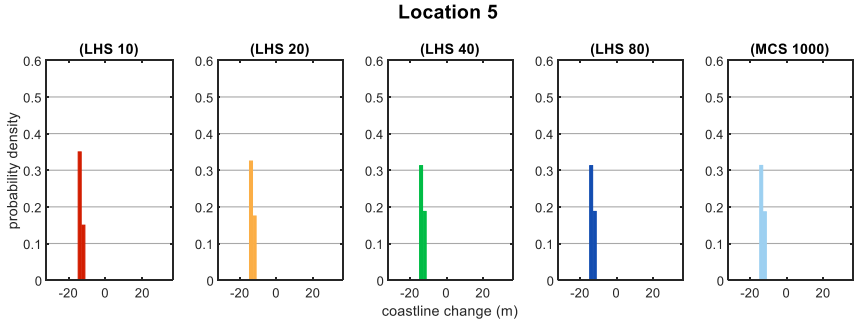
Location 5
(LHS 10)
(LHS 20)
(LHS 40)
(LHS 80)
(MCS 1000)
probability density
coastline change (m)

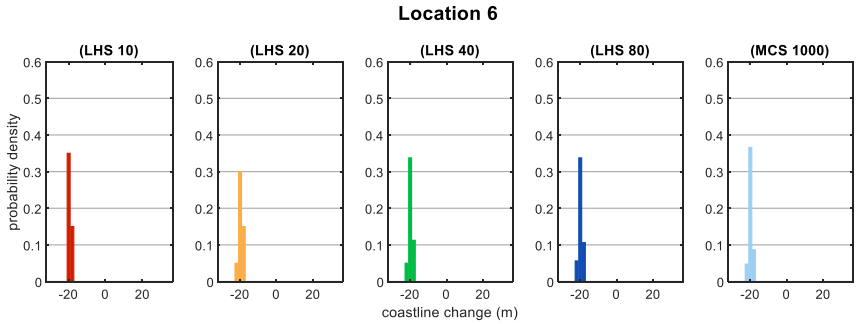
Location 6
(LHS 10)
(LHS 20)
(LHS 40)
(LHS 80)
(MCS 1000)
probability density
coastline change (m)

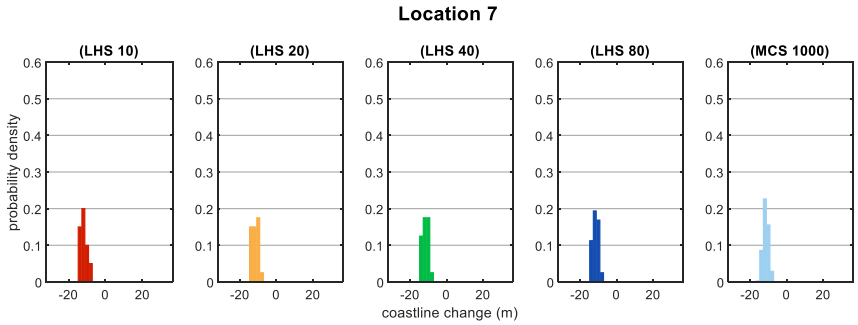
Location 7
(LHS 10)
(LHS 20)
(LHS 40)
(LHS 80)
(MCS 1000)
probability density
coastline change (m)

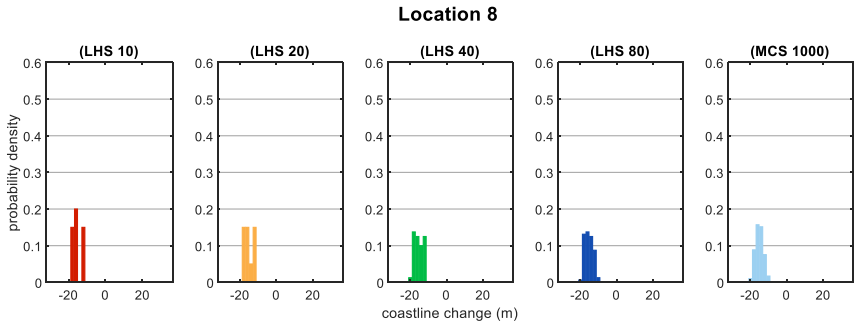
Location 8
(LHS 10)
(LHS 20)
(LHS 40)
(LHS 80)
(MCS 1000)
probability density
coastline change (m)

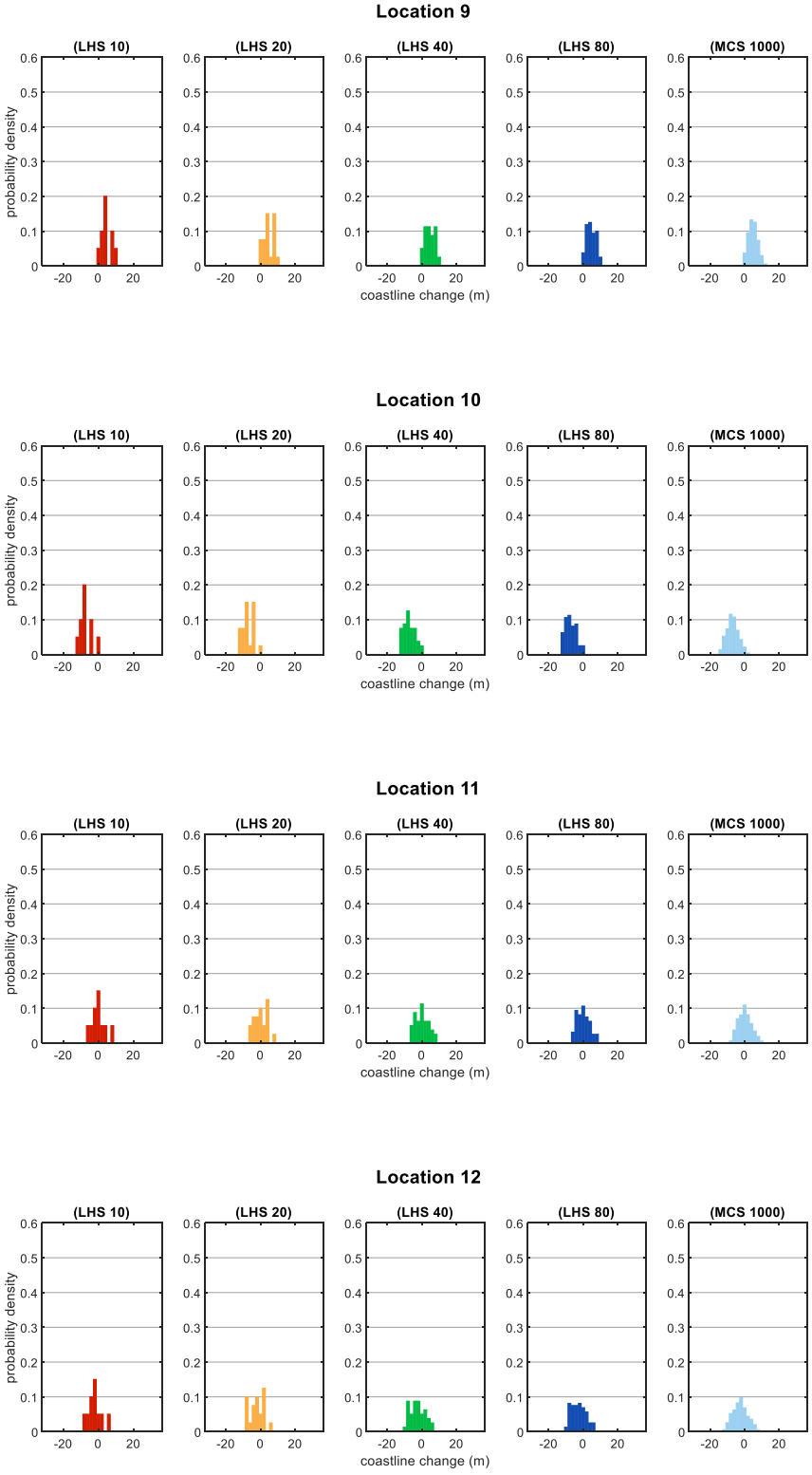

C.8: Probability density plots of coastline change at different cross-sections (as marked in Figure 4.1) along the coast for the different LH sample sizes (red: 10 samples, yellow: 20 samples, green: 40 samples and blue: 80 samples). Positive coastline change indicates accretion. Bin resolution is 2m.

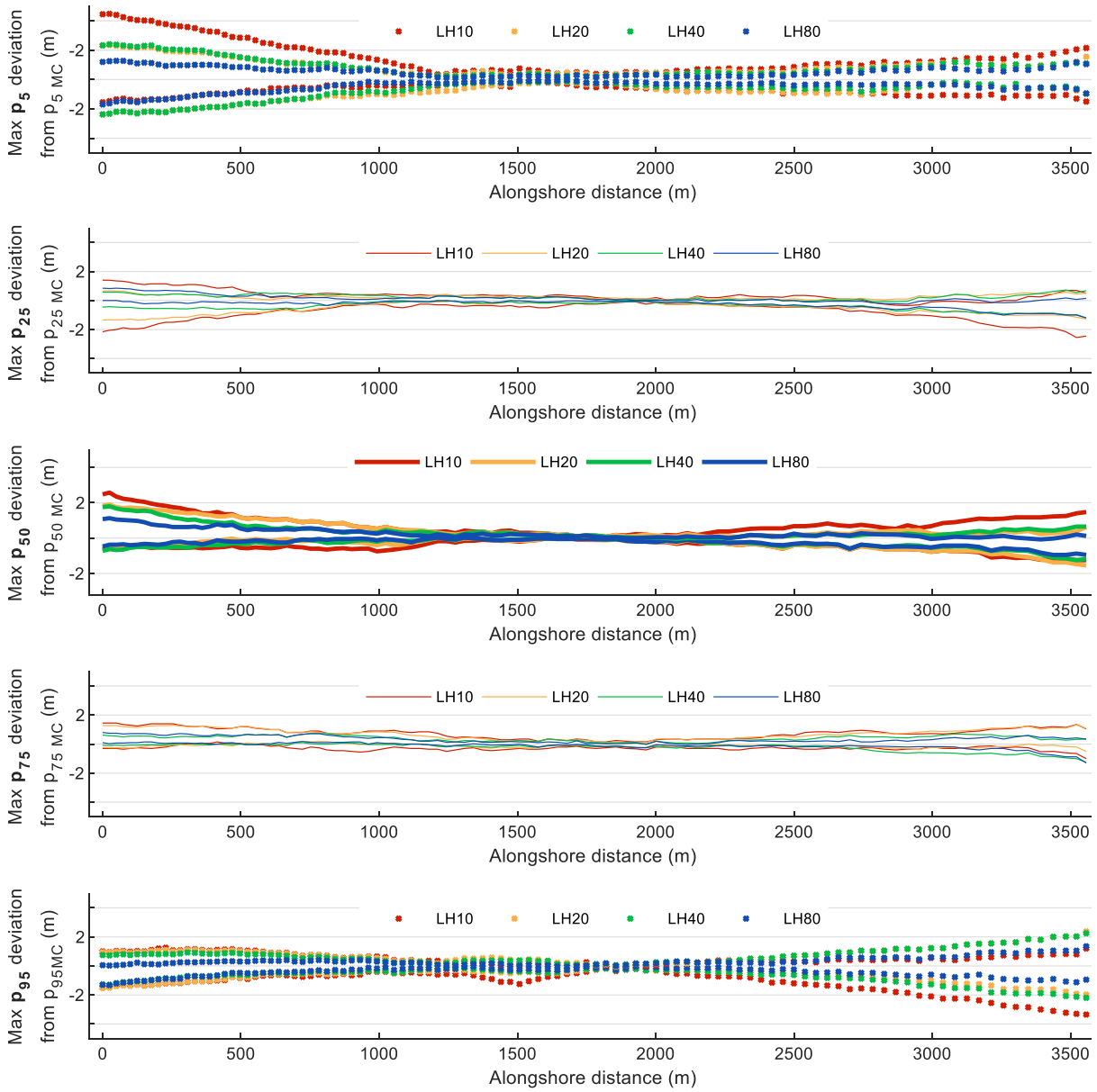

C.9: Alongshore distribution of percentile estimate spread for the 10 LHS realisations with different sample sizes (red: 10 samples, yellow: 20 samples, green: 40 samples, blue: 80 samples) around the respective SMC percentile estimates (1000 samples).

Appendix D: SMC, LHS comparison-supportive figures

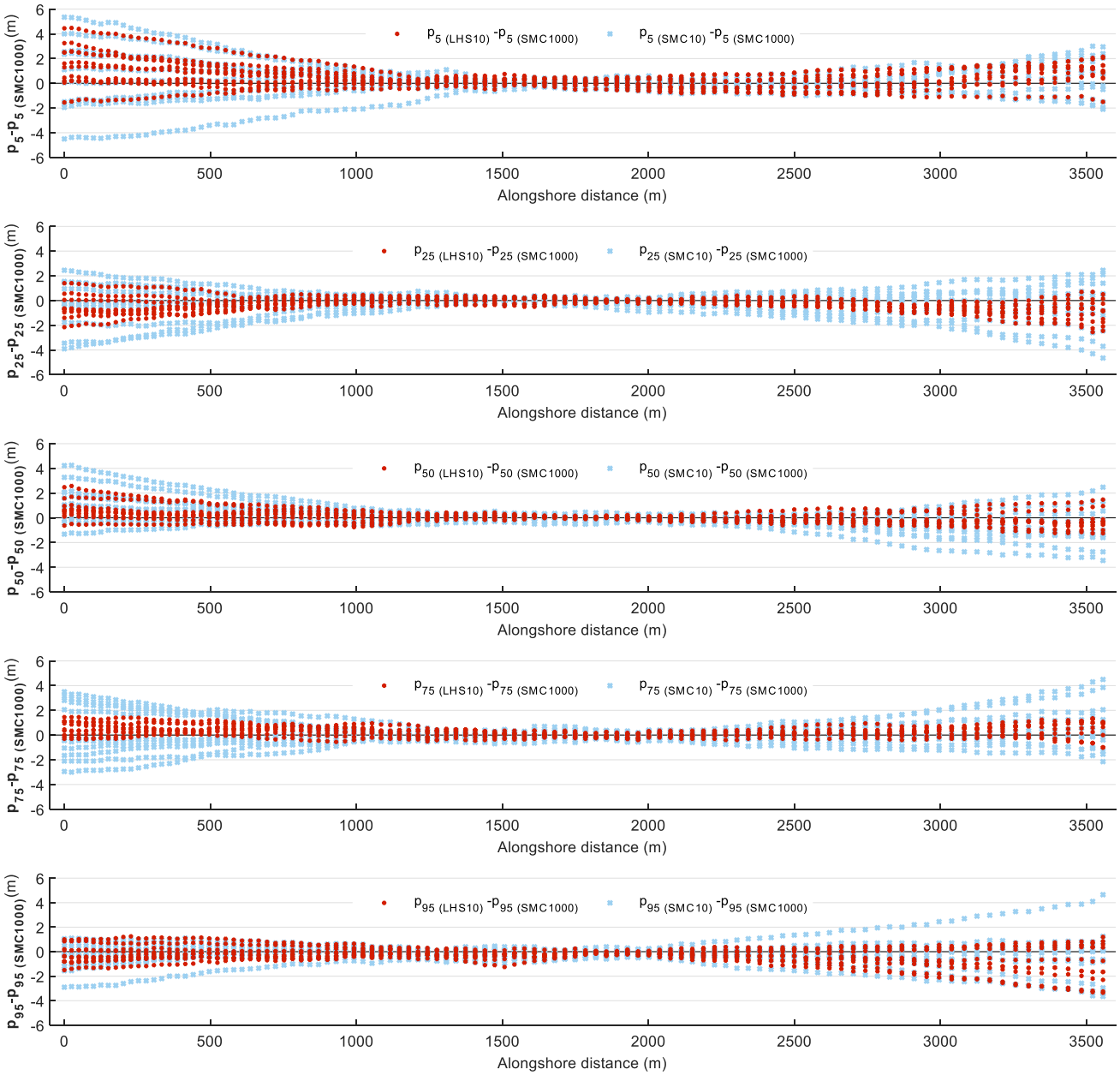

D.1: Alongshore distributions for different coastline change percentile realisations from 10 LHS/SMC iterations, relative to the percentile estimates from SMC (n=10). Red; percentile estimates from 1 LHS iteration (n=10). Blue: percentile estimates from 1 LHS iteration (n=10).

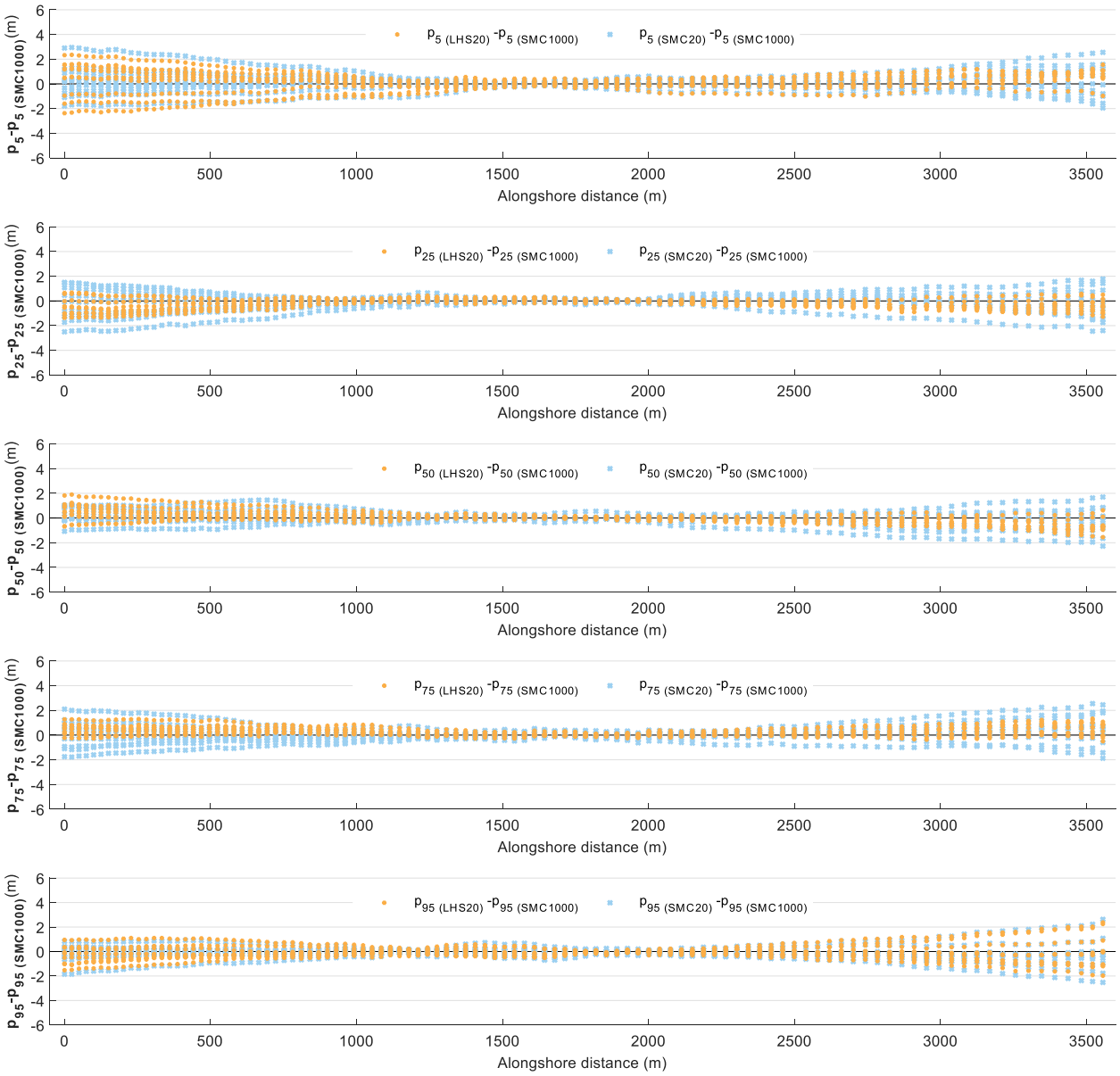

D.2: Alongshore distributions for different coastline change percentile realisations from 10 LHS/SMC iterations, relative to the percentile estimates from SMC (n=20). Red; percentile estimates from 1 LHS iteration (n=10). Blue: percentile estimates from 1 LHS iteration (n=20).

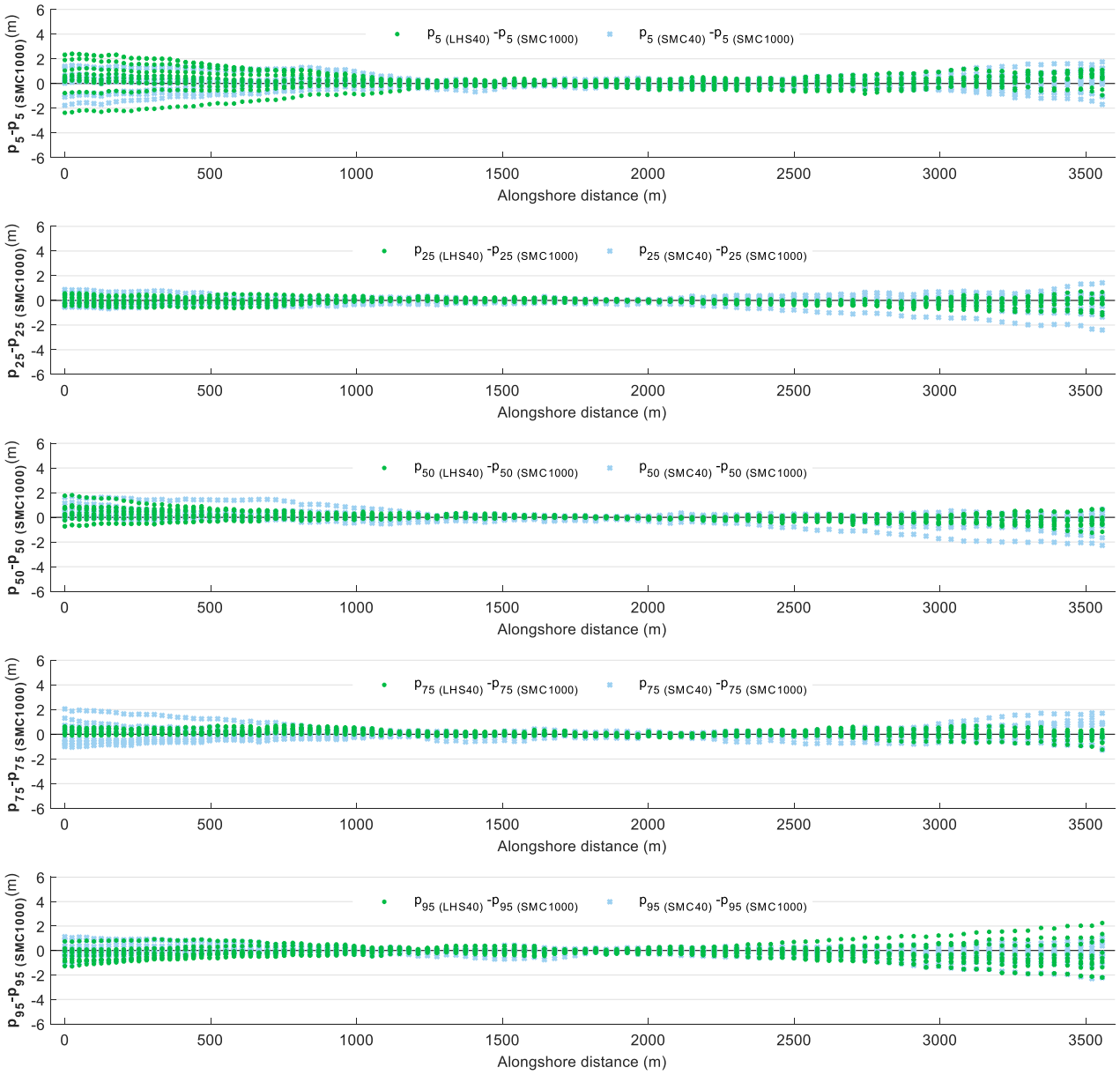

D.3: Alongshore distributions for different coastline change percentile realisations from 10 LHS/SMC iterations, relative to the percentile estimates from SMC (n=40). Red; percentile estimates from 1 LHS iteration (n=10). Blue: percentile estimates from 1 LHS iteration (n=40).

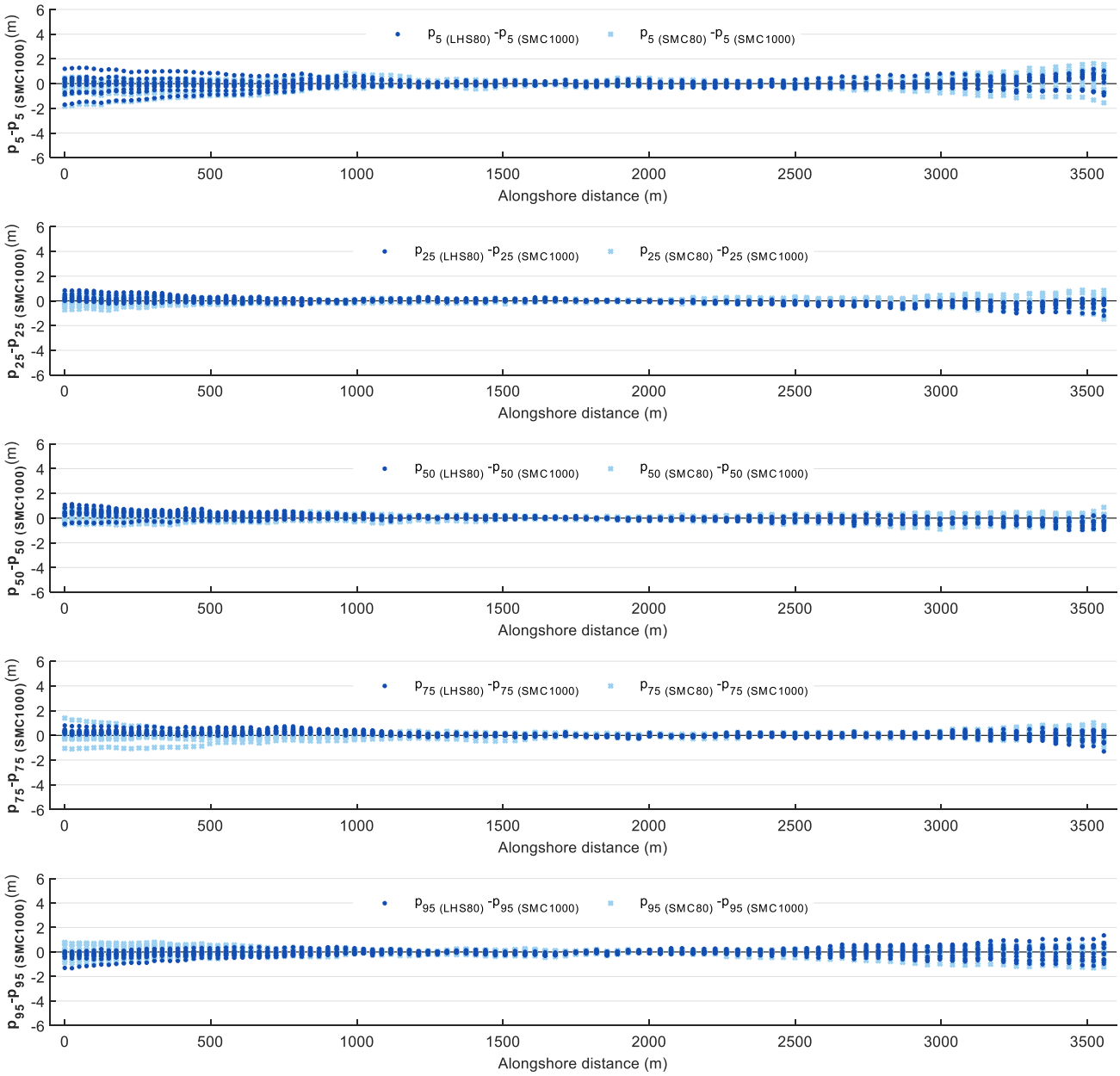

D.4: Alongshore distributions for different coastline change percentile realisations from 10 LHS/SMC iterations, relative to the percentile estimates from SMC (n=80). Red; percentile estimates from 1 LHS iteration (n=10). Blue: percentile estimates from 1 LHS iteration (n=80).

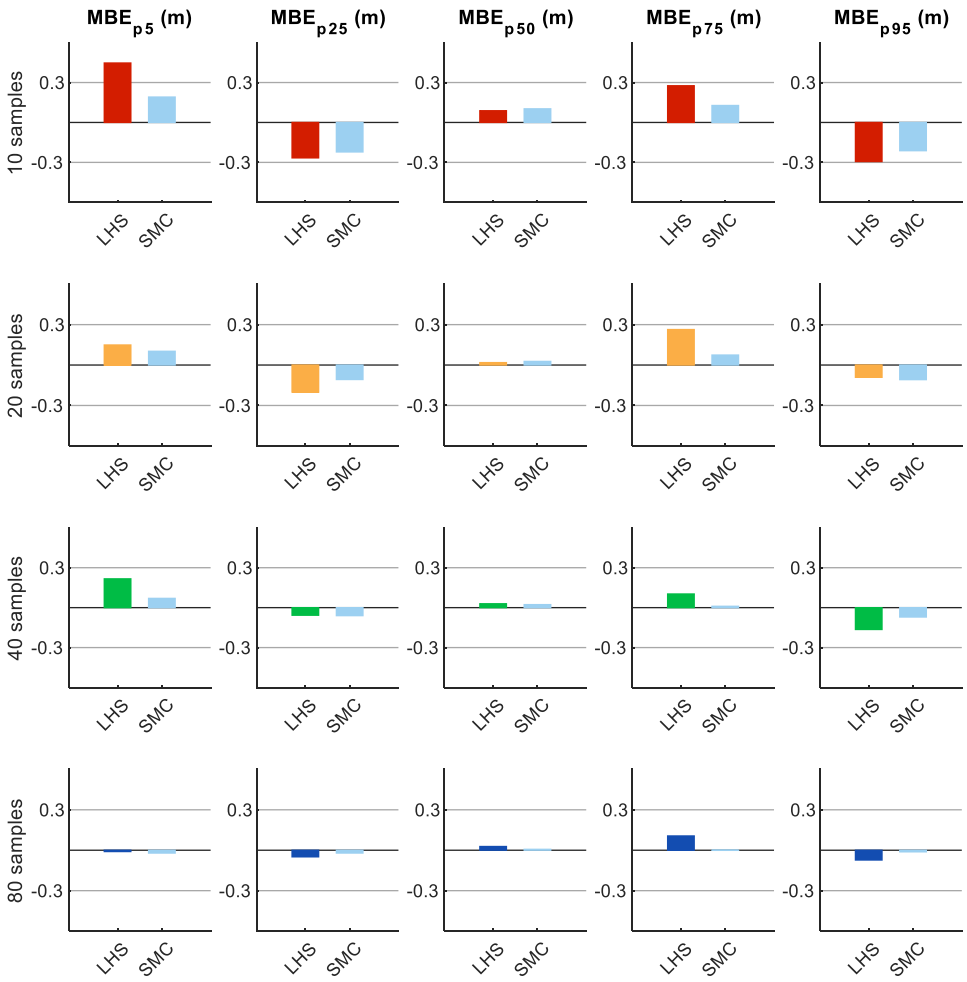

D.5: Alongshore averaged Mean Bias Error for the different coastline change percentile estimates, for SMC and LHS with different sample sets. The results are derived using 10 LHS and SMC realisations for each of the different sample set sizes. The percentile estimates derived using SMC (n=1000) were used as the 'true' values for the MBE calculation.

Appendix E: Uncertainty quantification, Delft3D - Supportive figures

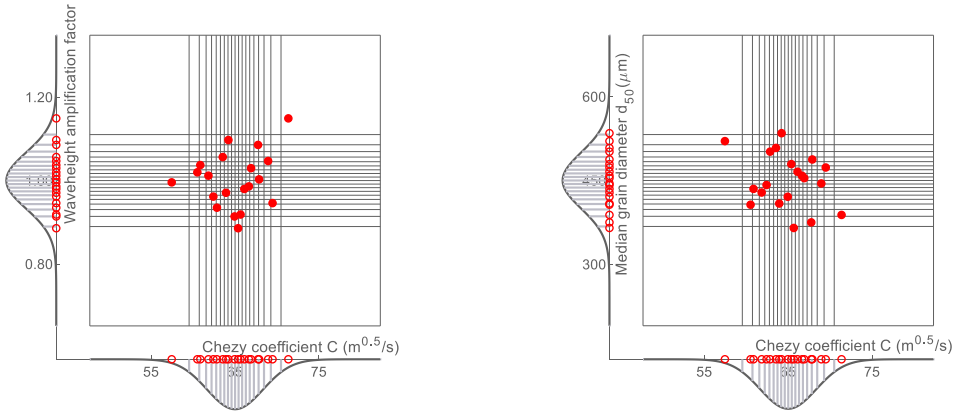

E.1:2D projections of the sample vectors (red dots) generated by LHS for D3D, (n=20). The sampled probability distributions of the variables (waveheight amplification factor, Chezy coefficient, median grain diameter) have been plotted on the sides along with the sampled values for each variable (red circles).

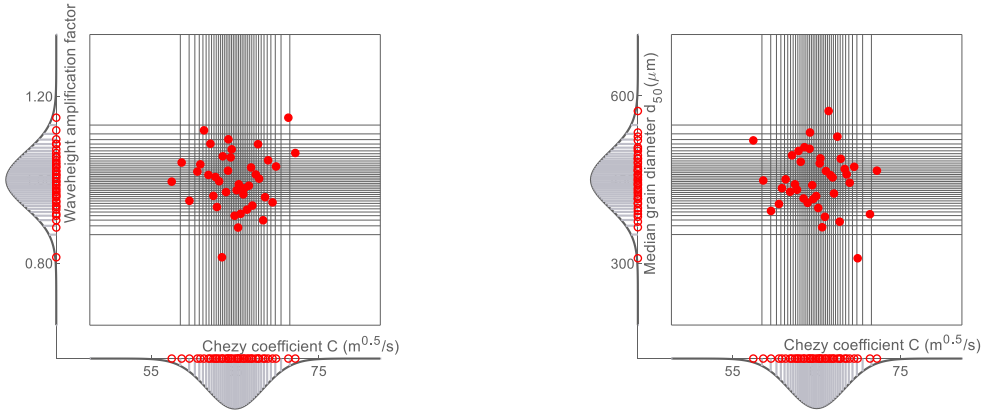

E.2: 2D projections of the sample vectors (red dots) generated by LHS for D3D, (n=40). The sampled probability distributions of the variables (waveheight amplification factor, Chezy coefficient, median grain diameter) have been plotted on the sides along with the sampled values for each variable (red circles).

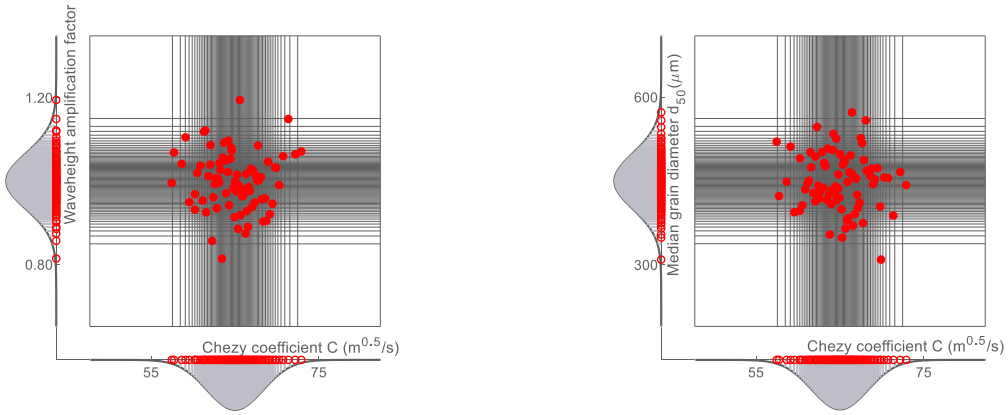

E.3: 2D projections of the sample vectors (red dots) generated by LHS for D3D, (n=80). The sampled probability distributions of the variables (waveheight amplification factor, Chezy coefficient, median grain diameter) have been plotted on the sides along with the sampled values for each variable (red circles).

Appendix F: Uncertainty aggregation methods comparison

Figures F.1 and F.2 present the results of uncertainty quantification in the coastline change estimates estimated using LHS or alternatively sensitivity analysis for the UNIBEST-CL+ schematization. The variables selected to introduce the uncertainty, the assigned sensitivity ranges and statistical characteristics can be found in Table 4 and Table 7. The results show that selecting the mean coastline change yields systematically more conservative values than the median coastline change estimated using the probabilistic approach: throughout the domain, larger erosion and smaller accretion are expected. More specifically, the deterministically defined coastline change consistently approaches the 25th percentile of coastline change. The sensitivity analysis derived minimum and maximum coastline change estimates were compared with the 1st and 99th percentile estimates of coastline change. For the cross-sections with low output uncertainty, the minimum/max estimates approach the 1st and 99th percentile estimates. However, towards the southern of the coast the differences in the extreme coastline change estimates are more pronounced. Using the deterministic method leads to overestimates of the maximum erosion and underestimates of the maximum accretion.

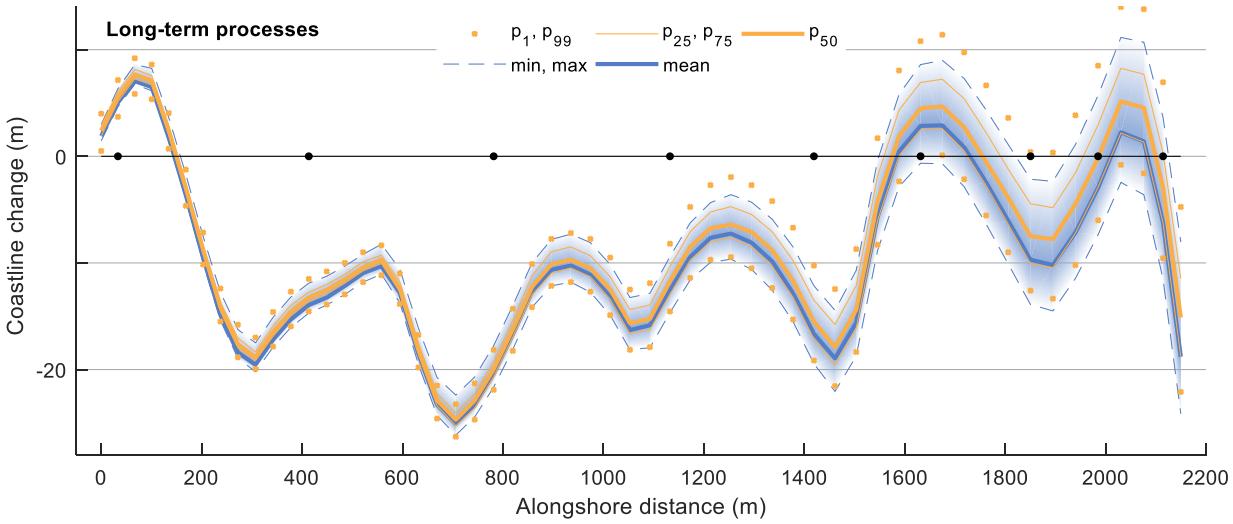

F.1: Overview of coastline change estimates under the effect of long term processes for Anmok beach using two different approaches. Percentiles of coastline change (yellow) were quantified using LHS (n=80) as described in Section 4.1.1 . Mean coastline change (blue continuous line) has been defined as the coastline change resulting from the UNIBEST-CL+ simulation with all uncertain variables evaluated at their mean values. Min/max coastline change (blue dashed lines) were estimated through sensitivity analysis. Positive values of coastline change indicate accretion. The black markings on the horizontal axis indicate the location of different cross-sections for which probability density plots are presented (Figure 4.23).

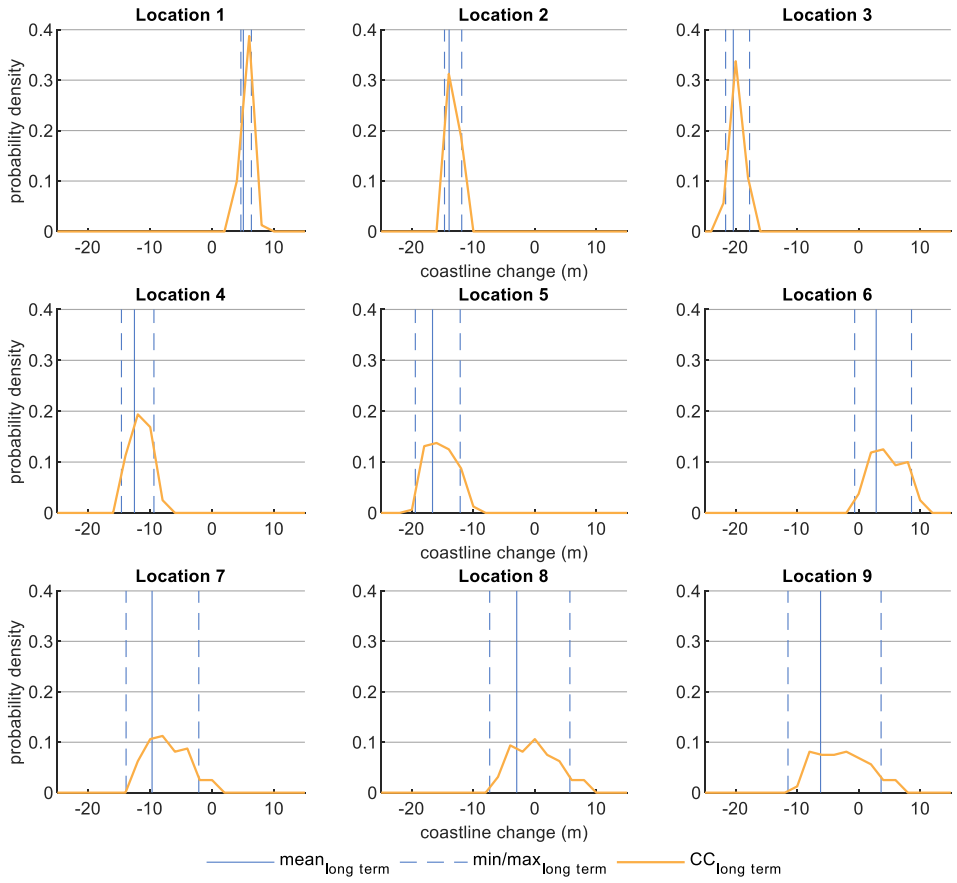

F.2: Coastline change estimates under the effect of long-term processes for different cross-sections along the coast (Figure 4.23) using two different approaches. Probability density plots (yellow) were evaluated using LHS (n=80) as described in Section 4.1.1 . Mean coastline change (blue continuous line) has been defined as the coastline change resulting from the UNIBEST-CL+ simulation with all uncertain variables evaluated at their mean values. Min/max coastline change (blue dashed lines) were estimated through sensitivity analysis. Positive values of coastline change indicate accretion.

Subsequently, the mean impact of the intervention of coastline change was evaluated as the difference in coastline change from two Delft3D simulations (with/without the submerged breakwater-nourishment) for which all the variables took their mean values. Minimum and maximum estimates of the intervention impact were derived from sensitivity simulations. The resulting mean, minimum and maximum estimates of coastline change are presented along with the probabilistically estimated percentiles in Figure F.3 and Figure F.4. We can see that the defined mean intervention impact on coastline position is a quite close approximation of the median coastline change. The uncertainty ranges defined by the minimum and maximum projected coastline change are generally smaller than the uncertainty ranges defined from the extreme percentiles, although better results can be observed in the area close to the submerged breakwater.

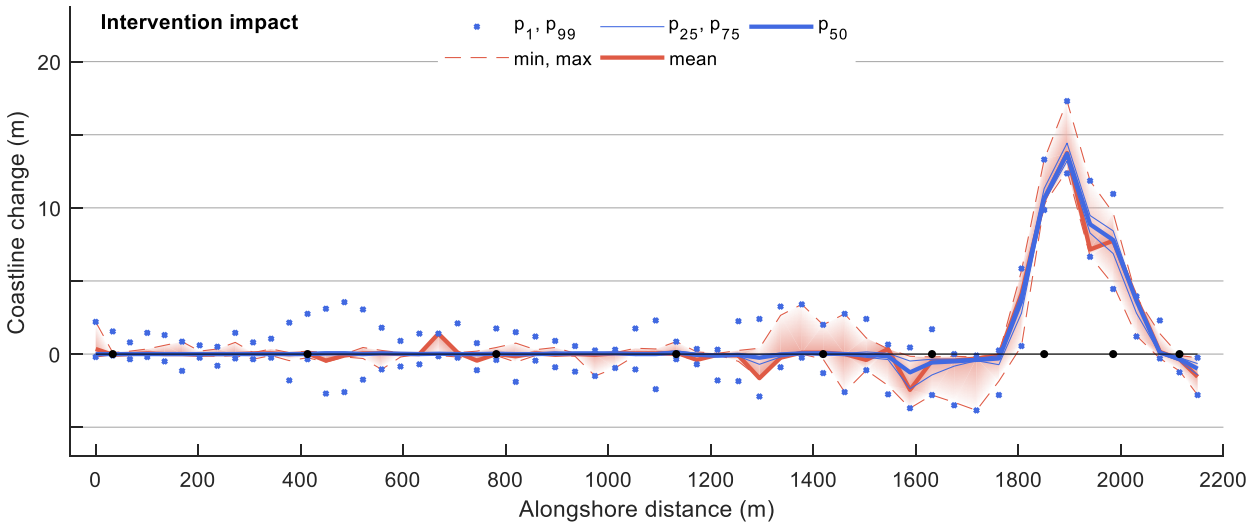

F.3: Overview of coastline change estimates under the effect of the intervention for Anmok beach using two different approaches. Percentiles of coastline change (blue) were evaluated using LHS (n=80) on two Delft3D simulations and convoluted using the SMC approach as described in Section 4.3.1 . Mean coastline change (blue continuous line) has been defined as the difference in coastline position between the two Delft3D simulations with all uncertain variables evaluated at their mean values. Min/max coastline change (blue dashed lines) have been estimated through sensitivity analysis. Positive values of coastline change indicate accretion. The black markings on the horizontal axis indicate the location of different cross-sections for which probability density plots are presented (Figure 4.23).

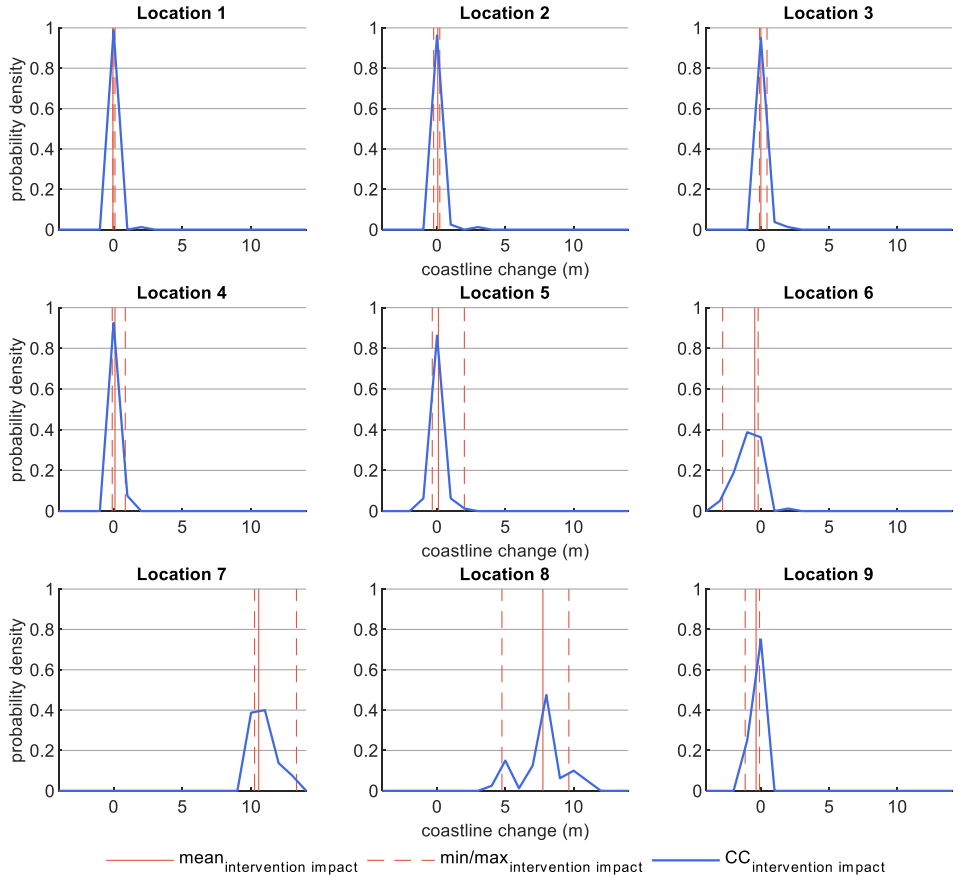

F.4: Coastline change estimates under the effect of long-term processes for different cross-sections along the coast (Figure 4.23) using two different approaches. Probability density plots (blue) were evaluated using LHS (n=80) on two Delft3D simulations and convoluted using the SMC approach as described in Section 4.3.1 . Mean coastline change (blue continuous line) has been defined as the difference in coastline position between the two Delft3D simulations with all uncertain variables evaluated at their mean values. Min/max coastline change (blue dashed lines) have been estimated through sensitivity analysis. Positive values of coastline change indicate accretion.

Appendix G: Alternative interventions

Emerged breakwater-nourishment

The first intervention considered includes an emerged breakwater and small-scale nourishment. The location, length, width and roughness characteristics were kept identical to that of the previously modelled submerged breakwater (Figure 4.32 c). However, the crest level was raised to the MSL, with the intention of further reducing the transmission coefficient for the incident wave heights. The nourishment characteristics were maintained identical to the original model schematization. Once again, a set of Delft3D simulations were used to quantify the uncertainty of the intervention impact on the coastline position. An overview of the process followed is presented in Table 14.

Process	Model	Simulated period	Uncertain Input	Uncertainty quantification method
Intervention impact (emerged breakwater-nourishment)	Delft3D	2015-2018	H_s N (1, 0.067) d_{50} N (450, 50) C N (65, 3.33)	LHS (n=80)

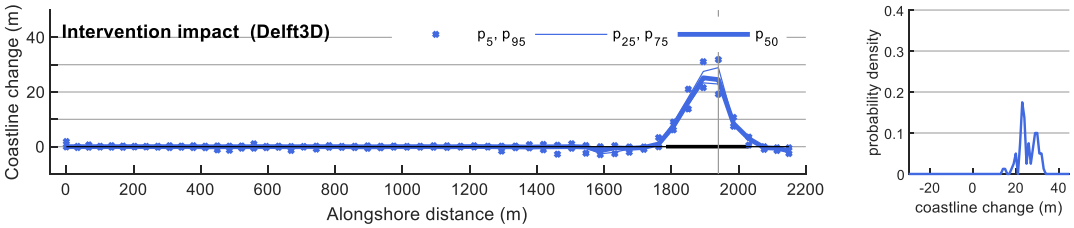

Table 14: Overview of the uncertainty quantification process for the Delft3D simulations used to assess the effect of the intervention (emerged breakwater and nourishment). On the left, the resulting alongshore distribution of different coastline change percentile estimates for intervention impact is presented. Positive coastline change indicates accretion. The location of the intervention has been marked on the horizontal axis. On the right, a probability distribution plot of coastline change for one location (marked with a grey vertical line in the left graphs) is presented.

The net impact of the emerged breakwater was evaluated as described in Section 4.3.1 ($CC_{intevention\ impact}$) and subsequently combined with the UNIBEST-CL+ derived probability distributions quantifying the uncertainty in the autonomous evolution and the effect of the long-term wave climate variations (Table 9). In Figure E.1 the alongshore distribution of percentile estimates of the aggregation components and the aggregation results are presented. The cumulative probability distributions of coastline change by 2035 are located in the negative side for the central part of the area considered. Accretion is projected for the area where the effect of the intervention is more pronounced (1500-2100m). In the area directly northern of the intervention (1500-1750m) the accretion projected in the autonomous scenario under the effect of the long-term wave climate variation counteracts the erosion caused from the submerged breakwater. In the shadow zone of the emerged breakwater the projected accretion (median) reaches up to 21m locally in contrast to the expected 8m of erosion when the emerged intervention is not considered. Lastly, behind the emerged breakwater a 17% increase in the 5-95 percentile range can be observed with respect to the range without the intervention impact.

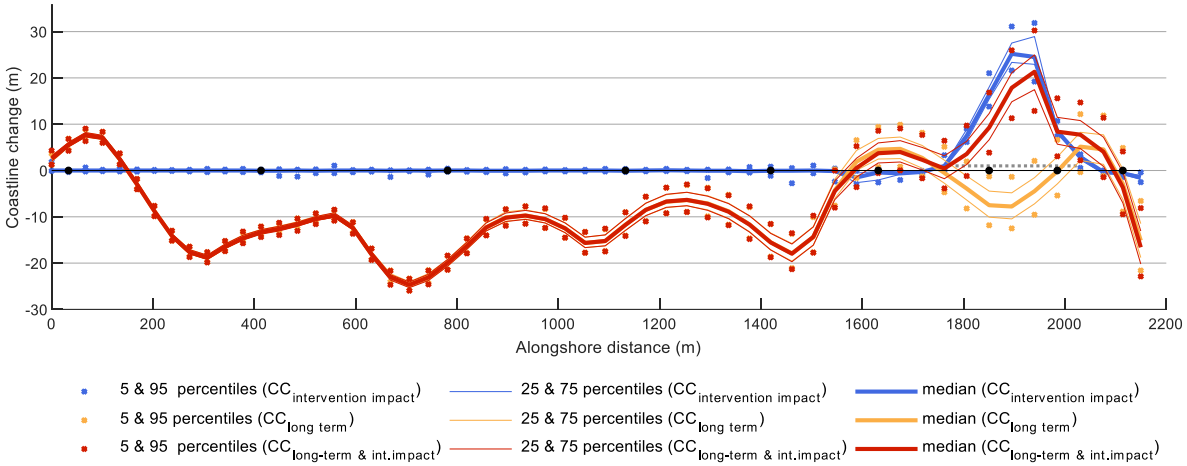

G.1: Overview of the coastline change percentile estimates for Anmok beach (blue: net intervention impact, yellow: climate change –wave climate variability, red: aggregated coastline change). The quartiles are shown with continuous lines, while the 5th and 95th percentile with x markings. Positive values of coastline change indicate accretion. The black markings on the horizontal axis indicate the location of different cross-sections (points 1 to 12) for which probability density plots are presented (Figure 4.23). The grey dotted line indicates the location of the intervention.

Set of submerged breakwaters-nourishment

A more complex intervention design consisting of a set of detached submerged breakwaters and a small-scale nourishment was alternatively included in the aggregation process. The design maintained the dimensions and parameterisation of the first intervention (submerged breakwater-nourishment) with the addition of one submerged detached breakwater attached to the north side of the Gangneung port breakwater (Figure 4.32 b). The design reflects the current condition of Anmok beach, where a second submerged breakwater has been constructed during 2016. The crest level of both submerged breakwaters is located 0.5m below MSL. The Delft3D simulations used to quantify the uncertainty of the intervention impact on the coastline position can be seen in Table 15.

Process	Model	Simulated period	Uncertain Input	Uncertainty quantification method
Intervention impact (2 submerged breakwaters-nourishment)	Delft3D	2015-2018	H_s N (1, 0.067) d_{50} N (450, 50) C N (65, 3.33)	LHS (n=80)

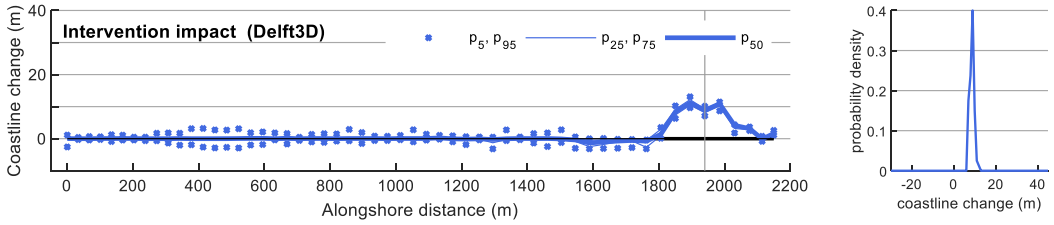

Table 15: Overview of the uncertainty quantification process for the Delft3D simulations used to assess the effect of the intervention (emerged breakwater and nourishment). On the left, the resulting alongshore distribution of different coastline change percentile estimates of the intervention impact is presented. Positive coastline change indicates accretion. The location of the intervention has been marked on the horizontal axis. On the right, the probability distribution plots of coastline change for one location (marked with a grey vertical line in the left graphs) is presented.

Following the net intervention impact assessment ($CC_{intevention\ impact}$), the uncertainty in the coastline change under the autonomous evolution and the combined effect of the intervention and long-term wave climate variations was evaluated following the steps described in Section 4.3.1 . The impact of the considered intervention is more pronounced at the south edge of the coast. The zone behind the breakwaters which was defined as erosive from the UNIBEST_CL+ simulations is mainly accretive when the effect of the intervention is considered. Under the cumulative effect of all the considered processes the expected coastline change in the area reaches up to 10m, the 5-95 percentile range increased by 3.6% on average, compared to the respective range when the intervention impact is not considered.

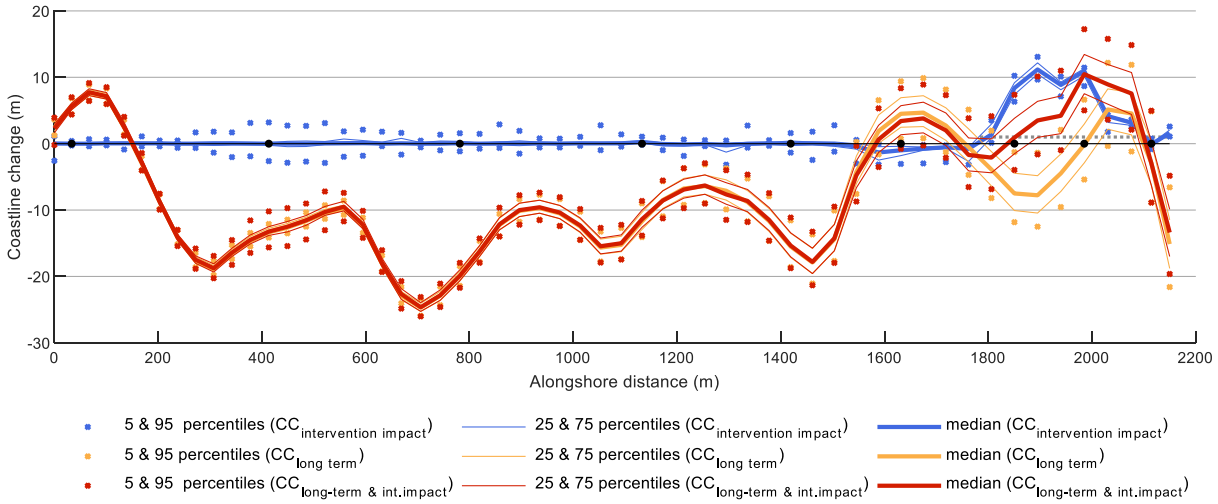

G.2: Overview of the coastline change percentile estimates for Anmok beach (blue: net intervention impact, yellow: climate change –wave climate variability, red: aggregated coastline change). The quartiles are shown with continuous lines, while the 5th and 95th percentile with x markings. Positive values of coastline change indicate accretion. The black markings on the horizontal axis indicate the location of different cross-sections (points 1 to 12) for which probability density plots are presented (Figure 4.23). The grey dotted line indicates the location of the intervention.